GRAVITY FIELD RECOVERY USING TWO LOW SATELLITES IN DIFFERENT ORBITAL PLANES

RUARAIDH ARMSTRONG MACKENZIE

Doctor of Philosophy

THE UNIVERSITY OF ASTON IN BIRMINGHAM

October 1995

THE UNIVERSITY OF ASTON IN BIRMINGHAM

GRAVITY FIELD RECOVERY USING TWO LOW SATELLITES IN DIFFERENT ORBITAL PLANES

RUARAIDH ARMSTRONG MACKENZIE

Doctor of Philosophy

October 1995

This study is concerned with gravity field recovery from low-low satellite to satellite range rate data. An improvement over a coplanar mission is predicted in the errors associated with certain parts of the geopotential by the separation of the orbital planes of the two satellites.

Using Hill's equations an analytical scheme to model the range rate residuals is developed. It is flexible enough to model equally well the residuals between pairs of satellites in the same orbital plane or whose planes are separated in right ascension. The possible benefits of such an orientation to gravity field recovery from range rate data can therefore be analysed, and this is done by means of an extensive error analysis. The results of this analysis show that for an optimal planar mission improvements can be made by separating the satellites in right ascension.

Gravity field recoveries are performed in order to verify and gauge the limitations of the analytical model, and to support the results of the error analysis. Finally the possible problem of the differential decay rates of two satellites due to the diurnal bulge are evaluated.

Key phrases

- Satellite to Satellite Tracking
- Range Rate Residuals

Acknowledgements

There are a number of people whose help or support I would like to acknowledge.

My supervisor Phil Moore for his patience and good humour during my time at Aston. Simon Ehlers and Chris Murphy for their help with Latex and PV-Wave. Chris Lam, Rob, Matt, Henno, Chris M., Rory and Stuart for the things they did.

Also I thank my family for financial support and for providing holiday homes and finally Lori for her continuous friendship, emotional sufferance and food over the last few years.

Contents

List of Figures

List of Tables

Chapter 1

Introduction

The Earth's gravity field has long been measured but the technology necessary for it's accurate global determination has only existed since the launch of artificial satellites. The motions of these satellites first provided information about the general shape of the geoid, or equipotential gravity surface, on a global scale; ie the ellipicity of the Earth, the low zonal harmonics (King-Hele, 1983). More accurate measurements of the satellite orbits produced further more detailed information, for example measurements of lumped harmonics from satellites in resonant orbits (King-Hele, 1981) and with the addition of data from more satellites the determination of individual coefficients within these lumped harmonics (King-Hele and Walker, 1985), but even today the full benefits our technology could afford us are not being realised.

Knowledge of the geoid is of considerable importance to earth scientists and oceanographers in the formation of models to understand and explain the physical processes that we experience on Earth. For example measurements of gravity indicate a correlation between geoidal highs and lows and areas of high geophysical activity. This suggests that such measurements provide less information about crustal elevations and more about the internal physical processes that determine

them (Stacy, 1977).

The fluidity of the oceans means that sea surface elevation reflects more accurately the nature of the equipotential surface. Using the sea surface as a geoid however disregards the important effects on the sea surface of ocean circulation. The ocean circulation is the dominant mode of heat transfer on earth and therefore of crucial importance to the climate system (Harries, 1990). By measuring the geoid, the effects of the currents on the sea surface can be isolated.

This thesis is concerned with the determination of the Earth's gravity field from space using satellite motions. Measuring the velocity or acceleration instead of the position of a satellite is beneficial because it improves the accuracy of recovery of more detailed gravity information, as does differencing the motions of nearby masses. Modern proposals for gravity missions such as Gradiometery (Rummel and Colombo, 1985), (CIGAR, 1995) and satellite to satellite tracking make use of these principles to measure high frequency gravity signal.

Several Satellite to Satellite Tracking (SST) missions have been proposed over the last twenty years eg (Keating T., 1986) and (Frey, 1993). To measure the gravity field to high resolution using this technique it is best that the satellites occupy low orbits and track each other continuously. The high-low variant is not as sensitive to the short wavelength features but has been proposed as a complimentary aspect of a gradiometer mission in (CIGAR, 1995) where the gradiometric satellite is tracked by the GPS network, thereby providing a full spectrum of the potential signal.

Both the range and the range rate have been suggested as the raw measurements for SST missions. The earlier proposals were to have used a doppler system to measure range rate but more recently eg in (Frey, 1993) a laser ranging system has been preferred. In the latter case the more useful range rate can be used as the observation by differencing range measurements in time.

In this work the satellites are assumed to be in orbits of the same or similar

heights so that they can track each other continuously and the observation used in the mathematical model is the range rate.

The thesis begins in chapter 2 with a general discussion of the gravity field and the principles of its recovery. Chapters 3 and 4 contain a description of the analytical model that has been developed in order to describe the case where the only restriction to the mission is that the satellites share the same mean motion and rate of change of their ascending node. This model allows the possibility that the spacecraft are in different orbital planes, separated in right ascension but with the same inclination. The effect of this on the recovery procedure, as well as that of height, inclination and separation are examined in detail in chapter 5 by means of an error analysis. Once an ideal mission scenario has been established, limited recoveries are performed in chapter 6 in order to verify the results of chapter 5.

More longitudinal information is present in the signal and therefore east-west variations in gravity are more accurately determined from separation of the orbital planes. Any problems in maintaining the along track separation between the satellites is significant. One such problem could be the differential decay rates these satellites suffer due to longitude dependent surface forces, in particular air drag. In chapter 7 these effects are analysed and in particular the effect of the diurnal bulge on the satellites is discussed to gauge the significance of the problem.

Chapter 2

Principles of Gravity Recovery

2.1 The Earth's Gravity Field

To a first approximation the effect of the Earth on an external mass such as an artificial satellite is that of a homogeneous sphere of mass $M_\oplus$. Hence the force of attraction between these bodies is given by Newton's universal law of gravitation, namely

$$F = G\frac{mM_\oplus}{r^2}, \tag{2.1.1}$$

where the satellite has mass m, the distance between the geocentre and the centre of mass of the satellite is r and G is the gravitational constant. Combined with Newton's second law of motion (2.1.1) gives the magnitude of the acceleration of the satellite in this direction (relative to an inertial reference frame) as

$$\begin{aligned} a &= G\frac{M_\oplus}{r^2} \\ &= \frac{\mu}{r^2}. \end{aligned} \tag{2.1.2}$$

This acceleration can also be expressed as the gradient of a scalar potential which is dependent only on the position of the satellite relative to the Earth,

$$\mathbf{a} = \nabla V, \tag{2.1.3}$$

where in spherical approximation

$$V = \frac{\mu}{r}. \tag{2.1.4}$$

The Earth however is a non spherical, non homogeneous mass and has a potential given by

$$V = G \int\int\int \frac{\rho(x,y,z)}{r(x,y,z)} dx\, dy\, dz \tag{2.1.5}$$

integrated over the whole Earth, where $\rho(x,y,z)$ is the density of the volume element at (x,y,z) and $r(x,y,z)$ the distance between that element and the satellite. If the mass of the satellite is negligible compared to the mass of the Earth then a Cartesian coordinate system with origin at the geocentre is consistent with equations (2.1.3), (2.1.4) and (2.1.5). (Kaula, 1966)

It can be shown from (2.1.4) or (2.1.5) that the external gravitational potential of a body satisfies Laplace's equation, which in the Cartesian system is written

$$\nabla^2 V = \frac{\partial^2 V}{\partial x^2} + \frac{\partial^2 V}{\partial y^2} + \frac{\partial^2 V}{\partial z^2} = 0. \tag{2.1.6}$$

This equation is expressed in spherical coordinates r, θ, λ (radial distance, latitude and longitude respectively) and the complete real solution obtained by the method of separation of variables. The solution can be written in the form (Bomford, 1980)

$$V = \frac{\mu}{R} \sum_{l=0}^{\infty} \left(\frac{R}{r}\right)^{(l+1)} \sum_{m=0}^{l} P_{lm}(\cos\theta) \left[c_{lm} \cos m\lambda + s_{lm} \sin m\lambda\right]$$

where R is the mean radius of the Earth, $P_{lm}(\cos\theta)$ are the normalised associated Legendre polynomials and c_{lm} and s_{lm} are the normalised gravity field coefficients, parameters which define the geopotential.

It is necessary to transform equation (2.1.7) into Keplerian elements a, e, I, ω, Ω, M, the semi major axis, eccentricity, inclination, argument of perigee, right ascension of the ascending node and mean anomaly of the satellite's orbital ellipse

respectively . This transformation is carried out in (Kaula, 1966) and results in the following expression, after choosing the geocentre as origin,

$$V = \frac{\mu}{r} + \frac{\mu}{R}\sum_{l=2}^{\infty}\sum_{m=0}^{l}\left(\frac{R}{a}\right)^{(l+1)}\sum_{p=0}^{l}F_{lmp}(i)\sum_{q=-\infty}^{+\infty}G_{lpq}(e) \times \sum_{\alpha=0}^{1}\cos\left(\psi_{lmpq}(t)+\phi_{lm\alpha}\right)c_{lm\alpha} \tag{2.1.7}$$

where

$$\psi_{lmpq} = (l-2p+q)(M+\omega) - q\omega + m(\Omega - \theta_G), \tag{2.1.8}$$

and

$$\phi_{lm\alpha} = -\frac{\pi}{4}\left(2\alpha + 1 - (-1)^{l-m}\right). \tag{2.1.9}$$

The $F_{lmp}(i)$ are the inclination functions and $G_{lpq}(e)$ the eccentricity functions. The notation $c_{lm0} = c_{lm}$ and $c_{lm1} = s_{lm}$ has been introduced for reasons of efficiency. This is the form in which the Earth's potential shall be expressed hereafter.

2.2 Satellite Motion and Gravity Field Determination

The motion of a satellite orbiting the Earth is dominated by it's gravity field but is also affected by atmospheric drag, solar radiation pressure and by the tidal accelerations of other bodies such as the moon, the sun, and the planets. The equation of motion can therefore be written

$$\mathbf{a} = \ddot{\mathbf{x}} = \nabla V + \mathbf{f}_{surface} + \mathbf{f}_{tidal}, \tag{2.2.1}$$

where $\mathbf{f}_{surface}$ and $\mathbf{f}_{tidal}$ are the surface force and tidal force vectors respectively. The motion of the spacecraft can be predicted by modelling these forces and the

Earth's gravity field and then integrating equation (2.2.1) forward from the satellite's initial state,

$$\mathbf{x}(t_0) = \mathbf{x}_0 \tag{2.2.2}$$

$$\dot{\mathbf{x}}(t_0) = \dot{\mathbf{x}}_0. \tag{2.2.3}$$

If $\mathbf{f}_{surface}$ and $\mathbf{f}_{tidal}$ are neglected then a solution can be obtained by calculating first order perturbations to the Keplerian elements from the Lagrange planetary equations. However by assuming the satellite's motion to be nearly circular and the orbit to have a fixed ascending node it is possible to solve for the motion using Hill's equations. This method will be discussed in chapter 3.

The complete equation (2.2.1) can be solved more accurately by numerical integration. In this manner the position and velocity of the spacecraft can be known if the models of V, $\mathbf{f}_{surface}$ and $\mathbf{f}_{tidal}$ are known.

Alternatively one can test an existing set of force models by making observations of the motions of one or more satellites , eg the range between an Earth based laser station and the satellite or the differential velocity or acceleration between two spacecraft. These observations are then compared to a simulated set of observations using the solution to equation (2.2.1) and the existing models of V, $\mathbf{f}_{surface}$ and $\mathbf{f}_{tidal}$. Suppose the observations are $S_{obs,i}$ and the simulated observations $S_{calc,i}$, then

$$S_{calc,i} = S_{calc,i}(\beta_{k,0}). \tag{2.2.4}$$

$\beta_{k,0}$ represents the 'known' values of all the parameters which affect the motion of the satellite or satellites, eg the initial state of the spacecraft, the gravity field parameters and the other forces the satellite experiences. Any mismodelling of these parameters will result in errors in the simulated observations. The observed residuals are

$$\Delta S_i = S_{obs,i} - S_{calc,i}(\beta_{k,0}). \tag{2.2.5}$$

These residuals can be used to improve the existing model by enabling one to calculate corrections to the parameters $\beta_{k,0}$. To this end equation (2.2.5) is equated to a Taylor series in the parameters β_k,

$$\Delta S_i = \sum_k \left(\frac{\partial S_{calc,i}}{\partial \beta_k} \right)_{\beta_{k,0}} \Delta\beta_k + \sum_k \sum_{k'} \left(\frac{\partial^2 S_{calc,i}}{\partial \beta_k \partial \beta_{k'}} \right)_{\beta_{k,0},\beta_{k',0}} \Delta\beta_k \Delta\beta_{k'} + ... \quad (2.2.6)$$

If the existing models are good then equation (2.2.6) can be truncated after the linear term and one obtains (Colombo, 1986)

$$\Delta S_i = \sum_k \left(\frac{\partial S_{calc,i}}{\partial \beta_k} \right)_{\beta_{k,0}} \Delta\beta_k + n_i, \quad (2.2.7)$$

where n_i is the noise due to modelling errors, truncation of the Taylor series, etc. Equation (2.2.7) with i ranging over all observations is used to solve for the unknown corrections $\Delta\beta_k$. These cannot be solved exactly because of their approximate nature and because of the existence of the noise in the observed residuals. The solution is obtained by the Least squares minimisation method which is discussed later in the thesis. Chapters 3 and 4 will deal with calculating the partial derivatives in (2.2.7).

An important factor limiting the accuracy in refining the gravity field coefficients is the sensitivity of an observation to errors in these coefficients. The partial derivatives in equation (2.2.7) are an indication of that sensitivity and shall be used later to measure the expected accuracy of the gravity coefficients for different mission scenarios. The importance of tailoring the observations so that they are sensitive to those parts of the gravity field one requires shall be discussed next.

2.3 Satellite Observations

Measurements of spacecraft motions have been used to calculate the geopotential coefficients ever since the first artificial satellites were launched. (Kozai, 1966) These observations were made from Earth based tracking stations using optical,

laser and radio-frequency measurements of the satellite's position. With this type of data, information can be obtained about the low degree and order coefficients in the harmonic expansion of the Earth's gravity field, corresponding to large scale variations in the geopotential, typically wavelengths of a few thousand kilometres.

This limitation is due to several factors:

- To measure the smaller wavelength features a very low orbit is essential and in such orbits satellites have a short lifetime due to the action of air drag. This limits the amount of data one can obtain unless the satellites are manoeuvered.

- Measurements made from Earth are subject to the perturbing effects of the atmosphere and are hence degraded.

- A large number of tracking stations are required to have a near continuous coverage.

- The position of a satellite is rather insensitive to gravity mismodelling except for the very lowest degree coefficients and certain resonant coefficients.

In order to model the shorter wavelength features a different approach is required. Traditional methods include land based gravimetry, and airborne gradiometry (Torge, 1980) but these techniques are limited by adverse geographic conditions, political problems and the great expense of creating global data sets. As a result terrestrial measurements are limited to providing local gravity models.

In recent years satellite altimetery has been used to map the global sea height, from which one may infer an equipotential gravity surface or geoid. The fact that these measurements cannot be made over land and the difficulties in separating the geoid from other oceanographic effects such as ocean currents, make this an insufficient source for a global high resolution field (Nerem, 1994).

The more modern proposals to provide a useful source involve satellites in very low orbits (160-400km). The problems of air drag are overcome by one of two methods. An accelerometer is used to measure the surface forces a satellite experiences. Then either the non conservative accelerations are continuously compensated for so the satellite is in a drag free environment, or manoeuvers are made periodically to keep the orbit from deteriorating and the measured accelerations are removed from the signal in post mission processing.

To overcome the problems of earth based tracking the satellites motion is measured from space. There are three types of mission that have been promoted in recent years. they are:-

- Tracking a low satellite by GPS.
- Tracking between two low satellites.
- Gradiometry. Using differential acceleration measurements of proof masses within a single low satellite.

All three missions have the important characteristic that the motion of at least one low satellite or proof mass is measured. Thus the attenuation with height due to the factor $\left(\frac{R}{a}\right)^{l+1}$ in (2.1.8) is less significant and the low satellite is subject to greater perturbations from high degree coefficients.

The GPS network provides a coverage which could be used to measure the orbit of a low satellite very accurately (Jekeli and Upadhyay, 1990). However the aim of a gravity mission is to provide an accurate, high resolution field and it has been found (Fischell and Pisacane, 1978) (Wakker K. et al, 1989) that low-low tracking is more suitable than the high-low variant for this purpose. This is because the separation of the satellites determines in part how gravity frequencies contribute to the total signal. For larger separations the high frequency contribution is smaller. Thus high-low tracking between satellites separated by a few thousand kilometres

has less high frequency signal than the low-low case where the separation is a few hundred km. In gradiometry the separation is much less, a metre or so, and this necessitates a much more accurate observation since the signal will be very low compared to SST.

Using relative velocity or acceleration measurements is also of benefit if the high degree coefficients are to be measured accurately, (Kaula, 1983), (Wolff, 1969), (Wagner, 1983). This is because the range measurements are the cumulative effects of velocity fluctuations over time and thus by measuring the relative velocity between spacecraft, more localised information is obtained. Similarly acceleration measurements are an improvement over velocity measurements in high frequency field recovery.

Proposals for a gravity field mission have therefore centred on either a low-low satellite to satellite tracking observation of the range rate or a gradiometric mission to measure the differential acceleration. Neither have been approved as yet. In the recent GAMES satellite to satellite tracking proposal (Frey, 1993) the use of a laser ranger was prefered. By differencing these range measurements a range rate dataset could be obtained, double differencing would provide a relative acceleration dataset but would introduce larger errors than by differencing just once.

In the remainder of this thesis only the case of the relative line of sight velocity between two satellites in low orbits shall be studied.

Chapter 3

The Variational Equations

3.1 Introduction

The purpose of this chapter is to derive, discuss and solve a set of equations which describe the sensitivity of a satellite's motion to a small perturbing force. If one assumes the spacecraft to be in a circular orbit which is fixed in space relative to some inertial reference frame, the equations greatly simplify. The price of this simplification is to restrict the applications of any solution to near polar orbits, which do not precess under the action of the Earth's flattening. Furthermore no satellite orbit can be truly circular because the Earth's non sphericity induces a slight eccentricity into an initially circular path. However the simple nature of the equations and their sufficient accuracy for near circular and near polar orbits needed for global gravity field improvement makes them useful for the task at hand.

3.2 Hill's Equations

The equations derived here resemble somewhat the approach used by G.W.Hill in his theory of the lunar orbit (Hill, 1878) and they shall be referred to as Hill's

equations hereafter. The derivation follows (Schrama, 1989). In order to obtain Hill's equations the equations of motion are first described in an inertial frame of reference with basis $\mathbf{I}, \mathbf{J}, \mathbf{K}$. The coordinates shall be Y_{In} in the $\mathbf{J}$ direction, pointing to the first point of Aries, X_{In} in the $\mathbf{I}$ direction, towards the north pole of the orbital plane and Z_{In} in the $\mathbf{K}$ direction, directed so that X_{In}, Y_{In}, Z_{In} form a right handed orthogonal coordinate system. Newton's equations of motion for a purely gravitational force are

$$\ddot{X}_{In}\mathbf{I} + \ddot{Y}_{In}\mathbf{J} + \ddot{Z}_{In}\mathbf{K} = \nabla V \tag{3.2.1}$$

where ∇V is the gradient of the geopotential V. In this coordinate system the gradient vector is easily expanded and in component form (3.2.1) becomes

$$\begin{bmatrix} \ddot{X}_{In} \\ \ddot{Y}_{In} \\ \ddot{Z}_{In} \end{bmatrix} = \begin{bmatrix} \frac{\partial V}{\partial X_{In}} \\ \frac{\partial V}{\partial Y_{In}} \\ \frac{\partial V}{\partial Z_{In}} \end{bmatrix}. \tag{3.2.2}$$

For a non precessing orbit it can be assumed that the satellite crosses the X_{In}, Y_{In} plane only on the Y_{In} axis without any loss of generality. Therefore to transform between the coordinates of the inertial frame and those of the satellite's 'local frame' with basis vectors $\mathbf{h}_1, \mathbf{h}_2, \mathbf{h}_3$ in the cross track, minus along track and radial directions respectively one must rotate the inertial coordinates through an angle $\theta = M + \omega - \frac{\pi}{2}$ about the X_{In} axis. The relationship between the coordinatesX_{In}, Y_{In}, Z_{In} and u, v, w, in the directions $\mathbf{h}_1, \mathbf{h}_2, \mathbf{h}_3$ is written

$$\mathbf{r}_{In} = \begin{bmatrix} X_{In} \\ Y_{In} \\ Z_{In} \end{bmatrix} = \begin{bmatrix} 1 & 0 & 0 \\ 0 & \cos\theta & -\sin\theta \\ 0 & \sin\theta & \cos\theta \end{bmatrix} \begin{bmatrix} u \\ v \\ w \end{bmatrix} = \mathbf{R}_1(\theta)\,\mathbf{x} \tag{3.2.3}$$

where $\mathbf{x}$ denotes the triplet u, v, w. Now because the orbit is circular a uniform rate of rotation can be assumed. Using Kepler's third law, as accurate as the spherical approximation of the earth, this means

$$\dot{\theta} = n_o = \sqrt{\frac{\mu}{a^3}} \tag{3.2.4}$$

where a and n_o are the semi major axis and mean motion respectively. The orbit being circular means $a = |\mathbf{r}_{In}|$.

From (3.2.3) it can be shown that

$$\dot{\mathbf{r}}_{In} = \dot{\mathbf{R}}_1(\theta)\,\mathbf{x} + \mathbf{R}_1(\theta)\,\dot{\mathbf{x}} \tag{3.2.5}$$

and

$$\ddot{\mathbf{r}}_{In} = \ddot{\mathbf{R}}_1(\theta)\,\mathbf{x} + \mathbf{R}_1(\theta)\,\ddot{\mathbf{x}} + 2\dot{\mathbf{R}}_1(\theta)\,\dot{\mathbf{x}}, \tag{3.2.6}$$

also

$$\dot{\mathbf{R}}_1(\theta)\,\dot{\mathbf{x}} = n_o \mathbf{R}_1(\theta) \begin{bmatrix} 0 \\ -\dot{w} \\ \dot{v} \end{bmatrix} \tag{3.2.7}$$

and

$$\ddot{\mathbf{R}}_1(\theta)\,\mathbf{x} = -n_o^2 \mathbf{R}_1(\theta) \begin{bmatrix} 0 \\ v \\ w \end{bmatrix}. \tag{3.2.8}$$

Now using (3.2.7) and (3.2.8) equation (3.2.6) becomes

$$\ddot{\mathbf{r}}_{In} = \mathbf{R}_1(\theta) \begin{bmatrix} \ddot{u} \\ \ddot{v} - 2n_o\dot{w} - n_o^2 v \\ \ddot{w} + 2n_o\dot{v} - n_o^2 w \end{bmatrix}, \tag{3.2.9}$$

which along with equation (3.2.2) gives the equations of motion in the rotating frame. The gradient vector can be transformed according to the same relationship as (3.2.3) so that

$$\begin{bmatrix} \frac{\partial V}{\partial X_{In}} \\ \frac{\partial V}{\partial Y_{In}} \\ \frac{\partial V}{\partial Z_{In}} \end{bmatrix} = \mathbf{R}_1(\theta) \begin{bmatrix} \frac{\partial V}{\partial u} \\ \frac{\partial V}{\partial v} \\ \frac{\partial V}{\partial w} \end{bmatrix}. \tag{3.2.10}$$

As a result of (3.2.10) and (3.2.2), (3.2.9) can be written

$$\begin{bmatrix} \frac{\partial V}{\partial u} \\ \frac{\partial V}{\partial v} \\ \frac{\partial V}{\partial w} \end{bmatrix} = \begin{bmatrix} \ddot{u} \\ \ddot{v} - 2n_o\dot{w} - n_o^2 v \\ \ddot{w} + 2n_o\dot{v} - n_o^2 w \end{bmatrix}. \tag{3.2.11}$$

Equations (3.2.11) are the equations of motion in the rotating frame. To obtain the variational equations one must vary a parameter upon which the motion depends eg. a gravity field coefficient, and determine the effect on equation (3.2.11). The effect of this on the spatial partial derivatives of the potential is both direct in the sense that the potential is a linear function of the coefficients and indirect in the sense that the potential is a function of position which of course is a function of the gravity coefficients. Mathematically this means that the sensitivity of (3.2.11) to the variation of some parameter β_k, which could be due to the gravity field or initial state errors or some other source of mismodelling, is

$$\begin{aligned} \frac{\partial}{\partial \beta_k} & \begin{bmatrix} \frac{\partial V}{\partial u} \\ \frac{\partial V}{\partial v} \\ \frac{\partial V}{\partial w} \end{bmatrix} + \begin{bmatrix} \frac{\partial^2 V}{\partial u^2} & \frac{\partial^2 V}{\partial u \partial v} & \frac{\partial^2 V}{\partial u \partial w} \\ \frac{\partial^2 V}{\partial v \partial u} & \frac{\partial^2 V}{\partial v^2} & \frac{\partial^2 V}{\partial v \partial w} \\ \frac{\partial^2 V}{\partial w \partial u} & \frac{\partial^2 V}{\partial w \partial v} & \frac{\partial^2 V}{\partial w^2} \end{bmatrix} \begin{bmatrix} \frac{\partial u}{\partial \beta_k} \\ \frac{\partial v}{\partial \beta_k} \\ \frac{\partial w}{\partial \beta_k} \end{bmatrix} = \\ = & \frac{\partial}{\partial \beta_k} \begin{bmatrix} \ddot{u} \\ \ddot{v} - 2n_o\dot{w} - n_o^2 v \\ \ddot{w} + 2n_o\dot{v} - n_o^2 w \end{bmatrix}. \end{aligned} \tag{3.2.12}$$

As long as β_k is not a function of time the operations taking the derivative with respect to time or space, and the partial derivative with respect to β_k commute. The second term in equation (3.2.12) contains as a factor the gravity tensor, in spherical approximation this becomes (Colombo, 1986)

$$\begin{bmatrix} \frac{\partial^2 V}{\partial u^2} & \frac{\partial^2 V}{\partial u \partial v} & \frac{\partial^2 V}{\partial u \partial w} \\ \frac{\partial^2 V}{\partial v \partial u} & \frac{\partial^2 V}{\partial v^2} & \frac{\partial^2 V}{\partial v \partial w} \\ \frac{\partial^2 V}{\partial w \partial u} & \frac{\partial^2 V}{\partial w \partial v} & \frac{\partial^2 V}{\partial w^2} \end{bmatrix} = -\frac{\mu}{r^3} \begin{bmatrix} 1 & 0 & 0 \\ 0 & 1 & 0 \\ 0 & 0 & -2 \end{bmatrix}$$

which, using (3.2.4) can be written

$$= -n_o^2 \begin{bmatrix} 1 & 0 & 0 \\ 0 & 1 & 0 \\ 0 & 0 & -2 \end{bmatrix}. \tag{3.2.13}$$

Replacing this in equation (3.2.12) the variational equations are obtained,

$$\frac{\partial}{\partial \beta_k} \begin{bmatrix} \frac{\partial V}{\partial u} \\ \frac{\partial V}{\partial v} \\ \frac{\partial V}{\partial w} \end{bmatrix} = \begin{bmatrix} \frac{\partial \ddot{u}}{\partial \beta_k} + n_o^2 \frac{\partial u}{\partial \beta_k} \\ \frac{\partial \ddot{v}}{\partial \beta_k} - 2n_o \frac{\partial \dot{w}}{\partial \beta_k} \\ \frac{\partial \ddot{w}}{\partial \beta_k} + 2n_o \frac{\partial \dot{v}}{\partial \beta_k} - 3n_o^2 \frac{\partial w}{\partial \beta_k} \end{bmatrix}. \tag{3.2.14}$$

Equations (3.2.14) is the set of equations that shall be used to obtain the orbit sensitivities used in the gravity field recovery procedure. It should be pointed out that the cross track equation is a simple harmonic oscillator with natural frequency n_o and is uncoupled from the other two equations. The solutions to (3.2.14) will resemble those of a perturbed mass spring system with natural frequency n_o where the force perturbations are given by the left hand side of the equation. However before discussing the solutions to (3.2.14) it is necessary to find an explicit form for these forcing partials in terms of the orbit and the gravity coefficients.

3.3 The forcing terms

Equation (2.1.8) gives the Earths potential, V, in terms of the Keplerian elements as

$$V = \frac{\mu}{r} + \frac{\mu}{R} \sum_{l=2}^{\infty} \sum_{m=0}^{l} \left(\frac{R}{a}\right)^{(l+1)} \sum_{p=0}^{l} F_{lmp}(i) \sum_{q=-\infty}^{+\infty} G_{lpq}(e) \times \sum_{\alpha=0}^{1} \cos\left(\psi_{lmpq}(t) + \phi_{lm\alpha}\right) c_{lm\alpha} \tag{3.3.1}$$

where

$$\psi_{lmpq} = (l - 2p + q)(M + \omega) - q\omega + m(\Omega - \theta_G), \tag{3.3.2}$$

and

$$\phi_{lm\alpha} = -\frac{\pi}{4}\left(2\alpha + 1 - (-1)^{l-m}\right). \tag{3.3.3}$$

Since a circular approximation to the nominal orbit has been assumed thus far the same will be assumed of the potential expression. Therefore F is defined as $M+\omega$, and only the $q = 0$ terms are nonzero. The potential is now written

$$V = \frac{\mu}{r} + \frac{\mu}{R}\sum_{l=2}^{\infty}\sum_{m=0}^{l}\left(\frac{R}{a}\right)^{(l+1)}\sum_{p=0}^{l}F_{lmp}(i)\sum_{\alpha=0}^{1}\cos\left(\psi_{lmp}(t) + \phi_{lm\alpha}\right)c_{lm\alpha} \tag{3.3.4}$$

where

$$\psi_{lmp} = (l-2p)F + m(\Omega - \theta_G). \tag{3.3.5}$$

According to the circular orbit assumption $a \equiv r$ and $\dot{F}$ will be constant and equal to the mean motion n_o. The variation in $\Omega - \theta_G$ is also assumed linear in time. Equation (3.3.4) is rewritten as

$$V = \frac{\mu}{r} + \sum_{l=2}^{\infty}\sum_{m=0}^{l}\sum_{\alpha=0}^{1}V_{lm\alpha}c_{lm\alpha} \tag{3.3.6}$$

where after substituting $j = l - 2p$,

$$V_{lm\alpha} = \frac{\mu}{R}\left(\frac{R}{r}\right)^{(l+1)}\sum_{j=-l[2]}^{l}F_{lm\frac{(l-j)}{2}}(i)\cos\left(\psi_{jm}(t) + \phi_{lm\alpha}\right) \tag{3.3.7}$$

and

$$\begin{aligned}\psi_{jm}(t) + \phi_{lm\alpha} &= jn_o t + m\left(\dot{\Omega} - \dot{\theta}_G\right)t + \psi_{jm}(t_o) + \phi_{lm\alpha} \\ &= \dot{\psi}_{jm}t + \psi_{jm}(t_o) + \phi_{lm\alpha}.\end{aligned} \tag{3.3.8}$$

Now to obtain the sensitivity of the forces in the directions of the coordinates u, v, w due to a perturbation in a coefficient $c_{lm\alpha}$ it is necessary to take the partial derivatives of the potential with respect to a coordinate and a gravity coefficient. From (3.3.6) it is clear that

$$\frac{\partial V}{\partial c_{lm\alpha}} = V_{lm\alpha}, \tag{3.3.9}$$

and so what is required is

$$\begin{aligned}
\frac{\partial V_{lm\alpha}}{\partial u} &= \text{across track sensitivity to } c_{lm\alpha} \\
\frac{\partial V_{lm\alpha}}{\partial v} &= \text{minus along track sensitivity to } c_{lm\alpha} \\
\frac{\partial V_{lm\alpha}}{\partial w} &= \text{radial sensitivity to } c_{lm\alpha}.
\end{aligned} \tag{3.3.10}$$

To formulate these partial derivatives it is necessary to use the chain rule to undertake the differentiation with respect to a curvilinear coordinate system. This will allow equation (3.3.7) to be used without any further change of coordinates. The possible curvilinear coordinate systems are r, F and either Ω or i. The system chosen here is denoted $r_\Omega, F_\Omega, i_\Omega$ with Ω acting as a parameter fixing the origin of the coordinates in the equatorial plane. In this system any point p in space can be described by the coordinates r, F, i see Figure 3.3.1. It's radial distance from the geocentre is r, then on the geocentric sphere of radius r, the angle between the equator and the great circle through p and o2 in Figure 3.3.1 is i_Ω, finally the angle between p and o2 is F_Ω. As long as Ω is chosen to be the right ascension of the ascending node of the orbit of a spacecraft and p is a point on the orbit, then $i_\Omega = i$ and $F_\Omega = F$ where i and F are the inclination and argument of latitude of the spacecraft. Now the partial derivatives of the potential with respect to the local frame coordinates can be described in terms of the derivatives with respect to the three curvilinear coordinates. Using the chain rule for partial derivatives,

$$\frac{\partial V_{lm\alpha}}{\partial u} = \frac{\partial V_{lm\alpha}}{\partial r}\frac{\partial r}{\partial u} + \frac{\partial V_{lm\alpha}}{\partial i}\frac{\partial i}{\partial u} + \frac{\partial V_{lm\alpha}}{\partial F}\frac{\partial F}{\partial u} \tag{3.3.11}$$

$$\frac{\partial V_{lm\alpha}}{\partial v} = \frac{\partial V_{lm\alpha}}{\partial r}\frac{\partial r}{\partial v} + \frac{\partial V_{lm\alpha}}{\partial i}\frac{\partial i}{\partial v} + \frac{\partial V_{lm\alpha}}{\partial F}\frac{\partial F}{\partial v} \tag{3.3.12}$$

$$\frac{\partial V_{lm\alpha}}{\partial w} = \frac{\partial V_{lm\alpha}}{\partial r}\frac{\partial r}{\partial w} + \frac{\partial V_{lm\alpha}}{\partial i}\frac{\partial i}{\partial w} + \frac{\partial V_{lm\alpha}}{\partial F}\frac{\partial F}{\partial w}. \tag{3.3.13}$$

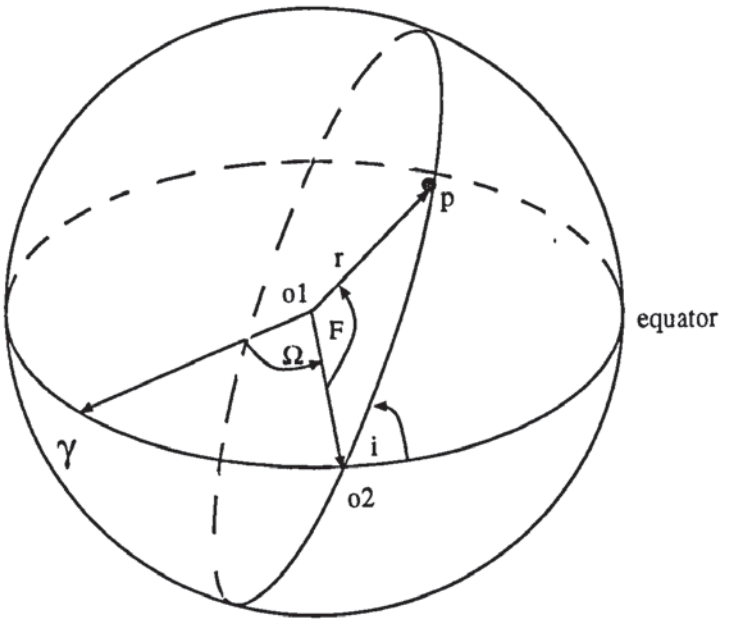

Figure 3.3.1

The r, F, i coordinate system, relative to the parameter Ω.

An important point is that all these partials are calculated along the circular orbit defined by $u = v = 0, w = r$. To obtain these partial derivatives the differentials in u, v and w must be expressed in terms of the curvilinear coordinates at the point $u = v = 0, w = r$ in the local coordinate system. This is done with the aid of Figures 3.3.2 and 3.3.3.

At the point in question $r \equiv w$, therefore the partials $\frac{\partial i}{\partial w}, \frac{\partial F}{\partial w}$ must be zero and $\frac{\partial r}{\partial w} = 1$. This means that (3.3.13) is rewritten

$$\frac{\partial V_{lm\alpha}}{\partial w} = \frac{\partial V_{lm\alpha}}{\partial r}. \tag{3.3.14}$$

Now from Figure 3.3.2 it can be seen that

$$r\delta F = -\delta v \tag{3.3.15}$$

and therefore

$$\frac{\partial F}{\partial v} = -\frac{1}{r} \tag{3.3.16}$$

at $u = v = 0, w = r$. The partial derivatives of F with respect to the other two local frame coordinates are zero at that point. Equation (3.3.12) is therefore (cf. (Colombo, 1984))

$$\frac{\partial V_{lm\alpha}}{\partial v} = -\frac{1}{r}\frac{\partial V_{lm\alpha}}{\partial F}. \tag{3.3.17}$$

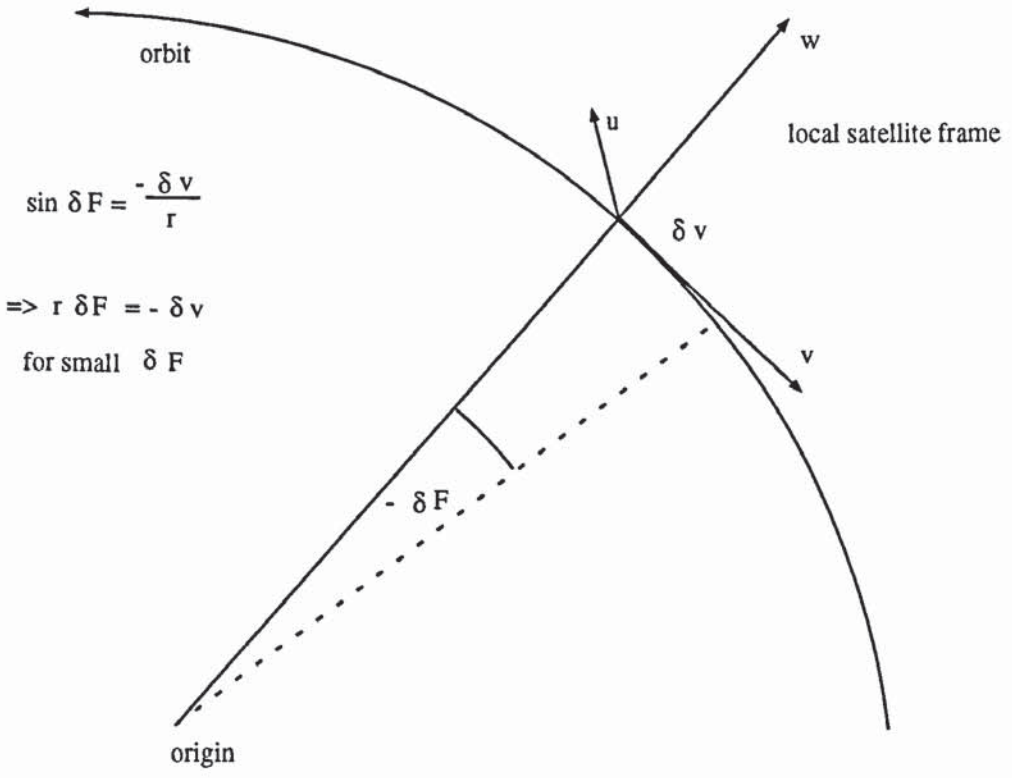

Figure 3.3.2

The along track partial derivative

In the same way from Figure 3.3.3 the partial

$$\frac{\partial i}{\partial u} = \frac{1}{r \sin F} \tag{3.3.18}$$

is found to be the only non zero derivative with respect to u in equation (3.3.11). The final partial is therefore (Koop, 1993)

$$\frac{\partial V_{lm\alpha}}{\partial u} = \frac{1}{r \sin F} \frac{\partial V_{lm\alpha}}{\partial i}. \tag{3.3.19}$$

Substituting (3.3.7) in (3.3.14) and (3.3.17) to obtain the force sensitivities in the orbital plane to an error in the coefficient $c_{lm\alpha}$ the following are obtained,

$$\frac{\partial V_{lm\alpha}}{\partial w} = \frac{\mu}{R^2}(-l-1)\left(\frac{R}{r}\right)^{(l+2)} \sum_{j=-l[2]}^{l} F_{lm\frac{(l-j)}{2}}(i) \cos\left(\psi_{jm}(t) + \phi_{lm\alpha}\right), \tag{3.3.20}$$

$$\frac{\partial V_{lm\alpha}}{\partial v} = \frac{\mu}{R^2}\left(\frac{R}{r}\right)^{(l+2)} \sum_{j=-l[2]}^{l} j F_{lm\frac{(l-j)}{2}}(i) \sin\left(\psi_{jm}(t) + \phi_{lm\alpha}\right). \tag{3.3.21}$$

(3.3.20) and (3.3.21) can now be used in equations (3.2.14) to obtain the in-plane orbital sensitivities to errors in the gravity field coefficient.

The cross track forcing term is given by equation (3.3.19) and is not as straightforward. It seems at first inspection that there is a singularity when $\sin F = 0$, further development reveals that this is not a real singularity since the factor $\frac{\partial V_{lm\alpha}}{\partial i}$ disappears at the points where $\sin F = 0$. To develop this term it is necessary to refer to the derivation of the terms $V_{lm} = V_{lm0} + V_{lm1}$ in (Kaula, 1966). Before the inclination functions have been defined the derivatives of equation (3.58) in (Kaula, 1966) are calculated with respect to inclination . The $\sin F$ term in (3.3.19) is then cancelled out with a term in the numerator to obtain an expression of the form

$$\frac{\partial V_{lm\alpha}}{\partial u} = -\left(\frac{R}{r}\right)^{(l+2)} \sum_{j=-l+2[2]}^{l} F^{*}_{lm\frac{(l-j)}{2}}(i) \sin\left(\psi_{jm}(t) - F + \phi_{lm\alpha}\right) \tag{3.3.22}$$

where the $F^*_{lm\frac{(l-i)}{2}}(i)$ are called the cross track inclination functions (Koop, 1993).

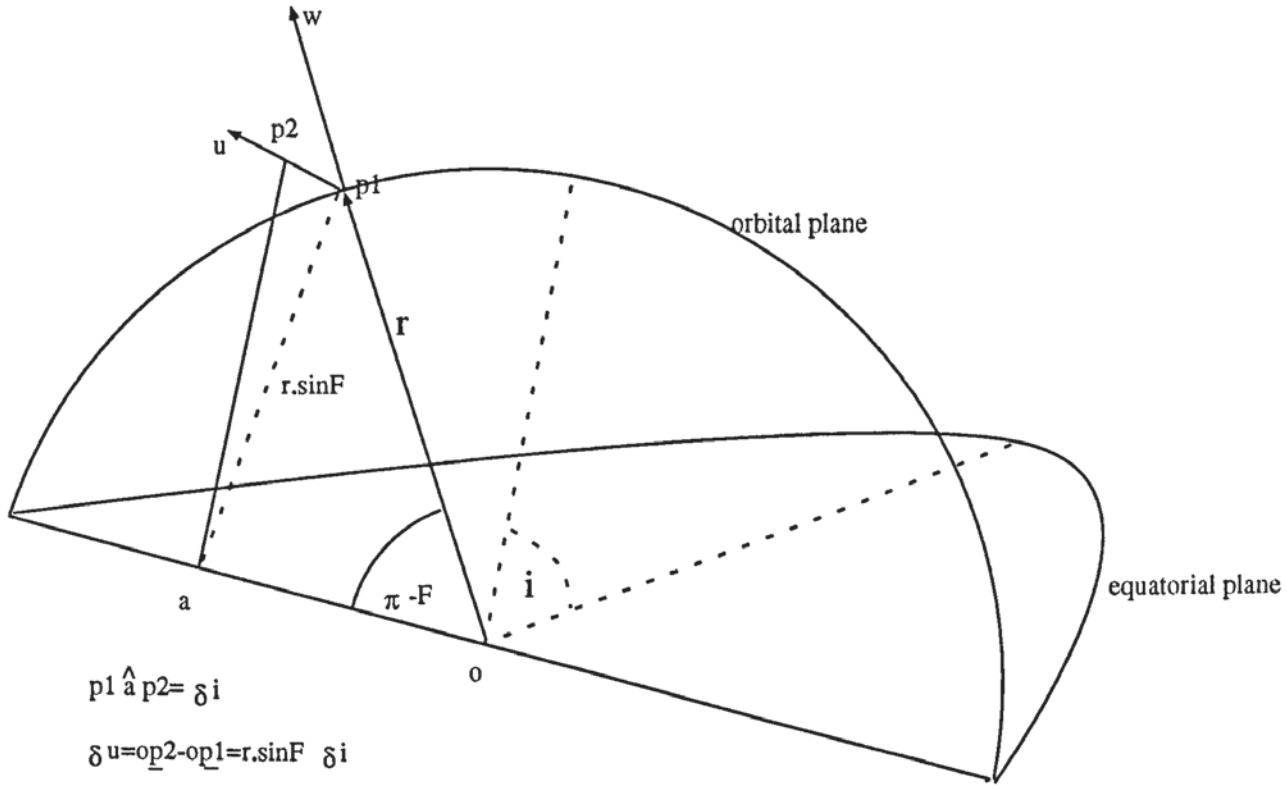

Figure 3.3.3

The cross track partial derivative

A well known problem with calculating the inclination functions which applies also to the cross track inclination functions is their numerical instability for high values of l, m. This problem has been overcome by using the Fast Fourier transform algorithm to compute the required functions, this method is used in (Koop, 1993)

but for completeness is described in Appendix A. Equations (3.3.20), (3.3.21) and (3.3.22) are the forcing partial required to solve Hill's equations (3.2.14). An outline of the method of solution is presented below.

3.4 Solving Hill's Equations

In the light of equations (3.3.20), (3.3.21) and (3.3.22), (3.2.14) can be rewritten for the specific case where $\beta_k = c_{lm\alpha}$ as

$$\begin{bmatrix} \frac{1}{r\sin F}\frac{\partial V_{lm\alpha}}{\partial i} \\ -\frac{1}{r}\frac{\partial V_{lm\alpha}}{\partial F} \\ \frac{\partial V_{lm\alpha}}{\partial r} \end{bmatrix} = \begin{bmatrix} \frac{\partial \ddot{u}}{\partial \beta_k} + n_o^2\frac{\partial u}{\partial \beta_k} \\ \frac{\partial \ddot{v}}{\partial \beta_k} - 2n_o\frac{\partial \dot{w}}{\partial \beta_k} \\ \frac{\partial \ddot{w}}{\partial \beta_k} + 2n_o\frac{\partial \dot{v}}{\partial \beta_k} - 3n_o^2\frac{\partial w}{\partial \beta_k} \end{bmatrix} \tag{3.4.1}$$

where the left hand side is made up of sums of sines and cosines whose arguments increase secularly with time. This fact, and the linear, time invariant nature of the equations makes them easy to solve, for example by the method of Laplace transforms in (Colombo, 1984). Since this technique for solving differential equations is an elementary one the procedure will not be carried out in this thesis and the solutions shall be presented without proof. For this see (Colombo, 1984), (Wiejak W., 1990).

The cross track equation (in u) is uncoupled from the other two; furthermore it is the equation of a simple harmonic oscillator. It can therefore be solved independently of the other two equations which, since they are mutually dependent, must be solved simultaneously. The method of Laplace transforms yields a pair of simultaneous algebraic equations from which the solutions are derived.

There are three different types of solution that are considered here

- The homogeneous solution for which the forcing terms are zero and the parameter β_k is one of the initial state parameters $u_o, v_o, w_o, \dot{u}_o, \dot{v}_o, \dot{w}_o$ which form the state vector of the spacecraft in it's local frame at the beginning of

the period of time for which the solution is required. The solutions will be the sensitivities of the orbits to errors in the initial state parameters.

- Secondly there is the response to an oscillation in the gravity field at a frequency that does not equal one of the critical resonant frequencies of the system.

- Finally the response to a resonant oscillation.

3.4.1 The homogeneous solution

The solution to

$$\begin{bmatrix} 0 \\ 0 \\ 0 \end{bmatrix} = \begin{bmatrix} \frac{\partial \ddot{u}}{\partial \beta_k} + n_o^2 \frac{\partial u}{\partial \beta_k} \\ \frac{\partial \ddot{v}}{\partial \beta_k} - 2n_o \frac{\partial \dot{w}}{\partial \beta_k} \\ \frac{\partial \ddot{w}}{\partial \beta_k} + 2n_o \frac{\partial \dot{v}}{\partial \beta_k} - 3n_o^2 \frac{\partial w}{\partial \beta_k} \end{bmatrix} \tag{3.4.2}$$

is given here, where β_k is one of $u_o, v_o, w_o, \dot{u}_o, \dot{v}_o, \dot{w}_o$, the position and velocity components at time $t = t_o$. The general forms of the solutions are

$$\begin{aligned} \frac{\partial u}{\partial \beta_k} &= A_{u\beta_k} \cos(n_o t) + B_{u\beta_k} \sin(n_o t) \\ \frac{\partial v}{\partial \beta_k} &= A_{v\beta_k} \cos(n_o t) + B_{v\beta_k} \sin(n_o t) + C_{v\beta_k} t + D_{v\beta_k} \\ \frac{\partial w}{\partial \beta_k} &= A_{w\beta_k} \cos(n_o t) + B_{w\beta_k} \sin(n_o t) + C_{w\beta_k}. \end{aligned} \tag{3.4.3}$$

The constants $A_{u\beta_k}, .., C_{w\beta_k}$ can easily be calculated but it is not necessary to do so here since the initial state will never be solved for. The forms of perturbations associated with a variation in the initial state are all that is required.

3.4.2 The response to an oscillation

If the forcing terms are sinusoidal in nature with frequency ω not equal to either zero or $\pm n_o$ then the response of the following equations will be non resonant,

$$\begin{bmatrix} a_u \cos(\omega t + \phi) + b_u \sin(\omega t + \phi) \\ a_v \cos(\omega t + \phi) + b_v \sin(\omega t + \phi) \\ a_w \cos(\omega t + \phi) + b_w \sin(\omega t + \phi) \end{bmatrix} = \begin{bmatrix} \frac{\partial \ddot{u}}{\partial \beta_k} + n_o^2 \frac{\partial u}{\partial \beta_k} \\ \frac{\partial \ddot{v}}{\partial \beta_k} - 2n_o \frac{\partial \dot{w}}{\partial \beta_k} \\ \frac{\partial \ddot{w}}{\partial \beta_k} + 2n_o \frac{\partial \dot{v}}{\partial \beta_k} - 3n_o^2 \frac{\partial w}{\partial \beta_k} \end{bmatrix} \tag{3.4.4}$$

where ϕ is a phase angle and β_k is the parameter giving rise to the forces. Equations (3.4.4) can be solved by Laplace Transforms to give a result which can be used to solve (3.4.1) due to the linear superposition of solutions of linear differential equations. The solution to equations (3.4.4) will include terms with the same frequency of response as the forcing terms, a consequence of the equations being linear with constant coefficients. The solutions are given below,

$$\begin{aligned} \frac{\partial u}{\partial \beta_k} &= \frac{a_u}{(n_o^2 - \omega^2)} \cos(\omega t + \phi) + \frac{b_u}{(n_o^2 - \omega^2)} \sin(\omega t + \phi) \\ &+ A^u \cos(n_o t) + B^u \sin(n_o t) \end{aligned} \tag{3.4.5}$$

$$\begin{aligned} \frac{\partial v}{\partial \beta_k} &= \frac{a_v (3n_o^2 + \omega^2) - 2n_o \omega b_w}{\omega^2 (n_o^2 - \omega^2)} \cos(\omega t + \phi) \\ &+ \frac{b_v (3n_o^2 + \omega^2) + 2n_o \omega a_w}{\omega^2 (n_o^2 - \omega^2)} \sin(\omega t + \phi) \\ &+ A^v \cos(n_o t) + B^v \sin(n_o t) + C^v t + D^v \end{aligned} \tag{3.4.6}$$

$$\begin{aligned} \frac{\partial w}{\partial \beta_k} &= \frac{a_w \omega - 2n_o b_v}{\omega (n_o^2 - \omega^2)} \cos(\omega t + \phi) \\ &+ \frac{b_w \omega + 2n_o a_v}{\omega (n_o^2 - \omega^2)} \sin(\omega t + \phi) \\ &+ A^w \cos(n_o t) + B^w \sin(n_o t) + C^w. \end{aligned} \tag{3.4.7}$$

The cross track equation is independent of the other two and is solved separately, the coefficients in the solutions are only functions of the cross track forces. Using

equation (3.3.22) as the forcing term, and applying the principle of linear superposition

$$\begin{aligned}\frac{\partial u}{\partial c_{lm\alpha}} &= -\frac{\mu}{R^2}\left(\frac{R}{r}\right)^{(l+2)} \sum_{j=-l+2[2]}^{l} \frac{F^*_{lm\frac{(l-j)}{2}}(i)}{\left(n_o^2 - \left(\dot{\psi}_{jm} - n_o\right)^2\right)} \\ &\quad \times \sin\left(\dot{\psi}_{jm}t - n_o t + \phi_{lm\alpha} + \psi^o_{jm} - F^o\right) \\ &+ A^u_{lm\alpha}\cos(n_o t) + B^u_{lm\alpha}\sin(n_o t) \end{aligned} \tag{3.4.8}$$

where ψ^o_{jm}, F^o are the initial values of these angles. Using

$$\dot{\psi}_{jm} = jn_o + m\left(\dot{\theta} - \dot{\Omega}\right) \tag{3.4.9}$$

(3.4.8) becomes

$$\begin{aligned}\frac{\partial u}{\partial c_{lm\alpha}} &= -\frac{\mu}{R^2}\left(\frac{R}{r}\right)^{(l+2)} \sum_{j=-l+2[2]}^{l} \frac{F^*_{lm\frac{(l-j)}{2}}(i)}{\left(n_o^2 - \left(\dot{\psi}_{j-1m}\right)^2\right)} \\ &\quad \times \sin\left(\dot{\psi}_{j-1m}t + \phi_{lm\alpha} + \psi^o_{j-1m}\right) \\ &+ A^u_{lm\alpha}\cos(n_o t) + B^u_{lm\alpha}\sin(n_o t) \end{aligned} \tag{3.4.10}$$

The two 'in plane' equations are coupled so are solved simultaneously. This means that the radial forces affect the along track position and vice-versa. From equations (3.3.20), (3.3.21) applied to the solutions (3.4.6) and (3.4.7) the in plane orbit sensitivities to a gravity coefficient error are

$$\begin{aligned}\frac{\partial v}{\partial c_{lm\alpha}} &= \frac{\mu}{R^2}\left(\frac{R}{r}\right)^{(l+2)} \sum_{j=-l[2]}^{l} F_{lm\frac{(l-j)}{2}}(i)\,\frac{j\left(3n_o^2 + \dot{\psi}^2_{jm}\right) - 2n_o\dot{\psi}^2_{jm}(l+1)}{\dot{\psi}^2_{jm}\left(n_o^2 - \dot{\psi}^2_{jm}\right)} \\ &\times \sin\left(\dot{\psi}_{jm}t + \phi_{lm\alpha} + \psi^o_{jm}\right) \\ &+ A^v_{lm\alpha}\cos(n_o t) + B^v_{lm\alpha}\sin(n_o t) + C^v_{lm\alpha}t + D^v_{lm\alpha} \end{aligned} \tag{3.4.11}$$

and

$$\begin{aligned}\frac{\partial w}{\partial c_{lm\alpha}} &= \frac{\mu}{R^2}\left(\frac{R}{r}\right)^{(l+2)} \sum_{j=-l[2]}^{l} F_{lm\frac{(l-j)}{2}}(i)\,\frac{-2jn_o - \dot{\psi}_{jm}(l+1)}{\dot{\psi}_{jm}\left(n_o^2 - \dot{\psi}^2_{jm}\right)} \\ &\times \cos\left(\dot{\psi}_{jm}t + \phi_{lm\alpha} + \psi^o_{jm}\right) \\ &+ A^w_{lm\alpha}\cos(n_o t) + B^w_{lm\alpha}\sin(n_o t) + C^w_{lm\alpha} \end{aligned} \tag{3.4.12}$$

3.4.3 Resonance

On examining equations (3.4.10), (3.4.11) and (3.4.12) it is clear that when the frequency $\dot{\psi}_{jm}$ is equal to $\pm n_o$ and for the in plane equations zero, the solutions are no longer valid. In fact it would seem that the response to a perturbation of this type is infinite.

When there is a gravity term which has frequency equal to the orbital frequency then the motion induced on the spacecraft is reinforced during every cycle. This is because the accelerations are occuring at a natural frequency of the system and much like a mass on a spring that is tapped at the same point during every cycle, the amplitudes of the motions at these frequencies are amplified by the small perturbing force. The resonant equations are given below, where β_k is the source of the resonant force perturbations,

$$\begin{bmatrix} a_u \cos(n_o t + \phi) + b_u \sin(n_o t + \phi) \\ a_v \cos(n_o t + \phi) + b_v \sin(n_o t + \phi) + c_v \\ a_w \cos(n_o t + \phi) + b_w \sin(n_o t + \phi) + c_w \end{bmatrix} = \begin{bmatrix} \frac{\partial \ddot{u}}{\partial \beta_k} + n_o^2 \frac{\partial u}{\partial \beta_k} \\ \frac{\partial \ddot{v}}{\partial \beta_k} - 2n_o \frac{\partial \dot{w}}{\partial \beta_k} \\ \frac{\partial \ddot{w}}{\partial \beta_k} + 2n_o \frac{\partial \dot{v}}{\partial \beta_k} - 3n_o^2 \frac{\partial w}{\partial \beta_k} \end{bmatrix} \tag{3.4.13}$$

and the general forms of the solutions are

$$\begin{aligned} \frac{\partial u}{\partial \beta_k} &= (A_{u\beta_k} + B_{u\beta_k} t)\cos(n_o t) + (C_{u\beta_k} + D_{u\beta_k} t)\sin(n_o t) \\ \frac{\partial v}{\partial \beta_k} &= (A_{v\beta_k} + B_{v\beta_k} t)\cos(n_o t) + (C_{v\beta_k} + D_{v\beta_k} t)\sin(n_o t) \\ &+ C_{v\beta_k} t^2 + D_{v\beta_k} t + E_{v\beta_k} \\ \frac{\partial w}{\partial \beta_k} &= (A_{w\beta_k} + B_{w\beta_k} t)\cos(n_o t) + (C_{w\beta_k} + D_{w\beta_k} t)\sin(n_o t) \\ &+ C_{w\beta_k} t + D_{w\beta_k}. \end{aligned} \tag{3.4.14}$$

From (3.4.14) it seems that the secular once per revolution terms would increase indefinitely. This is not so for two reasons, the damping of the motion of the spacecraft due to air drag would eventually become significant and would oppose

the motion. Secondly as the perturbations become large enough to be included in the nominal orbit upon which these solutions are based, one would find that resonance would begin to diminish.

3.5 The Orbital Sensitivities

In order to use the range rate residuals for gravity field analysis one must calculate the partials of the velocity and position with respect to the gravity coefficients. In the satellite's local frame equations (3.4.10), (3.4.11) and (3.4.12) give the position sensitivities. The derivatives of these with respect to time t give the velocity partials.

3.5.1 The Zonal Harmonics

If one or more of the frequencies ψ_{jm} , or ψ_{j-1m} for the cross track case, are equal to $\pm n_o$ or zero then the resonant solution must be incorporated into the partials. It is possible to choose an orbit for which the only significant coefficients that give rise to such terms have $m = 0$. This type of orbit is to be used in subsequent chapters, so if $m = 0$ and $j = 0, \pm 1$ the resonant solution must be used. This means that using (3.4.10), (3.4.11), (3.4.12) and (3.4.14) the $m = 0$ coefficients have the following associated orbit sensitivities,

$$\begin{aligned}\frac{\partial u}{\partial c_{l0\alpha}} &= -\frac{\mu}{R^2}\left(\frac{R}{r}\right)^{(l+2)} \sum_{j=-l+2[2]}^{l} \frac{F^*_{l0\frac{(l-j)}{2}}(i)}{\left(n_o^2 - \left(\dot{\psi}_{j-1,0}\right)^2\right)} \\ &\times \sin\left(\dot{\psi}_{j-1,0}t + \phi_{lm\alpha} + \psi^o_{j-1,0}\right) \\ &+ \left(A^u_{l0\alpha} + B^u_{l0\alpha}t\right)\cos\left(n_o t\right) + \left(C^u_{l0\alpha} + D^u_{l0\alpha}t\right)\sin\left(n_o t\right), \qquad (3.5.1)\end{aligned}$$

$$\frac{\partial v}{\partial c_{l0\alpha}} = \frac{\mu}{R^2}\left(\frac{R}{r}\right)^{(l+2)} \sum_{j=-l[2]}^{l} F_{l0\frac{(l-j)}{2}}(i)\, \frac{j\left(3n_o^2 + \dot{\psi}^2_{j0}\right) - 2n_o\dot{\psi}^2_{j0}(l+1)}{\dot{\psi}^2_{j0}\left(n_o^2 - \dot{\psi}^2_{j0}\right)}$$

$$\times \quad \sin\left(\dot{\psi}_{j0}t + \phi_{l0\alpha} + \psi^{o}_{j0}\right)$$
$$+ \quad (A^{v}_{l0\alpha} + B^{v}_{l0\alpha}t)\cos(n_o t) + (C^{v}_{l0\alpha} + D^{v}_{l0\alpha}t)\sin(n_o t) + E^{v}_{l0\alpha}t + F^{v}_{l0\alpha} \tag{3.5.2}$$

and

$$\frac{\partial w}{\partial c_{l0\alpha}} = \frac{\mu}{R^2}\left(\frac{R}{r}\right)^{(l+2)} \sum_{j=-l[2]}^{l} F_{l0\frac{(l-j)}{2}}(i)\,\frac{-2jn_o - \dot{\psi}_{j0}(l+1)}{\dot{\psi}_{j0}\left(n_o^2 - \dot{\psi}_{j0}^2\right)}$$
$$\times \quad \cos\left(\dot{\psi}_{j0}t + \phi_{l0\alpha} + \psi^{o}_{j0}\right)$$
$$+ \quad (A^{w}_{l0\alpha} + B^{w}_{l0\alpha}t)\cos(n_o t) + (C^{w}_{l0\alpha} + D^{w}_{l0\alpha}t)\sin(n_o t) + E^{w}_{l0\alpha}. \tag{3.5.3}$$

The coefficients $C_{v\beta_k}, C_{w\beta_k}$ in equation (3.4.14) are zero since they depend solely on the constant along track force provided by the $j = 0$ term in (3.3.21), which is zero. Therefore these terms are dropped from (3.5.1), (3.5.2) and (3.5.3).

3.5.2 A General Gravity Coefficient

A general form for the orbit sensitivities can now be written as

$$\frac{\partial x_i}{\partial c_{lm\alpha}} = \sum_{j=-l}^{l}\left[\mathcal{X}^{i}_{lm\alpha j}\cos\left(\dot{\psi}^{i}_{jm}t + \phi^{i}_{lm\alpha j}\right)\right]$$
$$+ \quad \left(\hat{C}^{i}_{lm\alpha} + \delta_{m0}\hat{D}^{i\beta}_{l0\alpha}t\right)\cos(n_o t) + \left(\hat{E}^{i}_{lm\alpha} + \delta_{m0}\hat{F}^{i}_{l0\alpha}t\right)\sin(n_o t)$$
$$+ \quad \hat{G}^{i}_{lm\alpha}t + \hat{H}^{i}_{lm\alpha} \tag{3.5.4}$$

where $x^i = 1, 2, 3$ refers to u, v and w. The phase angle

$$\phi^{i}_{lm\alpha j} = \phi_{lm\alpha} + \psi^{i0}_{jm} + \frac{\pi}{2} \tag{3.5.5}$$

for i=1,2 and

$$\phi^{3}_{lm\alpha j} = \phi_{lm\alpha} + \psi^{30}_{jm}. \tag{3.5.6}$$

The amplitudes $\mathcal{X}^i_{lm\alpha j}$ can be found by comparison of (3.5.4) with (3.4.10), (3.4.11) and (3.4.12), namely (cf. (Rosborough and Tapley, 1987))

$$\mathcal{X}^1_{lm\alpha j} = -\left(\frac{R}{r}\right)^{(l+2)} \frac{F^*_{lm\frac{(l-j)}{2}}(i)}{\left(n_o^2 - \left(\dot{\psi}_{jm} - n_o\right)^2\right)} \tag{3.5.7}$$

$$\mathcal{X}^2_{lm\alpha j} = \left(\frac{R}{r}\right)^{(l+2)} F_{lm\frac{(l-j)}{2}}(i) \frac{j\left(3n_o^2 + \dot{\psi}^2_{jm}\right) - 2n_o\dot{\psi}^2_{jm}(l+1)}{\dot{\psi}^2_{jm}\left(n_o^2 - \dot{\psi}^2_{jm}\right)} \tag{3.5.8}$$

$$\mathcal{X}^3_{lm\alpha j} = \left(\frac{R}{r}\right)^{(l+2)} F_{lm\frac{(l-j)}{2}}(i) \frac{-2jn_o - \dot{\psi}_{jm}(l+1)}{\dot{\psi}_{jm}\left(n_o^2 - \dot{\psi}^2_{jm}\right)}. \tag{3.5.9}$$

The frequencies are

$$\begin{aligned} \dot{\psi}^2_{jm} &= \dot{\psi}^3_{jm} = jn_o + m\left(\dot{\Omega} - \dot{\theta}_G\right) \\ \dot{\psi}^1_{jm} &= (j-1)n_o + m\left(\dot{\Omega} - \dot{\theta}_G\right). \end{aligned} \tag{3.5.10}$$

It should be noted that the summations over j in (3.5.1), (3.5.2), (3.5.3) (and (3.5.4) for $m = 0$) are restricted to values where $j \neq 0, \pm 1$. Equation (3.5.4) gives the general form for the sensitivity of the position of the spacecraft in it's local frame. To obtain the velocity sensitivities in the local frame this equation should be differentiated with respect to time. Because of the motion of the frame these velocities are not the same as one would obtain in an inertially static frame or a frame which moves relative to this one. In order to correctly model the relative velocity of two satellites using solutions to Hill's equations care must be taken to account for the relative motions that may exist between them.

Chapter 4

Satellite to Satellite Tracking

4.1 Introduction

In section 2.2 the general principles of refining an existing gravity field were outlined. The case of the range rate between two satellites in circular orbits will now be developed .The discussion here will be general enough to allow for the case when the satellites are in different orbital planes.

Using equation (2.2.7) , with $S_{obs\,i}$ replaced by $RR_{obs\,i}$, the i^{th} observed range rate measurement and $S_{calc\,i}$ replaced by $RR_{calc\,i}$,the i^{th} calculated range rate value then the Range Rate Residual

$$\Delta RR_i(\beta_{k_o}) = RR_{obs\,i} - RR_{calc\,i}(\beta_{k_o}) = \sum_{k=1}^{N_p} \frac{\partial RR_{calc\,i}(\beta_{k_o})}{\partial \beta_k} \Delta\beta_k. \qquad (4.1.1)$$

The β_k are the parameters which affect the motion of the satellites and hence the range rate.These can be split into gravitational and non gravitational parameters with (4.1.1) rewritten as

$$\Delta RR_i(\beta_{k_o}) = \sum_{l=2}^{Lmax} \sum_{m=0}^{l} \sum_{\alpha=0}^{1} \frac{\partial RR_{calc\,i}(c_{lm\alpha}, a_j)}{\partial c_{lm\alpha}} \Delta c_{lm\alpha}$$

$$+ \sum_{j=1}^{M} \frac{\partial RR_{calc\,i}(c_{lm\alpha}, a_j)}{\partial a_j} \Delta a_j \qquad (4.1.2)$$

where a_j are the M non gravitational parameters.

As far as this work is concerned the effect of the gravitational parameters $c_{lm\alpha}$ is of most interest. In the next part of this chapter a form will be derived for $\frac{\partial RR_{calc\,i}}{\partial c_{lm\alpha}}$,the so called partials.

Equation (4.1.2) is the linear (in terms of $\Delta c_{lm\alpha}$) Taylor expansion of $\Delta RR_i(\beta_{k_o})$. This implies that the partial derivatives in this and the next section are calculated using values β_{k_o} which are called the nominal values of the parameters. Consequently the positions and velocities used in calculating the partials are called the nominal positions and velocities.

4.2 The range rate residuals

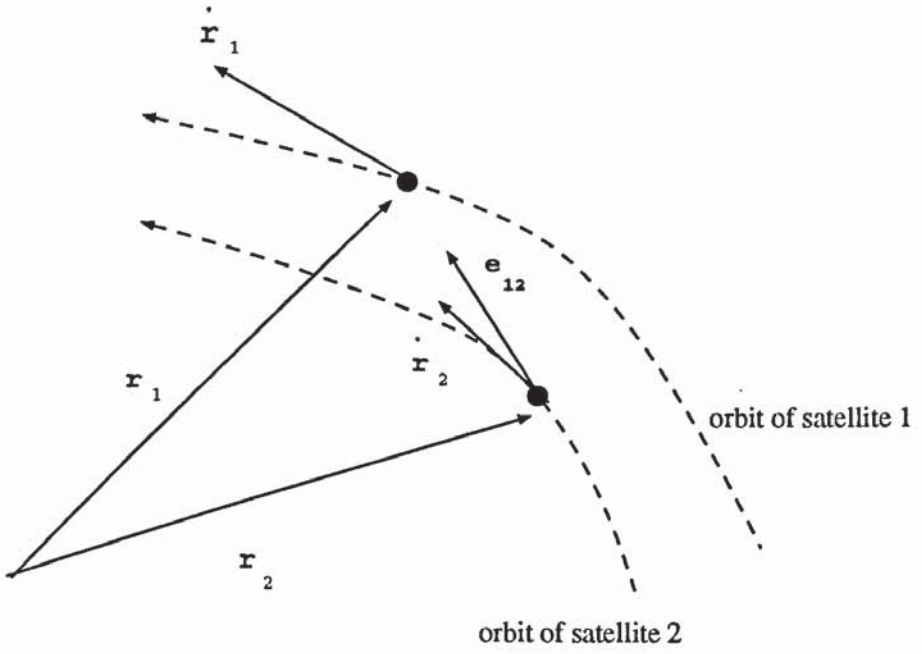

Figure 4.2.1

The relative orientations of the satellites

If the nominal position and velocity vectors of the two satellites in some arbitrary but consistent reference frame are given by $\mathbf{r}_{1_o}, \mathbf{r}_{2_o}, \dot{\mathbf{r}}_{1_o}, \dot{\mathbf{r}}_{2_o}$, then the nominal line of sight relative velocity between them is given by the scalar product of their relative velocity with the nominal unit vector pointing from one to the other, namely

$$RR_o = \frac{(\dot{\mathbf{r}}_{1_o} - \dot{\mathbf{r}}_{2_o}).(\mathbf{r}_{1_o} - \mathbf{r}_{2_o})}{|\mathbf{r}_{1_o} - \mathbf{r}_{2_o}|}. \tag{4.2.1}$$

eg (Groten, 1987), (Colombo, 1984).
This could also be written as

$$RR_o = (\dot{\mathbf{r}}_{1_o} - \dot{\mathbf{r}}_{2_o}).\mathbf{e}_{12_o} \tag{4.2.2}$$

where $\mathbf{e}_{12_o} = \frac{(\mathbf{r}_{1_o} - \mathbf{r}_{2_o})}{|\mathbf{r}_{1_o} - \mathbf{r}_{2_o}|}$ is the unit vector pointing from satellite 2 to satellite 1, see Figure 4.2.1 .

The nominal distance between the two satellites, is

$$\rho_o = |\mathbf{r}_{1_o} - \mathbf{r}_{2_o}| = \sqrt{((\mathbf{r}_{1_o} - \mathbf{r}_{2_o}).(\mathbf{r}_{1_o} - \mathbf{r}_{2_o}))}. \tag{4.2.3}$$

In order to derive $\frac{\partial RR_o}{\partial c_{lm\alpha}}$, the chain rule of partial differentiation is applied. Since $RR_o \equiv RR_o(\mathbf{r}_{1_o}, \mathbf{r}_{2_o}, \dot{\mathbf{r}}_{1_o}, \dot{\mathbf{r}}_{2_o})$

$$\begin{aligned} \frac{\partial RR_o}{\partial c_{lm\alpha}} &= \frac{\partial RR_o}{\partial \mathbf{r}_{1_o}}.\frac{\partial \mathbf{r}_{1_o}}{\partial c_{lm\alpha}} + \frac{\partial RR_o}{\partial \mathbf{r}_{2_o}}.\frac{\partial \mathbf{r}_{2_o}}{\partial c_{lm\alpha}} \\ &+ \frac{\partial RR_o}{\partial \dot{\mathbf{r}}_{1_o}}.\frac{\partial \dot{\mathbf{r}}_{1_o}}{\partial c_{lm\alpha}} + \frac{\partial RR_o}{\partial \dot{\mathbf{r}}_{2_o}}.\frac{\partial \dot{\mathbf{r}}_{2_o}}{\partial c_{lm\alpha}} \end{aligned} \tag{4.2.4}$$

where (4.2.1) and (4.2.2) are used to calculate the partials $\frac{\partial RR_o}{\partial \dot{\mathbf{r}}_{1_o}}, \frac{\partial RR_o}{\partial \dot{\mathbf{r}}_{2_o}}, \frac{\partial RR_o}{\partial \mathbf{r}_{1_o}}, \frac{\partial RR_o}{\partial \mathbf{r}_{2_o}}$

$$\frac{\partial RR_o}{\partial \dot{\mathbf{r}}_{1_o}} = \mathbf{e}_{12_o} \tag{4.2.5}$$

$$\frac{\partial RR_o}{\partial \dot{\mathbf{r}}_{2_o}} = -\mathbf{e}_{12_o} \tag{4.2.6}$$

$$\frac{\partial RR_o}{\partial \mathbf{r}_{1_o}} = (\dot{\mathbf{r}}_{1_o} - \dot{\mathbf{r}}_{2_o})\frac{1}{\rho_o} - \frac{1}{\rho_o^2}(\dot{\mathbf{r}}_{1_o} - \dot{\mathbf{r}}_{2_o}).(\mathbf{r}_{1_o} - \mathbf{r}_{2_o})\frac{\partial \rho_o}{\partial \mathbf{r}_{1_o}} \tag{4.2.7}$$

$$\frac{\partial RR_o}{\partial \mathbf{r}_{2_o}} = -(\dot{\mathbf{r}}_{1_o} - \dot{\mathbf{r}}_{2_o})\frac{1}{\rho_o} - \frac{1}{\rho_o^2}(\dot{\mathbf{r}}_{1_o} - \dot{\mathbf{r}}_{2_o}).(\mathbf{r}_{1_o} - \mathbf{r}_{2_o})\frac{\partial \rho_o}{\partial \mathbf{r}_{2_o}}. \tag{4.2.8}$$

From (4.2.3)

$$\begin{aligned}\frac{\partial \rho_o}{\partial \mathbf{r}_{1_o}} &= \frac{(\mathbf{r}_{1_o} - \mathbf{r}_{2_o})}{\rho_o} \\ &= \mathbf{e}_{12_o}\end{aligned} \tag{4.2.9}$$

$$\begin{aligned}\frac{\partial \rho_o}{\partial \mathbf{r}_{2_o}} &= \frac{-(\mathbf{r}_{1_o} - \mathbf{r}_{2_o})}{\rho_o} \\ &= -\mathbf{e}_{12_o}\end{aligned} \tag{4.2.10}$$

and on substituting these in (4.2.7) and (4.2.8)

$$\frac{\partial RR_o}{\partial \mathbf{r}_{1_o}} = (\dot{\mathbf{r}}_{1_o} - \dot{\mathbf{r}}_{2_o})\frac{1}{\rho_o} - \frac{1}{\rho_o^2}(\dot{\mathbf{r}}_{1_o} - \dot{\mathbf{r}}_{2_o}).(\mathbf{r}_{1_o} - \mathbf{r}_{2_o})\ \mathbf{e}_{12_o} \tag{4.2.11}$$

and

$$\frac{\partial RR_o}{\partial \mathbf{r}_{2_o}} = -(\dot{\mathbf{r}}_{1_o} - \dot{\mathbf{r}}_{2_o})\frac{1}{\rho_o} + \frac{1}{\rho_o^2}(\dot{\mathbf{r}}_{1_o} - \dot{\mathbf{r}}_{2_o}).(\mathbf{r}_{1_o} - \mathbf{r}_{2_o})\ \mathbf{e}_{12_o}. \tag{4.2.12}$$

Expressions (4.2.11) and (4.2.12) can be simplified if it is noted that the second term in each of the equations could be written as $\frac{1}{\rho_o}(\dot{\mathbf{r}}_{1_o} - \dot{\mathbf{r}}_{2_o}).\mathbf{e}_{12_o}\ \mathbf{e}_{12_o}$. This is the component of the first term in the $\mathbf{e}_{12_o}$ direction. Therefore if the first term

is split into three components in directions $\mathbf{e}_{12_o}, \mathbf{f}_{12_o}, \mathbf{g}_{12_o}$ which are defined as an orthonormal triad, then (4.2.11) and (4.2.12) can be written

$$\frac{\partial RR_o}{\partial \mathbf{r}_{1_o}} = \frac{1}{\rho_o}(\dot{\mathbf{r}}_{1_o} - \dot{\mathbf{r}}_{2_o}).\mathbf{f}_{12_o}\ \mathbf{f}_{12_o} + \frac{1}{\rho_o}(\dot{\mathbf{r}}_{1_o} - \dot{\mathbf{r}}_{2_o}).\mathbf{g}_{12_o}\ \mathbf{g}_{12_o} \tag{4.2.13}$$

$$\frac{\partial RR_o}{\partial \mathbf{r}_{2_o}} = -\frac{1}{\rho_o}(\dot{\mathbf{r}}_{1_o} - \dot{\mathbf{r}}_{2_o}).\mathbf{f}_{12_o}\ \mathbf{f}_{12_o} - \frac{1}{\rho_o}(\dot{\mathbf{r}}_{1_o} - \dot{\mathbf{r}}_{2_o}).\mathbf{g}_{12_o}\ \mathbf{g}_{12_o}. \tag{4.2.14}$$

Thus substituting (4.2.5), (4.2.6), (4.2.13) and (4.2.14) into (4.2.4)

$$\begin{aligned}\frac{\partial RR_o}{\partial c_{lm\alpha}} &= (\frac{\partial \dot{\mathbf{r}}_{1_o}}{\partial c_{lm\alpha}} - \frac{\partial \dot{\mathbf{r}}_{2_o}}{\partial c_{lm\alpha}}).\mathbf{e}_{12_o} \\ &+ \frac{1}{\rho_o}(\dot{\mathbf{r}}_{1_o} - \dot{\mathbf{r}}_{2_o}).\mathbf{f}_{12_o}(\frac{\partial \mathbf{r}_{1_o}}{\partial c_{lm\alpha}} - \frac{\partial \mathbf{r}_{2_o}}{\partial c_{lm\alpha}}).\mathbf{f}_{12_o} \\ &+ \frac{1}{\rho_o}(\dot{\mathbf{r}}_{1_o} - \dot{\mathbf{r}}_{2_o}).\mathbf{g}_{12_o}(\frac{\partial \mathbf{r}_{1_o}}{\partial c_{lm\alpha}} - \frac{\partial \mathbf{r}_{2_o}}{\partial c_{lm\alpha}}).\mathbf{g}_{12_o}\end{aligned} \tag{4.2.15}$$

(Colombo, 1984).

The first term in equation (4.2.15) is the vector sensitivity of the relative velocity along the direction $\mathbf{e}_{12_o}$ to perturbations in the gravity coefficient $c_{lm\alpha}$. This direction also depends on the gravity field and the range rate sensitivities take this into account in the next terms. The second and third terms in (4.2.15) add the relative velocity contributions from the directions perpendicular to $\mathbf{e}_{12_o}$ to the range rate sensitivities. Such terms contribute because although the directions $\mathbf{e}_{12_o}$ and $\mathbf{f}_{12_o}$ are perpendicular , the directions $\mathbf{f}_{12_o}$ and $\mathbf{e}_{12}$ are not and it is this direction along which the observations are made.

To illustrate this point it is seen from Fig (4.2.2) that

$$\rho \mathbf{e}_{12} = \rho_o \mathbf{e}_{12_o} + (\Delta \mathbf{r}_1 - \Delta \mathbf{r}_2) \tag{4.2.16}$$

where $\Delta \mathbf{r}_1$ and $\Delta \mathbf{r}_2$ are the differences between the nominal and true positions of satellites 1 and two respectively.

Now

$$(\Delta \mathbf{r}_1 - \Delta \mathbf{r}_2) = (\Delta \mathbf{r}_1 - \Delta \mathbf{r}_2).\mathbf{e}_{12_o}\ \mathbf{e}_{12_o}$$

$$
\begin{aligned}
&+ \quad (\Delta \mathbf{r}_1 - \Delta \mathbf{r}_2).\mathbf{f}_{12_o}\ \mathbf{f}_{12_o} \\
&+ \quad (\Delta \mathbf{r}_1 - \Delta \mathbf{r}_2).\mathbf{g}_{12_o}\ \mathbf{g}_{12_o} \\
&= \quad \Delta\rho_o \mathbf{e}_{12_o} \\
&+ \quad (\Delta \mathbf{r}_1 - \Delta \mathbf{r}_2).\mathbf{f}_{12_o}\ \mathbf{f}_{12_o} \\
&+ \quad (\Delta \mathbf{r}_1 - \Delta \mathbf{r}_2).\mathbf{g}_{12_o}\ \mathbf{g}_{12_o}. \qquad (4.2.17)
\end{aligned}
$$

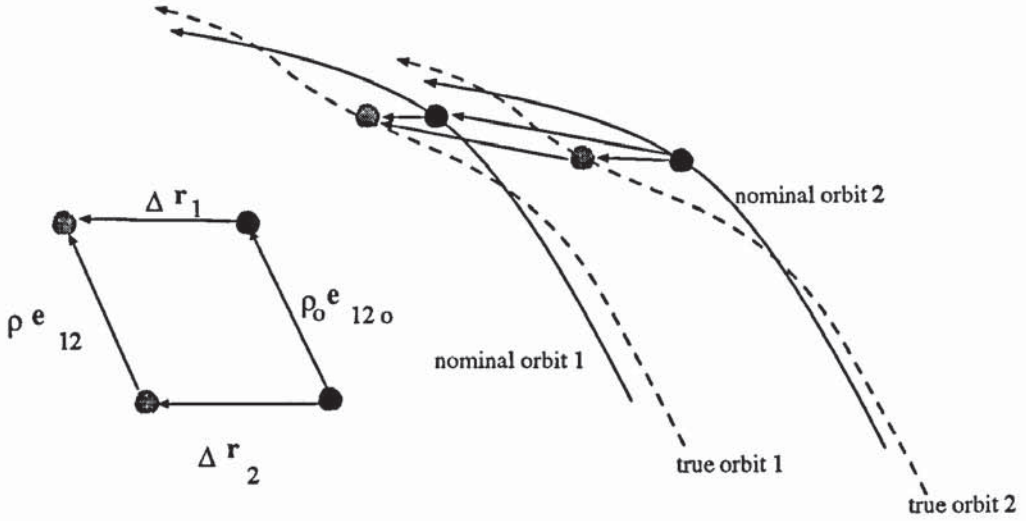

Figure 4.2.2

The true and nominal orbits

Thus for (4.2.16) and (4.2.17)

$$
\begin{aligned}
\rho \mathbf{e}_{12} &= (\rho_o + \Delta\rho_o)\mathbf{e}_{12_o} \\
&+ \quad (\Delta \mathbf{r}_1 - \Delta \mathbf{r}_2).\mathbf{f}_{12_o}\ \mathbf{f}_{12_o} \\
&+ \quad (\Delta \mathbf{r}_1 - \Delta \mathbf{r}_2).\mathbf{g}_{12_o}\ \mathbf{g}_{12_o}. \qquad (4.2.18)
\end{aligned}
$$

Dividing (4.2.18) by ρ gives

$$
\begin{aligned}
\mathbf{e}_{12} &= \mathbf{e}_{12_o} \\
&+ \quad \frac{1}{\rho}(\Delta \mathbf{r}_1 - \Delta \mathbf{r}_2).\mathbf{f}_{12_o}\ \mathbf{f}_{12_o} \\
&+ \quad \frac{1}{\rho}(\Delta \mathbf{r}_1 - \Delta \mathbf{r}_2).\mathbf{g}_{12_o}\ \mathbf{g}_{12_o}. \qquad (4.2.19)
\end{aligned}
$$

On taking the scalar product of (4.2.19) with the relative velocity of the satellites it can easily be shown that the difference between the range rate along the nominal and true satellite to satellite vectors is

$$\begin{aligned}(\dot{\mathbf{r}}_1 - \dot{\mathbf{r}}_2).(\mathbf{e}_{12} - \mathbf{e}_{12_o}) &= \frac{1}{\rho}(\Delta\mathbf{r}_1 - \Delta\mathbf{r}_2).\mathbf{f}_{12_o}\ \mathbf{f}_{12_o}.(\dot{\mathbf{r}}_{1_o} - \dot{\mathbf{r}}_{2_o}) \\ &+ \frac{1}{\rho}(\Delta\mathbf{r}_1 - \Delta\mathbf{r}_2).\mathbf{g}_{12_o}\ \mathbf{g}_{12_o}.(\dot{\mathbf{r}}_{1_o} - \dot{\mathbf{r}}_{2_o}). \quad (4.2.20)\end{aligned}$$

Comparing (4.2.20) with (4.2.15) illustrates the source of the second and third terms; namely the contribution to the mismodelling of the line of sight relative velocity from orbit errors affecting the line of sight.

In practice, (4.2.15) would be integrated along the paths $\mathbf{r}_{1_o}, \mathbf{r}_{2_o}$ which are determined by the nominal values of the parameters. In an analytical study however this is implausible and one must use nominal values for the paths which, whilst being close to the actual orbits, do not impede the elicitation of a simple solution to the problem. In the case under consideration where both satellites follow nearly circular paths one can consider three possible ways to simplify the orbital motion:-

- The motion can be approximated by creating an orbital path which varies from the circular in a periodical fashion. This method was employed by (Colombo, 1984) using a 9^{th} order zonal field. The orbit had additional symmetry about the point of highest latitude and was obtained by varying the initial state to converge the path using certain constraints.This is an accurate orbit and yet still allows for efficient gravity recovery. Hill's equations are then used to form the partials.

- A precessing ellipse is used and the Lagrange planetary equations employed (Wagner, 1983), (Kaula, 1983).

- A circular nominal orbit may be sufficient using Hill's equations again for the partials. (Wiejak W., 1990).

For the problem set out in this thesis, that is to make a comparative study of possible missions, it is considered unnecessary to use any but the most efficient and simplest models, namely a circular orbit. This is not inaccurate because of the near circularity of the desired orbits.

In the following it will be assumed that the nominal orbits are circular and (4.2.15) will be developed using the solutions to Hill's equations. Before this can be done however, it is necessary to study the relative motion of the satellites and how this affects the partials.

4.3 Frames of Reference

It appears that with equation (4.2.15) and the solutions to Hill's equations it should be possible to write down an explicit form for the partials $\frac{\partial RR}{\partial c_{lm\alpha}}$. It is important however not to ignore the question of reference frames, particularly when the satellites are not in the same orbital plane.

Suppose the components of the position vector of satellite 1 in the local frames 1 and 2 are denoted $(\mathbf{r}_1)_1, (\mathbf{r}_1)_2$ respectively. Similarly define the components of the trailing spacecraft's position vector by $(\mathbf{r}_2)_1, (\mathbf{r}_2)_2$. As long as both frames share the same origin,the geocentre, then these components are related by the rotation matrices $\mathbf{R}_{12}, \mathbf{R}_{21}$ as follows

$$\begin{aligned} (\mathbf{r}_\beta)_1 &= \mathbf{R}_{12}.(\mathbf{r}_\beta)_2 \\ (\mathbf{r}_\beta)_2 &= \mathbf{R}_{21}.(\mathbf{r}_\beta)_1 \end{aligned} \tag{4.3.1}$$

where $\beta = 1, 2$

In order to obtain these matrices it is necessary to refer both systems to a common reference frame. The relationships between the coordinates of a point in the common frame and the two local frames are obtained, and then used to connect the two local frames. For the reference frame an inertial system is chosen, with

the coordinates of some arbitrary point given by (X_I, Y_I, Z_I). The X_I axis points towards the first point of Aries, the Z_I axis points towards the north pole and the Y_I axis is defined such that X_I, Y_I, Z_I form a right handed orthogonal triplet.

To transform between these coordinates and the local coordinates relative to satellite β a sequence of basic rotations is performed (Kaula, 1966)

- An anti clockwise (positive) rotation about the Z (third) axis through an angle Ω_β ,so that the new X axis points towards the ascending node of the orbit of satellite β and is therefore in the orbital plane.

- An anti clockwise rotation about the X (first) axis through the angle I_β which is the inclination of the orbit. The new Z and Y axes are now normal to and in the orbital plane respectively.

- An anti clockwise rotation about this new Z axis through the angle $F_\beta - \pi/2$ so the Y axis (which is renamed the w axis) is pointing towards the satellite and the new X (v) axis is pointing against the direction of motion. The Z axis is relabelled u.

The final system is represented by (v, w, u) and

$$\begin{aligned}(\mathbf{r})_\beta &= \begin{pmatrix} v \\ w \\ u \end{pmatrix}_\beta = \mathbf{R}_3(F_\beta - \pi/2).\mathbf{R}_1(I_\beta).\mathbf{R}_3(\Omega_\beta).\begin{pmatrix} X_I \\ Y_I \\ Z_I \end{pmatrix} \\ &= \mathbf{R}_{\beta I}\,(\mathbf{r})_I \end{aligned} \tag{4.3.2}$$

or inversely

$$\begin{aligned}(\mathbf{r})_I &= \begin{pmatrix} X_I \\ Y_I \\ Z_I \end{pmatrix} = \mathbf{R}_3(-\Omega_\beta).\mathbf{R}_1(-I_\beta).\mathbf{R}_3(-F_\beta + \pi/2).\begin{pmatrix} v \\ w \\ u \end{pmatrix}_\beta \\ &= \mathbf{R}_{I\beta}\,(\mathbf{r})_\beta\,. \end{aligned} \tag{4.3.3}$$

Using these relationships the position components of a satellite in frame 1 relative to frame 2 can be described, namely

$$
\begin{aligned}
(\mathbf{r}_\beta)_1 &= \begin{pmatrix} v_\beta \\ w_\beta \\ u_\beta \end{pmatrix}_1 \\
&= \mathbf{R}_3(F_1 - \pi/2).\mathbf{R}_1(I_1).\mathbf{R}_3(\Omega_1) \\
&\quad . \ \mathbf{R}_3(-\Omega_2).\mathbf{R}_1(-I_2).\mathbf{R}_3(-F_2 + \pi/2). \begin{pmatrix} v_\beta \\ w_\beta \\ u_\beta \end{pmatrix}_2 \\
&= \mathbf{R}_{12}.(\mathbf{r}_\beta)_2 \qquad (4.3.4)
\end{aligned}
$$

the inverse relationship

$$
\begin{aligned}
(\mathbf{r}_\beta)_2 &= \begin{pmatrix} v_\beta \\ w_\beta \\ u_\beta \end{pmatrix}_2 \\
&= \mathbf{R}_3(F_2 - \pi/2).\mathbf{R}_1(I_2).\mathbf{R}_3(\Omega_2) \\
&\quad . \ \mathbf{R}_3(-\Omega_1).\mathbf{R}_1(-I_1).\mathbf{R}_3(-F_1 + \pi/2). \begin{pmatrix} v_\beta \\ w_\beta \\ u_\beta \end{pmatrix}_1 \\
&= \mathbf{R}_{21}.(\mathbf{r}_\beta)_1. \qquad (4.3.5)
\end{aligned}
$$

From (4.3.4) and (4.3.5) and from the properties of orthogonal transformations one can see that $\mathbf{R}_{21} = \mathbf{R}_{12}^T$. In equation (4.3.4) which defines $\mathbf{R}_{12}$ the ordering of the rows is negative along track, radial and cross track for 1,2,3 respectively. The rows of the matrices are reordered to be consistent with the notation of chapter 2 where 1,2,3 are u, v, w respectively. Therefore a cyclic permutation of the rows of the matrices is performed so that row 1 becomes row 2, row 2 becomes row 3, and row 3 becomes row 1.

Since the choice of reference frame to describe the partials is arbitrary, a choice can be made based on the simplicity of the algebra. When the satellites are in the same orbital plane so that $\Omega_1 = \Omega_2, I_1 = I_2$ then

$$\mathbf{R}_{12} = \mathbf{R}_3(F_1 - F_2) = \mathbf{R}_{21}^T. \tag{4.3.6}$$

Thus the transformations are time independent as the reference frames do not move with respect to each other. Further any comoving, coplanar frame will essentially have as simple a representation as any other.

For the solution under consideration where the satellites are not coplanar it is considered simpler to choose the frame in which to describe (4.2.15) as one of the local frames of the satellites. The leading satellite's frame is chosen arbitrarily.

On differentiating equation (4.3.4) with respect to time with $\beta = 2$ one gets the velocity components of satellite 2 relative to the local frame of satellite 1, ie

$$(\dot{\mathbf{r}_2})_1 = \mathbf{R}_{12}.(\dot{\mathbf{r}_2})_2 + \dot{\mathbf{R}}_{12}.(\mathbf{r}_2)_2 \tag{4.3.7}$$

and taking partial derivatives with respect to the $c_{lm\alpha}$

$$\left(\frac{\partial \dot{\mathbf{r}}_2}{\partial c_{lm\alpha}}\right)_1 = \mathbf{R}_{12}.\left(\frac{\partial \dot{\mathbf{r}}_2}{\partial c_{lm\alpha}}\right)_2 + \dot{\mathbf{R}}_{12}.\left(\frac{\partial \mathbf{r}_2}{\partial c_{lm\alpha}}\right)_2. \tag{4.3.8}$$

The first terms in (4.3.7) and (4.3.8) are the velocity components of satellite 2 or the velocity sensitivity to $c_{lm\alpha}$ as measured in its own local frame, with these components transformed to the local frame of the leading satellite .As will become clear it is immaterial which frame this terms components are expressed in as long as the correct choice of basis vectors are used to form the scalar products with $\mathbf{e}_{12}, \mathbf{f}_{12}, \mathbf{g}_{12}$. The second terms in (4.3.7) and (4.3.8) are related to the relative velocity of frames 1 and 2. If the planar case is considered then $\dot{\mathbf{R}}_{12}$ is zero so this term drops out. In the non-planar case both $\mathbf{R}_{12}$ and $\dot{\mathbf{R}}_{12}$ have complicated forms and in order to use (4.2.15) simplifications must be made to ease this problem.

First however (4.2.15) is rewritten with the new notation, and in the local frame of satellite 1 as

$$\begin{aligned}\frac{\partial RR_o}{\partial c_{lm\alpha}} &= \left(\left(\frac{\partial \dot{\mathbf{r}}_{1_o}}{\partial c_{lm\alpha}}\right)_1 - \left(\frac{\partial \dot{\mathbf{r}}_{2_o}}{\partial c_{lm\alpha}}\right)_1\right).(\mathbf{e}_{12_o})_1 \\ &+ \frac{1}{\rho_o}((\dot{\mathbf{r}}_{1_o})_1 - (\dot{\mathbf{r}}_{2_o})_1).(\mathbf{f}_{12_o})_1\left(\left(\frac{\partial \mathbf{r}_{1_o}}{\partial c_{lm\alpha}}\right)_1 - \left(\frac{\partial \mathbf{r}_{2_o}}{\partial c_{lm\alpha}}\right)_1\right).(\mathbf{f}_{12_o})_1 \\ &+ \frac{1}{\rho_o}((\dot{\mathbf{r}}_{1_o})_1 - (\dot{\mathbf{r}}_{2_o})_1).(\mathbf{g}_{12_o})_1\left(\left(\frac{\partial \mathbf{r}_{1_o}}{\partial c_{lm\alpha}}\right)_1 - \left(\frac{\partial \mathbf{r}_{2_o}}{\partial c_{lm\alpha}}\right)_1\right).(\mathbf{g}_{12_o})_1 \cdot\end{aligned} \tag{4.3.9}$$

The first simplification in (4.3.9) is to assume that the satellites both move in circular nominal orbits. This implies that both $(\dot{\mathbf{r}}_{1_o})_1$ and $(\dot{\mathbf{r}}_{2_o})_2$ are zero since the nominal position of a satellite will be stationary in its local frame. From (4.3.7)

$$(\dot{\mathbf{r}_2})_1 = \dot{\mathbf{R}}_{12}.(\mathbf{r}_2)_2. \tag{4.3.10}$$

The position vector $(\mathbf{r}_2)_2$, from the above assumption, can be written as

$$(\mathbf{r}_2)_2 = \begin{pmatrix} 0 \\ 0 \\ r_o \end{pmatrix} \tag{4.3.11}$$

in frame 2. In (4.3.11) $\mathbf{h}_{i\beta}, i = 1,2,3; \beta = 1,2$ denote the basis vectors in frame β in the directions i=1,2,3 (cross track, minus along track and radial respectively) and r_o is the common orbital height of the spacecraft .

On using (4.3.10) and (4.3.11)

$$\begin{aligned}(\dot{\mathbf{r}}_2)_1 &= r_o\dot{\mathbf{R}}_{12}.\begin{pmatrix} 0 \\ 0 \\ 1 \end{pmatrix} \\ &= r_o\sum_{i=1}^{3}\left(\dot{\mathbf{R}}_{12}\right)_{i3}\mathbf{h}_{i1}\end{aligned} \tag{4.3.12}$$

whilst

$$(\dot{\mathbf{r}}_1)_1 = 0 \tag{4.3.13}$$

in frame 1. Further substituting

$$\left(\frac{\partial \mathbf{r}_2}{\partial c_{lm\alpha}}\right)_1 = \mathbf{R}_{12}.\left(\frac{\partial \mathbf{r}_2}{\partial c_{lm\alpha}}\right)_2 \tag{4.3.14}$$

and (4.3.8) in (4.3.9), achieves

$$\begin{aligned}
\frac{\partial RR_o}{\partial c_{lm\alpha}} &= \left(\frac{\partial \dot{\mathbf{r}}_{1_o}}{\partial c_{lm\alpha}}\right)_1 . (\mathbf{e}_{12_o})_1 - \left[\mathbf{R}_{12}\left(\frac{\partial \dot{\mathbf{r}}_{2_o}}{\partial c_{lm\alpha}}\right)_2\right] . (\mathbf{e}_{12_o})_1 \\
&- \left[\dot{\mathbf{R}}_{12}\left(\frac{\partial \mathbf{r}_{2_o}}{\partial c_{lm\alpha}}\right)_2\right] . (\mathbf{e}_{12_o})_1 \\
&- \frac{r_o}{\rho_o}\left[\sum_{i=1}^{3}\left(\dot{\mathbf{R}}_{12}\right)_{i3}\mathbf{h}_{i1}\right] . (\mathbf{f}_{12_o})_1 \left[\left(\frac{\partial \mathbf{r}_{1_o}}{\partial c_{lm\alpha}}\right)_1 - \mathbf{R}_{12}\left(\frac{\partial \mathbf{r}_{2_o}}{\partial c_{lm\alpha}}\right)_2\right] . (\mathbf{f}_{12_o})_1 \\
&- \frac{r_o}{\rho_o}\left[\sum_{i=1}^{3}\left(\dot{\mathbf{R}}_{12}\right)_{i3}\mathbf{h}_{i1}\right] . (\mathbf{g}_{12_o})_1 \left[\left(\frac{\partial \mathbf{r}_{1_o}}{\partial c_{lm\alpha}}\right)_1 - \mathbf{R}_{12}\left(\frac{\partial \mathbf{r}_{2_o}}{\partial c_{lm\alpha}}\right)_2\right] . (\mathbf{g}_{12_o})_1 .
\end{aligned} \tag{4.3.15}$$

Equation (4.3.15) enables the partials to be written in terms of the solutions to Hill's equations which are the sensitivities of the motions in a spacecraft's own local frame.

Recall from chapter 3 that the solutions to Hill's equations are defined in the satellites local frame so are expressed in the form

$$\left(\frac{\partial \mathbf{r}_{\beta_o}}{\partial c_{lm\alpha}}\right)_\beta = \sum_{i=1}^{3}\frac{\partial x_{i\beta_o}}{\partial c_{lm\alpha}}\mathbf{h}_{i\beta} \tag{4.3.16}$$

and

$$\left(\frac{\partial \dot{\mathbf{r}}_{\beta_o}}{\partial c_{lm\alpha}}\right)_\beta = \sum_{i=1}^{3}\frac{\partial \dot{x}_{i\beta_o}}{\partial c_{lm\alpha}}\mathbf{h}_{i\beta}. \tag{4.3.17}$$

Each of the terms in equation (4.3.15) requires that one takes the scalar products of the basis vectors $\mathbf{h}_{i\beta}$ with one of the $\mathbf{e}_{12_o}, \mathbf{f}_{12_o}, \mathbf{g}_{12_o}$ system of vectors. As it stands the basis vectors used for each term would be the h_{i1}. That is the basis vectors of satellite 1's local frame. However it is not necessary to describe each

term with respect to the same basis vectors. In some terms it may be more efficient algebraically to express the components with respect to the trailing satellites local frame. The burden of consistency for each term is shifted to the requirement that the vectors that make up the scalar product in those terms are defined in the same reference frame.

With this in mind Equation (4.3.15) is rewritten, using (4.3.16), (4.3.17)

$$\begin{aligned}\frac{\partial RR_o}{\partial c_{lm\alpha}} &= \sum_{i=1}^{3}\left[\frac{\partial \dot{x}_{i1}}{\partial c_{lm\alpha}}\left(\mathbf{h}_{i1}.\mathbf{e}_{12_o}\right)_F - \frac{\partial \dot{x}_{i2}}{\partial c_{lm\alpha}}\left(\mathbf{h}_{i2}.\mathbf{e}_{12_o}\right)_F\right. \\ &- \left[\sum_{j=1}^{3}\left[\dot{\mathbf{R}}_{12}\right]_{ij}\left(\mathbf{h}_{i1}.\mathbf{e}_{12_o}\right)_F\frac{\partial x_{j2}}{\partial c_{lm\alpha}}\right] \\ &- \frac{r_o}{\rho_o}\left[\sum_{j=1}^{3}\left(\dot{\mathbf{R}}_{12}\right)_{j3}\left(\mathbf{h}_{j1}.\mathbf{f}_{12_o}\right)_F\right]\left(\frac{\partial x_{i1}}{\partial c_{lm\alpha}}\left(\mathbf{h}_{i1}.\mathbf{f}_{12_o}\right)_F - \frac{\partial x_{i2}}{\partial c_{lm\alpha}}\left(\mathbf{h}_{i2}.\mathbf{f}_{12_o}\right)_F\right) \\ &- \left.\frac{r_o}{\rho_o}\left[\sum_{j=1}^{3}\left(\dot{\mathbf{R}}_{12}\right)_{j3}\left(\mathbf{h}_{j1}.\mathbf{g}_{12_o}\right)_F\right]\left(\frac{\partial x_{i1}}{\partial c_{lm\alpha}}\left(\mathbf{h}_{i1}.\mathbf{g}_{12_o}\right)_F - \frac{\partial x_{i2}}{\partial c_{lm\alpha}}\left(\mathbf{h}_{i2}.\mathbf{g}_{12_o}\right)_F\right)\right]. \end{aligned} \tag{4.3.18}$$

where the subscript F on the scalar products indicates that they are calculated in some arbitrary reference frame.

If the following notation is introduced for the scalars

$$V_f = -\frac{r_o}{\rho_o}\sum_{i=1}^{3}\left[\dot{\mathbf{R}}_{12}\right]_{i3}\left(\mathbf{h}_{i1}.\mathbf{f}_{12_o}\right)_F \tag{4.3.19}$$

and

$$V_g = -\frac{r_o}{\rho_o}\sum_{i=1}^{3}\left[\dot{\mathbf{R}}_{12}\right]_{i3}\left(\mathbf{h}_{i1}.\mathbf{g}_{12_o}\right)_F \tag{4.3.20}$$

and the matrix

$$V_{ij} = \left[\dot{\mathbf{R}}_{12}\right]_{ij}\left(\mathbf{h}_{i1}.\mathbf{e}_{12_o}\right)_F \tag{4.3.21}$$

then (4.3.18) can be written

$$\frac{\partial RR_o}{\partial c_{lm\alpha}} = \sum_{i=1}^{3}\left[\sum_{\beta=1}^{2}(-1)^{\beta-1}\left(\frac{\partial \dot{x}_{i\beta_o}}{\partial c_{lm\alpha}}\left(\mathbf{h}_{i\beta}.\mathbf{e}_{12_o}\right)_F\right.\right.$$

$$+ \quad \frac{\partial x_{i\beta_o}}{\partial c_{lm\alpha}} \left[V_f \left(\mathbf{h}_{i\beta} . \mathbf{f}_{12_o} \right)_F + V_g \left(\mathbf{h}_{i\beta} . \mathbf{g}_{12_o} \right)_F \right] \Bigg) + \sum_{j=1}^{3} V_{ij} \frac{\partial x_{j2_o}}{\partial c_{lm\alpha}} \Bigg]$$

$$= \sum_{i=1}^{3} \Bigg[\sum_{\beta=1}^{2} (-1)^{\beta-1} \left(\frac{\partial \dot{x}_{i\beta_o}}{\partial c_{lm\alpha}} \left(\mathbf{h}_{i\beta} . \mathbf{e}_{12_o} \right)_F + \frac{\partial x_{i\beta_o}}{\partial c_{lm\alpha}} \left[V_{X,i\beta} \right] \right)$$

$$+ \quad \sum_{j=1}^{3} V_{ij} \frac{\partial x_{j2_o}}{\partial c_{lm\alpha}} \Bigg] \tag{4.3.22}$$

where

$$V_{X,i\beta} = V_f \left(\mathbf{h}_{i\beta} . \mathbf{f}_{12_o} \right)_F + V_g \left(\mathbf{h}_{i\beta} . \mathbf{g}_{12_o} \right)_F . \tag{4.3.23}$$

In order to arrive at a usable form for equation (4.3.22) the following must be modelled:-

- The nine elements of the matrix V_{ij}
- Six terms $V_{X,i\beta}$
- The scalar products $\mathbf{h}_{i\beta} . \mathbf{e}_{12_o}$

and in order to calculate these , $\mathbf{h}_{i\beta} . \mathbf{f}_{12_o}, \mathbf{h}_{i\beta} . \mathbf{g}_{12_o}$ and the elements of $\dot{\mathbf{R}}_{12}$ must also be modelled.

The scalar products are always frame invariant. This is very useful in calculating them because it means that all of the above can be approximated using only the transformation matrices defined in (4.3.2) and (4.3.3), ie

$$\mathbf{R}_{I\beta} = \mathbf{R}_3(-\Omega_\beta) . \mathbf{R}_1(-I_\beta) . \mathbf{R}_3(-F_\beta + \pi/2) \tag{4.3.24}$$

$$\mathbf{R}_{\beta I} = \mathbf{R}_3(F_\beta - \pi/2) . \mathbf{R}_1(I_\beta) . \mathbf{R}_3(\Omega_\beta), \ \beta = 1, 2 \tag{4.3.25}$$

and their derivatives.

First however $\mathbf{f}_{12_o}$ and $\mathbf{g}_{12_o}$ must be defined and then along with $\mathbf{e}_{12_o}$ written in terms of the basis vectors.These vectors form an orthonormal triad and $\mathbf{e}_{12_o}$ points from the trailing satellite to the leading one so this can be written

$$\mathbf{e}_{12_o} = \frac{r_o \left(\mathbf{h}_{31} - \mathbf{h}_{32} \right)}{\left| r_o \left(\mathbf{h}_{31} - \mathbf{h}_{32} \right) \right|}$$

$$= \frac{(\mathbf{h}_{31} - \mathbf{h}_{32})}{|(\mathbf{h}_{31} - \mathbf{h}_{32})|}. \tag{4.3.26}$$

The vectors $\mathbf{f}_{12_o}$ and $\mathbf{g}_{12_o}$ are arbitrarily defined in the plane perpendicular to $\mathbf{e}_{12_o}$ but since frame 1 is being used as the reference frame, define

$$\mathbf{f}_{12_o} = \frac{(\mathbf{h}_{31} \times \mathbf{e}_{12_o})}{|\mathbf{h}_{31} \times \mathbf{e}_{12_o}|} \tag{4.3.27}$$

and

$$\mathbf{g}_{12_o} = (\mathbf{e}_{12_o} \times \mathbf{f}_{12_o}) \tag{4.3.28}$$

Now because the scalar products are frame invariant, they are all calculated in the previously defined inertial frame I. From equation (4.3.3) the components of the basis vectors can be calculated in this inertial frame using $\mathbf{R}_{I\beta}$

$$(\mathbf{h}_{i\beta})_I = \mathbf{R}_{I\beta}\,(\mathbf{h}_{i\beta})_\beta \tag{4.3.29}$$

Thus the j^{th} element of $(\mathbf{h}_{i\beta})_I$ is the element of $\mathbf{R}_{I\beta}$ in the j^{th} row and i^{th} column. In this manner all basis vectors are calculated in the Inertial frame.

Explicitly, the components of the basis vectors in the inertial frame are given by elements of the transformation matrices.

$$\left[(\mathbf{h}_{i\beta})_I\right]_j = [\mathbf{R}_{I\beta}]_{ji} \tag{4.3.30}$$

From these elements the components of the nominal satellite to satellite vectors $\mathbf{e}_{12_o}$,$\mathbf{f}_{12_o}$ and $\mathbf{g}_{12_o}$ in the inertial frame I can be calculated from (4.3.26), (4.3.27) and (4.3.28) respectively. Once all nine of the unit vectors have been calculated in the inertial frame it is a simple procedure to form the scalar products $\mathbf{h}_{i\beta}.\mathbf{e}_{12_o}$,$\mathbf{h}_{i\beta}.\mathbf{f}_{12_o}$ and $\mathbf{h}_{i\beta}.\mathbf{g}_{12_o}$.

As for the elements of the matrix V_{ij} and the six elements labelled $V_{X,i\beta}$, these are given in terms of the scalar products and the elements of the matrix which transforms between the two satellites local frames $\left[\dot{\mathbf{R}}_{12}\right]_{ij}$ in equations (4.3.19), (4.3.20), (4.3.21) and (4.3.23). This matrix is the derivative of,

$$\mathbf{R}_{12} = \mathbf{R}_{1I}.\mathbf{R}_{I2} \tag{4.3.31}$$

and so can be written

$$\dot{\mathbf{R}}_{12} = \dot{\mathbf{R}}_{1I}.\mathbf{R}_{I2} + \mathbf{R}_{1I}.\dot{\mathbf{R}}_{I2} \tag{4.3.32}$$

which in elemental form is

$$\left[\dot{\mathbf{R}}_{12}\right]_{ij} = \sum_{k=1}^{3} \left[\dot{\mathbf{R}}_{1I}\right]_{ik} \left[\mathbf{R}_{I2}\right]_{kj} + \left[\mathbf{R}_{1I}\right]_{ik} \left[\dot{\mathbf{R}}_{I2}\right]_{kj}. \tag{4.3.33}$$

Hence all the required products and functions in (4.3.22) which link the solutions to Hill's equations in the two different frames to the scalar values of the range rate partials can, in theory, be formed from the products of different elements of the matrices $\mathbf{R}_{\beta I}$, their inverses $\mathbf{R}_{I\beta}$ and the derivatives of these matrices.

The problem with this method is the tremendous amount of tedious algebraic manipulations that would be required to arrive at forms for all the functions needed. A much more efficient way of approximating the elements is to numerically calculate a time series for each. This cannot be used in the analytical formulae directly so each required product's or element's time series is solved by least squares for the dominant constant and periodic terms.

Equations (4.3.24) and (4.3.25) give the matrices required in terms of three basic angles,Ω_β,I_β and F_β. Thus to derive the elements of $\mathbf{R}_{I\beta}$ and its derivatives, for example (4.3.24) is used and the elements of these matrices are evaluated at time intervals dt using a choice of initial values of $I_\beta, F_\beta, \Omega_\beta$ and using constant values for the gradients so that the p^{th} value of the angles are

$$I_\beta(t_o + p.dt) = I_0 \tag{4.3.34}$$

$$F_\beta(t_o + p.dt) = F_{\beta,0} + \dot{F}.p.dt \tag{4.3.35}$$

$$\Omega_\beta(t_o + p.dt) = \Omega_{\beta,0} + \dot{\Omega}.p.dt \tag{4.3.36}$$

where $p = 0, 1, ..., N_p - 1$ (Engelis, 1987), (Wiejak W., 1990). The satellites have the same values for their basic frequencies $\dot{F}, \dot{\Omega}$ and therefore the same inclination.

The elements of the matrices can now be calculated at successive time steps and are written $[\mathbf{R}_{\beta I}]^p_{ij}$,$[\mathbf{R}_{I\beta}]^p_{ij}$ $\left[\dot{\mathbf{R}}_{\beta I}\right]^p_{ij}$,$\left[\dot{\mathbf{R}}_{I\beta}\right]^p_{ij}$ where $\beta = 1, 2$; $p = 0, 1, 2, .., N_p -$

$1; i, j = 1, 2, 3$. As described earlier the scalar products can now be formed at each time step. For example $\mathbf{e}_{12_o}.\mathbf{h}_{i\beta}$

$$\begin{aligned}(\mathbf{e}_{12_o}.\mathbf{h}_{i\beta})^p &= \left[\frac{(\mathbf{h}_{31}-\mathbf{h}_{32})}{|(\mathbf{h}_{31}-\mathbf{h}_{32})|}.\mathbf{h}_{i\beta}\right]^p \\ &= \frac{\sum_{j=1}^{3}\left([\mathbf{R}_{I1}]_{j3}^p - [\mathbf{R}_{I2}]_{j3}^p\right)[\mathbf{R}_{I\beta}]_{ji}^p}{\sqrt{\sum_{k=1}^{3}\left([\mathbf{R}_{I1}]_{k3}^p - [\mathbf{R}_{I2}]_{k3}^p\right)^2}} \end{aligned} \tag{4.3.37}$$

on using equations (4.3.26) and (4.3.30).The other scalar products are formed in the same way using (4.3.27), (4.3.28) with a value found at each time step.

From (4.3.19) and (4.3.32)

$$V_f = \frac{r_o}{\rho_o}\sum_{i=1}^{3}\left[\dot{\mathbf{R}}_{12}\right]_{i3}(\mathbf{h}_{i1}.\mathbf{f}_{12_o})$$

and

$$\begin{aligned}V_f^p &= \left(\frac{1}{\sqrt{\sum_{j=1}^{3}\left([\mathbf{R}_{I1}]_{j3}^p - [\mathbf{R}_{I2}]_{j3}^p\right)^2}}\right) \\ &\cdot \sum_{i=1}^{3}\sum_{k=1}^{3}\left(\left[\dot{\mathbf{R}}_{1I}\right]_{ik}^p[\mathbf{R}_{I2}]_{k3}^p + [\mathbf{R}_{1I}]_{ik}^p\left[\dot{\mathbf{R}}_{I2}\right]_{k3}^p\right)(\mathbf{h}_{i1}.\mathbf{f}_{12_o})^p \end{aligned} \tag{4.3.38}$$

with V_g^p found in the same way (replace the $\mathbf{f}_{12_o}$ above with $\mathbf{g}_{12_o}$). Using both these and the scalar products the elements $V_{X,i\beta}^p$ can be found, ie

$$V_{X,i\beta}^p = V_f^p(\mathbf{h}_{i\beta}.\mathbf{f}_{12_o})^p + V_g^p(\mathbf{h}_{i\beta}.\mathbf{g}_{12_o})^p \tag{4.3.39}$$

and finally

$$\begin{aligned}V_{ij} &= \left[\dot{\mathbf{R}}_{12}\right]_{ij}\mathbf{h}_{i1}.\mathbf{e}_{12_o} \\ V_{ij}^p &= \sum_{k=1}^{3}\left(\left[\dot{\mathbf{R}}_{1I}\right]_{ik}^p[\mathbf{R}_{I2}]_{kj}^p + [\mathbf{R}_{1I}]_{ik}^p\left[\dot{\mathbf{R}}_{I2}\right]_{kj}^p\right)(\mathbf{h}_{i1}.\mathbf{e}_{12_o})^p . \end{aligned} \tag{4.3.40}$$

Equations (4.3.37) and (4.3.40) are used to approximate their respective functions and scalar products and the results presented in Figures (4.3.1-4), first for coplanar satellites for the non zero scalar products and then for non coplanar satellites.Throughout a value of $r_o = 6600km$ and inclination 96.4° was assumed

whilst the initial angle values are given.The units on the time axes are numbers of revolutions and the value for the orbital period, T is approximated from Kepler's equation $n_o^2 r_o^3 = \mu$ namely

$$T = 2\pi\sqrt{\left(\frac{r_o^3}{\mu}\right)}. \tag{4.3.41}$$

For the planar case in Figure (4.3.1) only the along track and radial scalar products are non zero and the radial one is small. In fact their constant values are $-\cos(\Delta F)$ and $\sin(\Delta F)$ respectively where ΔF is the along track separation.

The non planar case exhibits large periodic variations in the along track scalar product with the satellite to satellite vector. Also a sinusoidal variation in the cross track scalar product is introduced. The terms $V_{X,i\beta}$ and V_{ij} for this non planar case are all small with the largest ones due to the effect of the cross track relative velocity of the satellites introducing cross track orbit error into the partials.

In the following sections the variations are all supposed to be harmonics of the orbital frequency, an observation supported by Figures (4.3.1) to (4.3.4). Furthermore although several terms are small all terms have been included in the analysis for completeness as their inclusion does not complicate the work significantly.

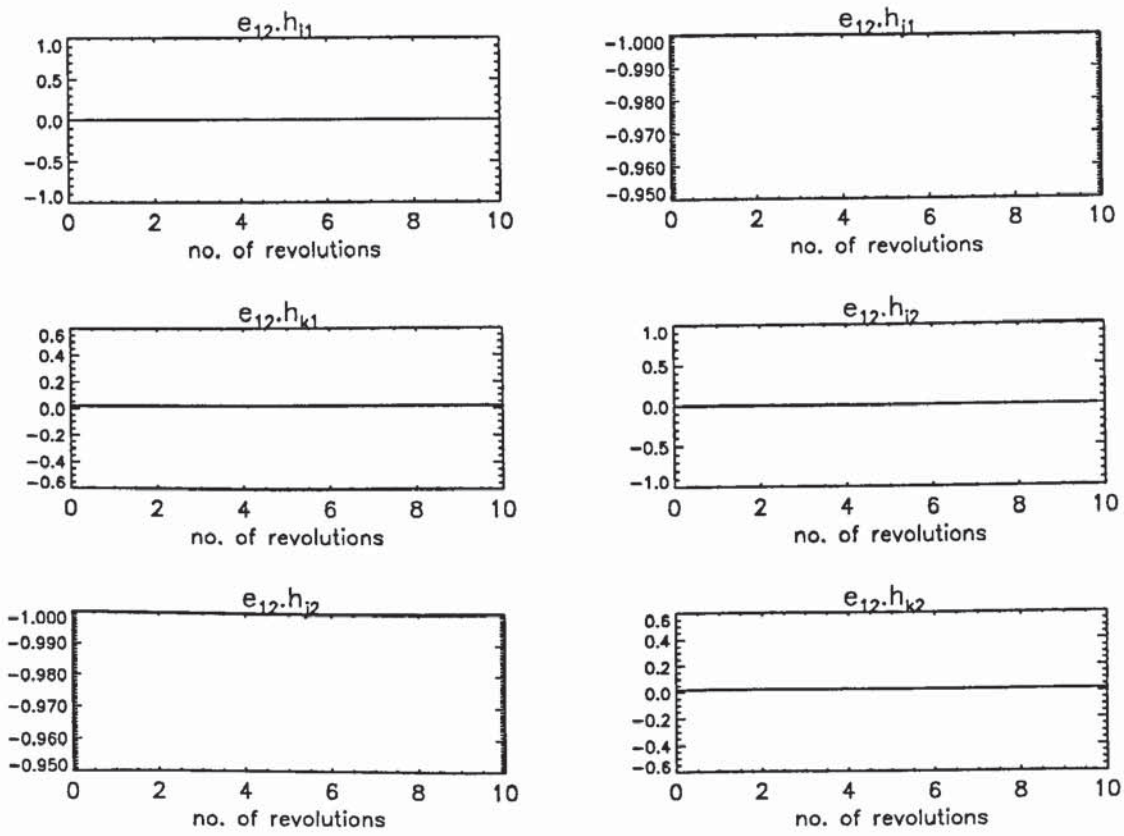

Figure 4.3.1 scalar products $(\mathbf{h}_{i\beta}.\mathbf{e}_{12_o})$.

Separation 2.4° along track satellites in same plane.

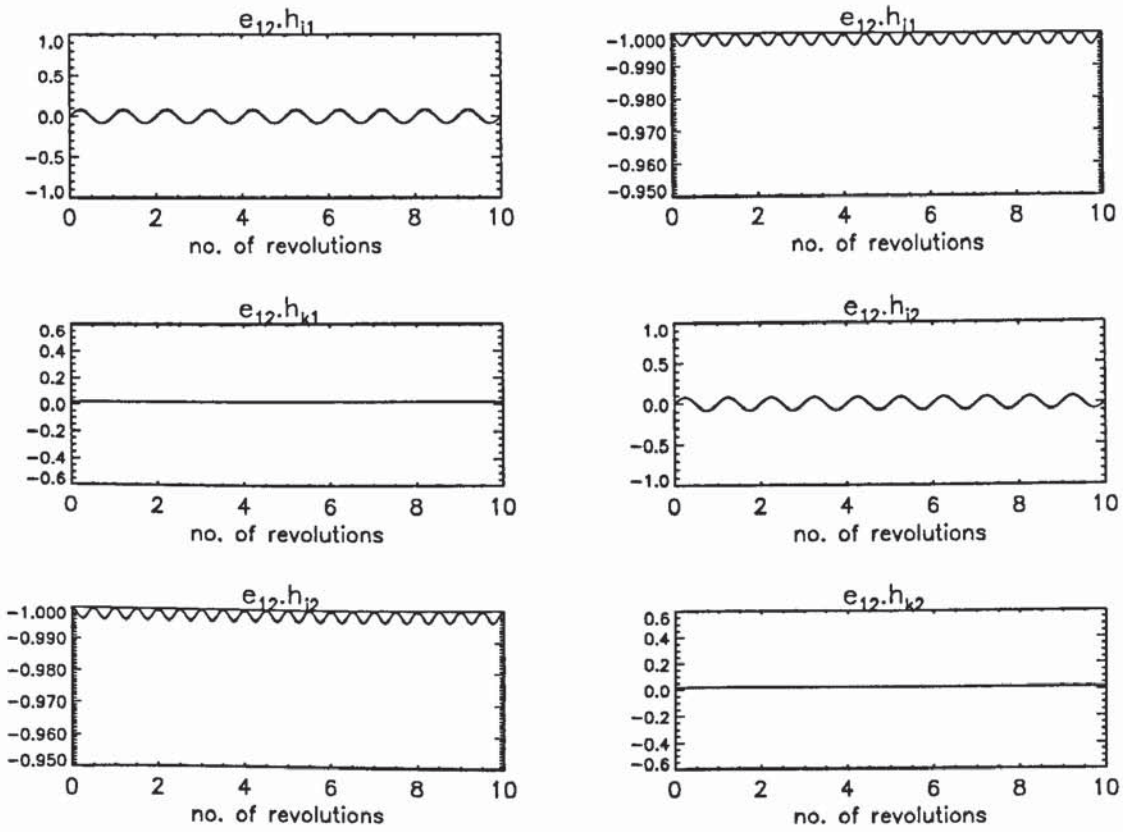

Figure 4.3.2 The scalar products $(\mathbf{h}_{i\beta}.\mathbf{e}_{12_o})$.

Separation 2.4° along track 0.2° in right ascension.

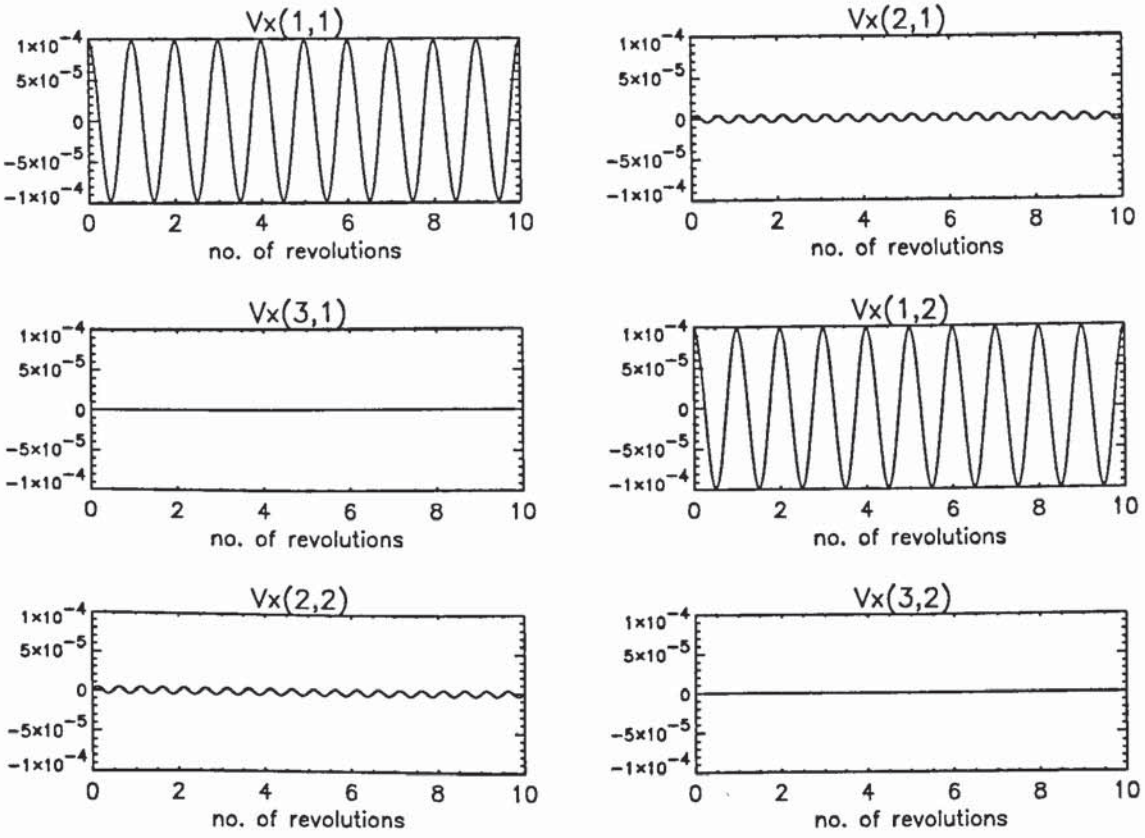

Figure 4.3.3 The functions $V_{X,i\beta}$.

Separation 2.4° along track 0.2° in right ascension.

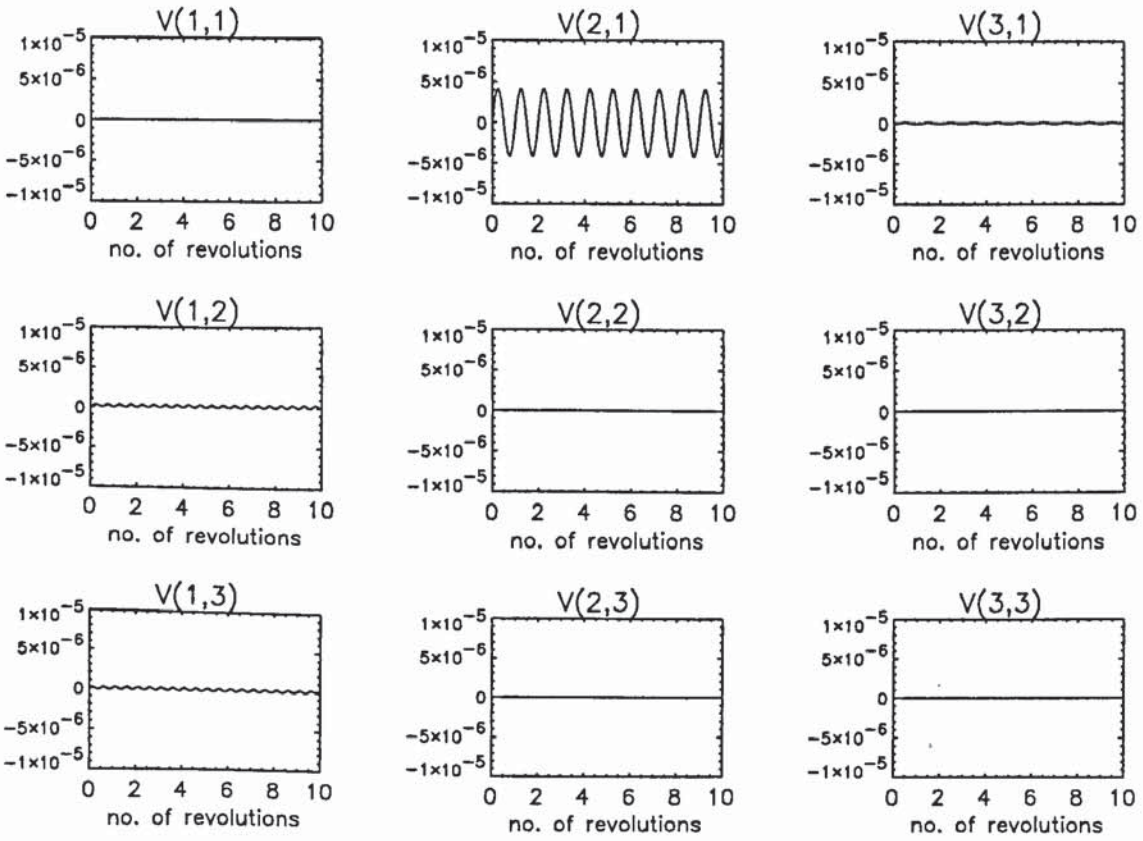

Figure 4.3.4 The elements of V_{ij}.

Separation 2.4° along track 0.2° in right ascension.

4.4 The signal equation

Based on the findings of the previous section the following approximations can reasonably be made:-

$$V_{X,i\beta} = \sum_{k=0}^{k_{max}} b_{i\beta,k}\cos\left(k\dot{F}t\right) + c_{i\beta,k}\sin\left(k\dot{F}t\right) \tag{4.4.1}$$

$$V_{ij} = \sum_{k=0}^{k_{max}} e_{ij,k}\cos\left(k\dot{F}t\right) + f_{ij,k}\sin\left(k\dot{F}t\right) \tag{4.4.2}$$

$$\mathbf{h}_{i\beta}.\mathbf{e}_{12_o} = \sum_{k=0}^{k_{max}} m_{i\beta,k}\cos\left(k\dot{F}t\right) + q_{i\beta,k}\sin\left(k\dot{F}t\right). \tag{4.4.3}$$

Using equation (3.5.4), namely

$$\begin{aligned}\frac{\partial x_{oi}}{\partial c_{lm\alpha}} &= \sum_{j=-l}^{l}\left[\mathcal{X}^i_{lm\alpha j}\cos\left(\dot{\psi}^i_{jm}t + \phi^i_{lm\alpha j}\right)\right] \\ &+ \left(\hat{C}^i_{lm\alpha} + \delta_{m0}\hat{D}^i_{l0\alpha}t\right)\cos\left(n_o t\right) + \left(\hat{E}^i_{lm\alpha} + \delta_{m0}\hat{F}^i_{l0\alpha}t\right)\sin\left(n_o t\right) \\ &+ \hat{G}^i_{lm\alpha}t + \hat{H}^i_{lm\alpha}\end{aligned} \tag{4.4.4}$$

it is possible to derive expressions for the sensitivities of the motions of both satellites. In the case considered here the spacecraft's orbits have the same height and inclination and therefore the same basic frequencies $\dot{F}$ and $\dot{\Omega}$. The only differences are in the initial values of the angles F and Ω (F_o and Ω_o). Therefore to indicate which satellite is under consideration the index $\beta = 1, 2$ is introduced to the phase angle $\phi^i_{lm\alpha j}$ in (4.4.4). Equation (4.4.4) is now written

$$\begin{aligned}\frac{\partial x_{i\beta_o}}{\partial c_{lm\alpha}} &= \sum_{j=-l}^{l}\left[\mathcal{X}^i_{lm\alpha j}\cos\left(\dot{\psi}^i_{jm}t + \phi^{i\beta_o}_{lm\alpha j}\right)\right] \\ &+ \left(\hat{C}^{i\beta}_{lm\alpha} + \delta_{m0}\hat{D}^{i\beta}_{l0\alpha}t\right)\cos\left(n_o t\right) + \left(\hat{E}^{i\beta}_{lm\alpha} + \delta_{m0}\hat{F}^{i\beta}_{l0\alpha}t\right)\sin\left(n_o t\right) \\ &+ \hat{G}^{i\beta}_{lm\alpha}t + \hat{H}^{i\beta}_{lm\alpha}\end{aligned} \tag{4.4.5}$$

Now using (4.4.5) one can write

$$\frac{\partial \dot{x}_{i\beta_o}}{\partial c_{lm\alpha}} = \sum_{j=-l}^{l}\left[A^{i\beta}_{lm\alpha j}\cos\left(\dot{\psi}^i_{jm}t\right) + B^{i\beta}_{lm\alpha j}\sin\left(\dot{\psi}^i_{jm}t\right)\right]$$

$$+ \left(C^{i\beta}_{lm\alpha} + \delta_{m0} D^{i\beta}_{l0\alpha} t\right) \cos\left(\dot{F}t\right) + \left(E^{i\beta}_{lm\alpha} + \delta_{m0} F^{i\beta}_{l0\alpha} t\right) \sin\left(\dot{F}t\right)$$
$$+ G^{i\beta}_{lm\alpha} \tag{4.4.6}$$

as the derivative of

$$\begin{aligned}\frac{\partial x_{i\beta_o}}{\partial c_{lm\alpha}} &= \sum_{j=-l}^{l} \left[\hat{A}^{i\beta}_{lm\alpha j} \cos\left(\dot{\psi}^{i}_{jm} t\right) + \hat{B}^{i\beta}_{lm\alpha j} \sin\left(\dot{\psi}^{i}_{jm} t\right)\right] \\ &+ \left(\hat{C}^{i\beta}_{lm\alpha} + \delta_{m0} \hat{D}^{i\beta}_{l0\alpha} t\right) \cos\left(\dot{F}t\right) + \left(\hat{E}^{i\beta}_{lm\alpha} + \delta_{m0} \hat{F}^{i\beta}_{l0\alpha} t\right) \sin\left(\dot{F}t\right) \\ &+ \hat{G}^{i\beta}_{lm\alpha} t + H^{i\beta}_{lm\alpha}, \end{aligned} \tag{4.4.7}$$

where

$$\begin{aligned} A^{i\beta}_{lm\alpha j} &= -\dot{\psi}^{i}_{jm} \mathcal{X}^{i}_{lmj} \sin\left(\phi^{i\beta}_{lm\alpha j}\right) \\ B^{i\beta}_{lm\alpha j} &= -\dot{\psi}^{i}_{jm} \mathcal{X}^{i}_{lmj} \cos\left(\phi^{i\beta}_{lm\alpha j}\right), \end{aligned}$$

and

$$\begin{aligned} \hat{A}^{i\beta}_{lm\alpha j} &= \mathcal{X}^{i}_{lmj} \cos\left(\phi^{i\beta}_{lm\alpha j}\right) \\ \hat{B}^{i\beta}_{lm\alpha j} &= -\mathcal{X}^{i}_{lmj} \sin\left(\phi^{i\beta}_{lm\alpha j}\right). \end{aligned}$$

$\phi^{i\beta}_{lm\alpha j}$ is given by

$$\phi^{i\beta}_{lm\alpha j} = \phi_{lm\alpha} + \psi^{i\beta_o}_{jm} + \frac{\pi}{2} \tag{4.4.8}$$

for i=1,2 and

$$\phi^{3\beta}_{lm\alpha j} = \phi_{lm\alpha} + \psi^{3\beta_o}_{jm} \tag{4.4.9}$$

where

$$\begin{aligned} \psi^{2\beta_o}_{jm} &= \psi^{3\beta_o}_{jm} = jF_{\beta_o} + m\left(\Omega_{\beta_o} - \theta_{G,o}\right) \\ \psi^{1\beta_o}_{jm} &= (j-1) F_{\beta_o} + m\left(\Omega_{\beta_o} - \theta_{G,o}\right). \end{aligned} \tag{4.4.10}$$

From (3.5.10)

$$\begin{aligned} \dot{\psi}^{2}_{jm} &= \dot{\psi}^{3}_{jm} = j\dot{F} + m\left(\dot{\Omega} - \dot{\theta}_G\right) \\ \dot{\psi}^{1}_{jm} &= (j-1)\dot{F} + m\left(\dot{\Omega} - \dot{\theta}_G\right) \end{aligned} \tag{4.4.11}$$

and so

$$\dot{\psi}^i_{jm} + k\dot{F} = \dot{\psi}^i_{j+km}. \tag{4.4.12}$$

Equation (4.3.22) namely

$$\begin{aligned}\frac{\partial RR_o}{\partial c_{lm\alpha}} &= \sum_{i=1}^{3}\left[\sum_{\beta=1}^{2}(-1)^{\beta-1}\left(\frac{\partial \dot{x}_{i\beta_o}}{\partial c_{lm\alpha}}\mathbf{h}_{i\beta}.\mathbf{e}_{12_o} + \frac{\partial x_{i\beta_o}}{\partial c_{lm\alpha}}V_{X,i\beta}\right)\right. \\ &+ \left.\sum_{j=1}^{3}V_{ji}\frac{\partial x_{j2_o}}{\partial c_{lm\alpha}}\right]\end{aligned} \tag{4.4.13}$$

will be developed. The first step is to examine the cross track partials (ie $i = 1$) and to express these in the same form as the other partials. From equations (4.4.6) and (4.4.11) and writing $\dot{\psi}^i_{jm}$ for $i = 2, 3$ as $\dot{\psi}_{jm}$

$$\begin{aligned}\frac{\partial \dot{x}_{1\beta_o}}{\partial c_{lm\alpha}} &= \sum_{j=-l}^{l}\left[A^{1\beta}_{lm\alpha j}\cos\left(\dot{\psi}_{j-1m}t\right) + B^{1\beta}_{lm\alpha j}\sin\left(\dot{\psi}_{j-1m}t\right)\right] \\ &+ \left(C^{1\beta}_{lm\alpha} + \delta_{m0}D^{1\beta}_{l0\alpha}t\right)\cos\left(\dot{F}t\right) + \left(E^{1\beta}_{lm\alpha} + \delta_{m0}F^{1\beta}_{l0\alpha}t\right)\sin\left(\dot{F}t\right) \\ &+ G^{1\beta}_{lm\alpha}.\end{aligned} \tag{4.4.14}$$

Now if the j summation is replaced by a summation over $j' = j - 1$ then the summation limits become $j' = -l - 1$ and $l - 1$ and equation (4.4.14) is rewritten as

$$\begin{aligned}\frac{\partial \dot{x}_{1\beta_o}}{\partial c_{lm\alpha}} &= \sum_{j'=-l-1}^{l-1}\left[A^{1\beta}_{lm\alpha j'+1}\cos\left(\dot{\psi}_{j'm}t\right) + B^{1\beta}_{lm\alpha j'+1}\sin\left(\dot{\psi}_{j'm}t\right)\right] \\ &+ \left(C^{1\beta}_{lm\alpha} + \delta_{m0}D^{1\beta}_{l0\alpha}t\right)\cos\left(\dot{F}t\right) + \left(E^{1\beta}_{lm\alpha} + \delta_{m0}F^{1\beta}_{l0\alpha}t\right)\sin\left(\dot{F}t\right) \\ &+ G^{1\beta}_{lm\alpha}.\end{aligned} \tag{4.4.15}$$

The primed notation can now be dropped with the result that all partials are of the same form except for their summation limits. A general term is now

$$\begin{aligned}\frac{\partial \dot{x}_{i\beta_o}}{\partial c_{lm\alpha}} &= \sum_{j=-l-\delta_{i1}}^{l-\delta_{i1}}\left[A^{i\beta}_{lm\alpha j+\delta_{i1}}\cos\left(\dot{\psi}_{jm}t\right) + B^{i\beta}_{lm\alpha j+\delta_{i1}}\sin\left(\dot{\psi}_{jm}t\right)\right] \\ &+ \left(C^{i\beta}_{lm\alpha} + \delta_{m0}D^{i\beta}_{l0\alpha}t\right)\cos\left(\dot{F}t\right) + \left(E^{i\beta}_{lm\alpha} + \delta_{m0}F^{i\beta}_{l0\alpha}t\right)\sin\left(\dot{F}t\right) \\ &+ G^{i\beta}_{lm\alpha}.\end{aligned} \tag{4.4.16}$$

Equation (4.4.13) is now further developed. The terms in (4.4.13) are all similar algebraically. Thus the first term is derived carefully and the other terms inferred from this. The constant, once per revolution and secular terms at the end of (4.4.16) are not explicitly worked out in the following although the period of their variations are carefully noted.

Using (4.4.3) the first term in (4.4.13) is

$$\begin{aligned}\frac{\partial \dot{x}_{i\beta_o}}{\partial c_{lm\alpha}}\mathbf{h}_{i\beta}.\mathbf{e}_{12_o} &= \left(\sum_{j=-l-\delta_{i1}}^{l-\delta_{i1}}\left[A^{i\beta}_{lm\alpha j+\delta_{i1}}\cos\left(\dot{\psi}_{jm}t\right)+B^{i\beta}_{lm\alpha j+\delta_{i1}}\sin\left(\dot{\psi}_{jm}t\right)\right]\right.\\ &+ \left(C^{i\beta}_{lm\alpha}+\delta_{m0}D^{i\beta}_{l0\alpha}t\right)\cos\left(\dot{F}t\right)+\left(E^{i\beta}_{lm\alpha}+\delta_{m0}F^{i\beta}_{l0\alpha}t\right)\sin\left(\dot{F}t\right)\\ &+ \left.G^{i\beta}_{lm\alpha}\right)\\ &\times \left(\sum_{k=0}^{k_{max}} m_{i\beta,k}\cos\left(k\dot{F}t\right)+q_{i\beta,k}\sin\left(k\dot{F}t\right)\right) \qquad (4.4.17)\end{aligned}$$

which on using the following trigonometric results

$$\begin{aligned}2\cos(a)\cos(b) &= \cos(a+b)+\cos(a-b)\\ 2\sin(a)\sin(b) &= -\cos(a+b)+\cos(a-b)\\ 2\sin(a)\cos(b) &= \sin(a+b)+\sin(a-b)\\ 2\cos(a)\sin(b) &= \sin(a+b)-\sin(a-b) \qquad (4.4.18)\end{aligned}$$

and (4.4.12) can be written as

$$\begin{aligned}\frac{\partial \dot{x}_{i\beta_o}}{\partial c_{lm\alpha}}\mathbf{h}_{i\beta}.\mathbf{e}_{12_o} &= \frac{1}{2}\sum_{j=-l-\delta_{i1}}^{l-\delta_{i1}}\sum_{k=0}^{k_{max}}\left(A^{i\beta}_{lm\alpha j+\delta_{i1}}m_{i\beta,k}-B^{i\beta}_{lm\alpha j+\delta_{i1}}q_{i\beta,k}\right)\cos\left(\dot{\psi}_{j+km}t\right)\\ &+ \left(A^{i\beta}_{lm\alpha j+\delta_{i1}}m_{i\beta,k}+B^{i\beta}_{lm\alpha j+\delta_{i1}}q_{i\beta,k}\right)\cos\left(\dot{\psi}_{j-km}t\right)\\ &+ \left(A^{i\beta}_{lm\alpha j+\delta_{i1}}q_{i\beta,k}+B^{i\beta}_{lm\alpha j+\delta_{i1}}m_{i\beta,k}\right)\sin\left(\dot{\psi}_{j+km}t\right)\\ &+ \left(-A^{i\beta}_{lm\alpha j+\delta_{i1}}q_{i\beta,k}+B^{i\beta}_{lm\alpha j+\delta_{i1}}m_{i\beta,k}\right)\sin\left(\dot{\psi}_{j-km}t\right)\\ &+ \sum_{k'=0}^{k_m+1}\left[\left(C^{\star i\beta k'}_{lm\alpha}+D^{\star i\beta k'}_{lm\alpha}t\right)\cos\left(k'\dot{F}t\right)\right.\\ &+ \left.\left(E^{\star i\beta k'}_{lm\alpha}+F^{\star i\beta k'}_{lm\alpha}t\right)\sin\left(k'\dot{F}t\right)\right]. \qquad (4.4.19)\end{aligned}$$

To see how this can be simplified look at the term

$$\sum_{j=-l-\delta_{i1}}^{l-\delta_{i1}} \sum_{k=0}^{k_{max}} \left(A^{i\beta}_{lm\alpha j+\delta_{i1}} m_{i\beta,k} - B^{i\beta}_{lm\alpha j+\delta_{i1}} q_{i\beta,k} \right) \cos\left(\dot{\psi}_{j+km} t\right).$$

By interchanging the order of summations and replacing the j summation by $j' = j + k$ the term becomes

$$\sum_{k=0}^{k_{max}} \sum_{j'=-l-\delta_{i1}+k}^{l-\delta_{i1}+k} \left(A^{i\beta}_{lm\alpha(j'-k+\delta_{i1})} m_{i\beta,k} - B^{i\beta}_{lm\alpha(j'-k+\delta_{i1})} q_{i\beta,k} \right) \cos\left(\dot{\psi}_{j'm} t\right).$$

Again reverse the order of the summation to give

$$\sum_{j'=-l-\delta_{i1}+k_{max}}^{l-\delta_{i1}+k_{max}} \left(\sum_{k=0}^{k_{max}} \left(A^{i\beta}_{lm\alpha(j'-k+\delta_{i1})} m_{i\beta,k} - B^{i\beta}_{lm\alpha(j'-k+\delta_{i1})} q_{i\beta,k} \right) \right) \cos\left(\dot{\psi}_{j'm} t\right)$$

When j' has a value outside the bounds given in the last equation then the value of the bracketed index in the amplitudes is outside that defined in chapter 3. In chapter 3 $A^{i\beta}_{lm\alpha j}$ was defined for $j = -l - \delta_{i1}$ to $l - \delta_{i1}$ in steps of two from the lower to the upper bound. If the value of any amplitude with index j outside those values is defined as zero then the summation limits and the index j can be generalised for the first four terms of equation (4.3.15) in the form

$$\begin{aligned}
\frac{\partial \dot{x}_{i\beta_o}}{\partial c_{lm\alpha}} \mathbf{h}_{i\beta} . \mathbf{e}_{12_o} &= \frac{1}{2} \sum_{j=-l-\delta_{i1}-k_{max}}^{l-\delta_{i1}+k_{max}} \left[\sum_{k=0}^{k_{max}} \left(A^{i\beta}_{lm\alpha(j-k+\delta_{i1})} m_{i\beta,k} - B^{i\beta}_{lm\alpha(j-k+\delta_{i1})} q_{i\beta,k} \right.\right. \\
&+ \left.\left. A^{i\beta}_{lm\alpha(j+k+\delta_{i1})} m_{i\beta,k} + B^{i\beta}_{lm\alpha(j+k+\delta_{i1})} q_{i\beta,k} \right) \right] \cos\left(\dot{\psi}_{jm} t\right) \\
&+ \left[\sum_{k=0}^{k_{max}} \left(A^{i\beta}_{lm\alpha(j-k+\delta_{i1})} q_{i\beta,k} + B^{i\beta}_{lm\alpha(j-k+\delta_{i1})} m_{i\beta,k} \right.\right. \\
&- \left.\left. A^{i\beta}_{lm\alpha(j+k+\delta_{i1})} q_{i\beta,k} + B^{i\beta}_{lm\alpha(j+k+\delta_{i1})} m_{i\beta,k} \right) \right] \sin\left(\dot{\psi}_{jm} t\right) \\
&+ \sum_{k'=0}^{k_m+1} \left[\left(C^{\star i\beta k'}_{lm\alpha} + D^{\star i\beta k'}_{lm\alpha} t \right) \cos\left(k' \dot{F} t\right) \right. \\
&+ \left. \left(E^{\star i\beta k'}_{lm\alpha} + F^{\star i\beta k'}_{lm\alpha} t \right) \sin\left(k' \dot{F} t\right) \right] \qquad (4.4.20)
\end{aligned}$$

Introduce the new notation

$$\begin{aligned}\Lambda^{i\beta}_{lm\alpha j} &= \frac{1}{2}\left[\sum_{k=0}^{k_{max}}\left(A^{i\beta}_{lm\alpha(j-k+\delta_{i1})}m_{i\beta,k} - B^{i\beta}_{lm\alpha(j-k+\delta_{i1})}q_{i\beta,k}\right.\right.\\ &+ \left.\left. A^{i\beta}_{lm\alpha(j+k+\delta_{i1})}m_{i\beta,k} + B^{i\beta}_{lm\alpha(j+k+\delta_{i1})}q_{i\beta,k}\right)\right] \qquad (4.4.21)\\ \Gamma^{i\beta}_{lm\alpha j} &= \frac{1}{2}\left[\sum_{k=0}^{k_{max}}\left(A^{i\beta}_{lm\alpha(j-k+\delta_{i1})}q_{i\beta,k} + B^{i\beta}_{lm\alpha(j-k+\delta_{i1})}m_{i\beta,k}\right.\right.\\ &- \left.\left. A^{i\beta}_{lm\alpha(j+k+\delta_{i1})}q_{i\beta,k} + B^{i\beta}_{lm\alpha(j+k+\delta_{i1})}m_{i\beta,k}\right)\right] \qquad (4.4.22)\end{aligned}$$

then

$$\begin{aligned}\frac{\partial \dot{x}_{i\beta_o}}{\partial c_{lm\alpha}}\mathbf{h}_{i\beta}.\mathbf{e}_{12_o} &= \frac{1}{2}\sum_{j=-l-\delta_{i1}-k_{max}}^{l-\delta_{i1}+k_{max}}\left(\Lambda^{i\beta}_{lm\alpha j}\cos\left(\dot{\psi}_{jm}t\right) + \Gamma^{i\beta}_{lm\alpha j}\sin\left(\dot{\psi}_{jm}t\right)\right)\\ &+ \sum_{k'=0}^{k_m+1}\left[\left(C^{\star i\beta k'}_{lm\alpha} + D^{\star i\beta k'}_{lm\alpha}t\right)\cos\left(k'\dot{F}t\right)\right.\\ &+ \left.\left(E^{\star i\beta k'}_{lm\alpha} + F^{\star i\beta k'}_{lm\alpha}t\right)\sin\left(k'\dot{F}t\right)\right]. \qquad (4.4.23)\end{aligned}$$

Similarly one can show

$$\begin{aligned}\frac{\partial x_{i\beta_o}}{\partial c_{lm\alpha}}V_{Xi\beta} &= \frac{1}{2}\sum_{j=-l-\delta_{i1}-k_{max}}^{l-\delta_{i1}+k_{max}}\left(\hat{\Lambda}^{i\beta}_{lm\alpha j}\cos\left(\dot{\psi}_{jm}t\right) + \hat{\Gamma}^{i\beta}_{lm\alpha j}\sin\left(\dot{\psi}_{jm}t\right)\right)\\ &+ \sum_{k'=0}^{k_m+1}\left[\left(\hat{C}^{\star i\beta k'}_{lm\alpha} + \hat{D}^{\star i\beta k'}_{lm\alpha}t\right)\cos\left(k'\dot{F}t\right)\right.\\ &+ \left.\left(\hat{E}^{\star i\beta k'}_{lm\alpha} + \hat{F}^{\star i\beta k'}_{lm\alpha}t\right)\sin\left(k'\dot{F}t\right)\right] \qquad (4.4.24)\end{aligned}$$

where

$$\begin{aligned}\hat{\Lambda}^{i\beta}_{lm\alpha j} &= \frac{1}{2}\left[\sum_{k=0}^{k_{max}}\left(\hat{A}^{i\beta}_{lm\alpha(j-k+\delta_{i1})}b_{i\beta,k} - \hat{B}^{i\beta}_{lm\alpha(j-k+\delta_{i1})}c_{i\beta,k}\right.\right.\\ &+ \left.\left. \hat{A}^{i\beta}_{lm\alpha(j+k+\delta_{i1})}b_{i\beta,k} + \hat{B}^{i\beta}_{lm\alpha(j+k+\delta_{i1})}c_{i\beta,k}\right)\right] \qquad (4.4.25)\\ \hat{\Gamma}^{i\beta}_{lm\alpha j} &= \frac{1}{2}\left[\sum_{k=0}^{k_{max}}\left(\hat{A}^{i\beta}_{lm\alpha(j-k+\delta_{i1})}c_{i\beta,k} + \hat{B}^{i\beta}_{lm\alpha(j-k+\delta_{i1})}b_{i\beta,k}\right.\right.\end{aligned}$$

$$- \quad \hat{A}^{i\beta}_{lm\alpha(j+k+\delta_{i1})} c_{i\beta,k} + \hat{B}^{i\beta}_{lm\alpha(j+k+\delta_{i1})} b_{i\beta,k} \Big) \Bigg] . \tag{4.4.26}$$

The final term in (4.4.13) is written

$$\sum_{r=1}^{3} V_{ir} \frac{\partial x_{r2_o}}{\partial c_{lm\alpha}} \tag{4.4.27}$$

with each component expressible in the same way as the other two terms of equation (4.4.11) except for an extra index r which is needed,ie

$$\begin{aligned} V_{ir} \frac{\partial x_{r2_o}}{\partial c_{lm\alpha}} &= \frac{1}{2} \sum_{j=-l-\delta_{i1}-k_{max}}^{l-\delta_{i1}+k_{max}} \left(\Upsilon^{i2r}_{lm\alpha j} \cos\left(\dot{\psi}_{jm} t\right) + \Xi^{i2r}_{lm\alpha j} \sin\left(\dot{\psi}_{jm} t\right) \right) \\ &+ \sum_{k'=0}^{k_m+1} \Big[\left(\hat{C}^{*i2rk'}_{lm\alpha} + \hat{D}^{*i2rk'}_{lm\alpha} t \right) \cos\left(k' \dot{F} t\right) \\ &+ \left(\hat{E}^{*i2rk'}_{lm\alpha} + \hat{F}^{*i2rk'}_{lm\alpha} t \right) \sin\left(k' \dot{F} t\right) \Big] \end{aligned} \tag{4.4.28}$$

where

$$\begin{aligned} \Upsilon^{i2r}_{lm\alpha j} &= \frac{1}{2} \Bigg[\sum_{k=0}^{k_{max}} \left(\hat{A}^{r2}_{lm\alpha(j-k+\delta_{i1})} e_{ri,k} - \hat{B}^{r2}_{lm\alpha(j-k+\delta_{i1})} f_{ri,k} \right. \\ &+ \left. \hat{A}^{r2}_{lm\alpha(j+k+\delta_{i1})} e_{ri,k} + \hat{B}^{r2}_{lm\alpha(j+k+\delta_{i1})} f_{ri,k} \right) \Bigg] \end{aligned} \tag{4.4.29}$$

$$\begin{aligned} \Xi^{i2r}_{lm\alpha j} &= \frac{1}{2} \Bigg[\sum_{k=0}^{k_{max}} \left(\hat{A}^{r2}_{lm\alpha(j-k+\delta_{i1})} f_{ri,k} + \hat{B}^{r2}_{lm\alpha(j-k+\delta_{i1})} e_{ri,k} \right. \\ &- \left. \hat{A}^{r2}_{lm\alpha(j+k+\delta_{i1})} f_{ri,k} + \hat{B}^{r2}_{lm\alpha(j+k+\delta_{i1})} e_{ri,k} \right) \Bigg] . \end{aligned} \tag{4.4.30}$$

Hence the final term in (4.4.13) is given by

$$\begin{aligned} \sum_{r=1}^{3} V_{ir} \frac{\partial x_{r2_o}}{\partial c_{lm\alpha}} &= \sum_{j=-l-\delta_{i1}-k_{max}}^{l-\delta_{i1}+k_{max}} \left(\left[\sum_{r=1}^{3} \Upsilon^{i2r}_{lm\alpha j} \right] \cos\left(\dot{\psi}_{jm} t\right) + \left[\sum_{r=1}^{3} \Xi^{i2r}_{lm\alpha j} \right] \sin\left(\dot{\psi}_{jm} t\right) \right) \\ &+ \sum_{k'=0}^{k_m+1} \Big[\left(\hat{C}^{*i2rk'}_{lm\alpha} + \hat{D}^{*i2rk'}_{lm\alpha} t \right) \cos\left(k' \dot{F} t\right) \\ &+ \left(\hat{E}^{*i2rk'}_{lm\alpha} + \hat{F}^{*i2rk'}_{lm\alpha} t \right) \sin\left(k' \dot{F} t\right) \Big] . \end{aligned} \tag{4.4.31}$$

Using equations (4.4.23),(4.4.24) and (4.4.31) in (4.4.13) and interchanging the β and j summations

$$\begin{aligned}\frac{\partial RR_o}{\partial c_{lm\alpha}} &= \sum_{i=1}^{3}\Bigg\{\sum_{j=-l-\delta_{i1}-k_{max}}^{l-\delta_{i1}+k_{max}} \\ &\quad \left[\sum_{\beta=1}^{2}(-1)^{\beta-1}\left(\Lambda_{lm\alpha j}^{i\beta}+\hat{\Lambda}_{lm\alpha j}^{i\beta}+\left[\sum_{r=1}^{3}\Upsilon_{lm\alpha j}^{i2r}\right]\right)\cos\left(\dot{\psi}_{jm}t\right)\right. \\ &\quad \left.+\sum_{\beta=1}^{2}(-1)^{\beta-1}\left(\Gamma_{lm\alpha j}^{i\beta}+\hat{\Gamma}_{lm\alpha j}^{i\beta}+\left[\sum_{r=1}^{3}\Xi_{lm\alpha j}^{i2r}\right]\right)\sin\left(\dot{\psi}_{jm}t\right)\right] \\ &\quad +\sum_{k'=0}^{k_m+1}\left[\left(\tilde{C}_{lm\alpha}^{i2k'}+\tilde{D}_{lm\alpha}^{i2k'}t\right)\cos\left(k'\dot{F}t\right)+\left(\tilde{E}_{lm\alpha}^{*i2k'}+\tilde{F}_{lm\alpha}^{i2k'}t\right)\sin\left(k'\dot{F}t\right)\right]\Bigg\},\end{aligned} \tag{4.4.32}$$

where the $\tilde{C}_{lm\alpha}^{i2k'}$ etc. are a summation of the appropriate amplitudes. By reversing the order of the i and j summations and expanding the limits of the j summation equation (4.4.32) may be written more compactly. In detail

$$\begin{aligned}\frac{\partial RR_o}{\partial c_{lm\alpha}} &= \sum_{j=-l-1-k_{max}}^{l+k_{max}}\left[\mathcal{A}_{lm\alpha j}\cos\left(\dot{\psi}_{jm}t\right)+\mathcal{B}_{lm\alpha j}\sin\left(\dot{\psi}_{jm}t\right)\right] \\ &\quad +\sum_{k'=0}^{k_m+1}\left[\left(\tilde{C}_{lm\alpha}^{i2k'}+\tilde{D}_{lm\alpha}^{i2k'}t\right)\cos\left(k'\dot{F}t\right)+\left(\tilde{E}_{lm\alpha}^{*i2k'}+\tilde{F}_{lm\alpha}^{i2k'}t\right)\sin\left(k'\dot{F}t\right)\right]\end{aligned} \tag{4.4.33}$$

where

$$\mathcal{A}_{lm\alpha j} = \sum_{i=0}^{3}\left[\sum_{\beta=1}^{2}(-1)^{\beta-1}\left(\Lambda_{lm\alpha j}^{i\beta}+\hat{\Lambda}_{lm\alpha j}^{i\beta}\right)+\left[\sum_{r=1}^{3}\Upsilon_{lm\alpha j}^{i2r}\right]\right] \tag{4.4.34}$$

$$\mathcal{B}_{lm\alpha j} = \sum_{i=0}^{3}\left[\sum_{\beta=1}^{2}(-1)^{\beta-1}\left(\Gamma_{lm\alpha j}^{i\beta}+\hat{\Gamma}_{lm\alpha j}^{i\beta}\right)+\left[\sum_{r=1}^{3}\Xi_{lm\alpha j}^{i2r}\right]\right] \tag{4.4.35}$$

$$\begin{aligned}\Lambda_{lm\alpha j}^{i\beta} &= \frac{1}{2}\left[\sum_{k=0}^{k_{max}}\left(A_{lm\alpha(j-k+\delta_{i1})}^{i\beta}m_{i\beta,k}-B_{lm\alpha(j-k+\delta_{i1})}^{i\beta}q_{i\beta,k}\right.\right. \\ &\quad \left.\left.+A_{lm\alpha(j+k+\delta_{i1})}^{i\beta}m_{i\beta,k}+B_{lm\alpha(j+k+\delta_{i1})}^{i\beta}q_{i\beta,k}\right)\right],\end{aligned} \tag{4.4.36}$$

$$\Gamma^{i\beta}_{lm\alpha j} = \frac{1}{2}\left[\sum_{k=0}^{k_{max}}\left(A^{i\beta}_{lm\alpha(j-k+\delta_{i1})}q_{i\beta,k} + B^{i\beta}_{lm\alpha(j-k+\delta_{i1})}m_{i\beta,k}\right.\right.$$
$$\left.\left. - A^{i\beta}_{lm\alpha(j+k+\delta_{i1})}q_{i\beta,k} + B^{i\beta}_{lm\alpha(j+k+\delta_{i1})}m_{i\beta,k}\right)\right], \qquad (4.4.37)$$

$$\hat{\Lambda}^{i\beta}_{lm\alpha j} = \frac{1}{2}\left[\sum_{k=0}^{k_{max}}\left(\hat{A}^{i\beta}_{lm\alpha(j-k+\delta_{i1})}b_{i\beta,k} - \hat{B}^{i\beta}_{lm\alpha(j-k+\delta_{i1})}c_{i\beta,k}\right.\right.$$
$$\left.\left. + \hat{A}^{i\beta}_{lm\alpha(j+k+\delta_{i1})}b_{i\beta,k} + \hat{B}^{i\beta}_{lm\alpha(j+k+\delta_{i1})}c_{i\beta,k}\right)\right], \qquad (4.4.38)$$

$$\hat{\Gamma}^{i\beta}_{lm\alpha j} = \frac{1}{2}\left[\sum_{k=0}^{k_{max}}\left(\hat{A}^{i\beta}_{lm\alpha(j-k+\delta_{i1})}c_{i\beta,k} + \hat{B}^{i\beta}_{lm\alpha(j-k+\delta_{i1})}b_{i\beta,k}\right.\right.$$
$$\left.\left. - \hat{A}^{i\beta}_{lm\alpha(j+k+\delta_{i1})}c_{i\beta,k} + \hat{B}^{i\beta}_{lm\alpha(j+k+\delta_{i1})}b_{i\beta,k}\right)\right], \qquad (4.4.39)$$

$$\Upsilon^{i2r}_{lm\alpha j} = \frac{1}{2}\left[\sum_{k=0}^{k_{max}}\left(\hat{A}^{r2}_{lm\alpha(j-k+\delta_{i1})}e_{ri,k} - \hat{B}^{r2}_{lm\alpha(j-k+\delta_{i1})}f_{ri,k}\right.\right.$$
$$\left.\left. + \hat{A}^{r2}_{lm\alpha(j+k+\delta_{i1})}e_{ri,k} + \hat{B}^{r2}_{lm\alpha(j+k+\delta_{i1})}f_{ri,k}\right)\right] \qquad (4.4.40)$$

and

$$\Xi^{i2r}_{lm\alpha j} = \frac{1}{2}\left[\sum_{k=0}^{k_{max}}\left(\hat{A}^{r2}_{lm\alpha(j-k+\delta_{i1})}f_{ri,k} + \hat{B}^{r2}_{lm\alpha(j-k+\delta_{i1})}e_{ri,k}\right.\right.$$
$$\left.\left. - \hat{A}^{r2}_{lm\alpha(j+k+\delta_{i1})}f_{ri,k} + \hat{B}^{r2}_{lm\alpha(j+k+\delta_{i1})}e_{ri,k}\right)\right]. \qquad (4.4.41)$$

$A^{i\beta}_{lm\alpha j}$, $B^{i\beta}_{lm\alpha j}$, etc., in terms of the amplitudes of the solutions to Hill's equations are given by

$$A^{i\beta}_{lm\alpha j} = -\dot{\psi}^{i}_{jm}\mathcal{X}^{i}_{lmj}\sin\left(\phi^{i\beta}_{lm\alpha j}\right)$$
$$B^{i\beta}_{lm\alpha j} = -\dot{\psi}^{i}_{jm}\mathcal{X}^{i}_{lmj}\cos\left(\phi^{i\beta}_{lm\alpha j}\right), \qquad (4.4.42)$$

$$\hat{A}^{i\beta}_{lm\alpha j} = \mathcal{X}^{i}_{lmj}\cos\left(\phi^{i\beta}_{lm\alpha j}\right)$$
$$\hat{B}^{i\beta}_{lm\alpha j} = -\mathcal{X}^{i}_{lmj}\sin\left(\phi^{i\beta}_{lm\alpha j}\right). \qquad (4.4.43)$$

Equations (4.4.33), to (4.4.43) provide the relationship between the partial derivatives of the range rate residuals with respect to a gravity coefficient, and the amplitudes of the solutions to Hill's Equations, the $V_{ij}, V_{X i\beta}$ and the scalar products. The amplitudes of the solutions to Hill's Equations $\mathcal{X}^i_{lmj}$ are in turn given in terms of the orbital elements and the values of the indices in equations (3.5.7) to (3.5.9).

Equation (4.4.33), its subsidiary equations (4.4.34) to (4.4.43) and the procedure to calculate all the coefficients $m_{i\beta k}, q_{i\beta k}, b_{i\beta k}, c_{i\beta k}, e_{ijk}, f_{ij,k}$ from equations (4.4.1-3) as discussed in the previous section is the basis of the work that follows. The formulism is flexible enough to model the range rate residuals, or to recover a gravity field, providing the satellites share the same orbital height, the same inclination, the same near zero eccentricity but not necessarily the same orbital plane.

In particular the methodology permits investigation of the extent that satellites in different orbital planes may affect the recovery procedure. The premise is that the relative orientation of the satellites as reflected in the increasing periodic variations in the scalar products and subsequent terms introduces extra cross track information into the signal. This extra information may then help recover certain coefficients which are poorly determined when the spacecraft follow each other in a plane.

4.5 Additional effects on the Range Rate Residuals

So far the effects of the periodic, non resonant perturbations of the satellite's motions on the range rate have been discussed. In addition to these there are the effects of the zonal harmonics which, at the once per revolution or constant fre-

quency accelerations for odd and even zonals respectively, give rise to the resonant response discussed in chapter 3. Furthermore the response of the satellites to an error in the initial state vector is an effect which was examined in chapter 2. These will now be discussed briefly since they do not provide additional information on the gravity field that can be used in the recovery. It is important therefore only to derive the form of response that these parameters have on the line of sight relative velocity, and not to detail their effects in terms of the zonal gravity coefficients or initial state errors.

The contribution to the Range Rate Residuals from the once per revolution and constant gravity signal, and the initial state errors can be calculated in the same way as the other gravity signal. Equations (3.4.3) and (3.4.14) give the perturbations to the satellites motions due to these effects. Their combined effects can be represented by equations of the form (eg (Wiejak W., 1990))

$$\begin{aligned}
\Delta u_{res/init} &= (A_u + B_u t)\cos\left(\dot{F}t\right) + (C_u + D_u t)\sin\left(\dot{F}t\right) + E_u \\
\Delta v_{res/init} &= (A_v + B_v t)\cos\left(\dot{F}t\right) + (C_v + D_v t)\sin\left(\dot{F}t\right) + E_v t + F_v \qquad (4.5.1) \\
\Delta w_{res/init} &= (A_w + B_w t)\cos\left(\dot{F}t\right) + (C_w + D_w t)\sin\left(\dot{F}t\right) + E_w.
\end{aligned}$$

Equation (4.3.22) with the partial derivatives replaced by the differentials in (4.5.1), and using equations (4.4.1),(4.4.2) and (4.4.3) to take some account of the relative motions of the satellites, give the general form for the perturbation in the range rate due to the initial state error and resonant effects. It is written as

$$\Delta RR_{res/init} = \sum_{k=0}^{k_m+1} (A_k + B_k t)\cos\left(k\dot{F}t\right) + (C_k + D_k t)\sin\left(k\dot{F}t\right). \qquad (4.5.2)$$

$A_k, .., D_k$ are due to the combined effects of the once per revolution and constant gravity accelerations and the initial state errors.

Now using equations (4.1.2), (4.4.31) and (4.5.2) the Range Rate Residuals due to all the effects so far discussed are written

$$\Delta RR = \sum_{l=2}^{L_{max}} \sum_{m=0}^{l} \sum_{\alpha=0}^{1} \sum_{j=-l-1-k_{max}}^{l+k_{max}} \left[\mathcal{A}_{lm\alpha j} \cos\left(\dot{\psi}_{jm} t\right) + \mathcal{B}_{lm\alpha j} \sin\left(\dot{\psi}_{jm} t\right)\right]$$
$$+ \sum_{k=0}^{k_m+1} \left[\left(\tilde{A}^k + \tilde{B}^k t\right) \cos\left(k\dot{F}t\right) + \left(\tilde{C}^k + \tilde{D}^k t\right) \sin\left(k\dot{F}t\right)\right] \qquad (4.5.3)$$

where now $\tilde{A}_k, .., \tilde{D}_k$ are due to the combined effects of the once per revolution and constant gravity accelerations and the initial state errors but also the other effects of the zonals at these frequencies. This places a restriction on the j summation for the zonals. For $m = 0$, $|j| > k_m + 1$.

A new notation is now introduced. The partial derivatives filtered for the combined effects of the constant once and up to $k_m + 1$ times per revolution gravity accelerations and the initial state errors are called the filtered partial derivatives, they are written

$$\frac{\partial RR_{o,f}}{\partial c_{lm\alpha}} = \sum_{j=-l-1-k_{max}}^{l+k_{max}} \left[\mathcal{A}_{lm\alpha j} \cos\left(\dot{\psi}_{jm} t\right) + \mathcal{B}_{lm\alpha j} \sin\left(\dot{\psi}_{jm} t\right)\right] \qquad (4.5.4)$$

with the restrictions on the summation mentioned above implied. The equations of the form (4.5.4) are the basis for the next chapter and provide the complete description of range rate residuals between satellites in a drag free near circular orbit under the influence of gravity and initial state vector mismodelling.

Chapter 5

Range Rate Error Analysis

5.1 Introduction

The previous chapter saw the derivation of the partials $\frac{\partial RR_{calc_i}}{\partial c_{lm\alpha}}$, namely the sensitivities of the Range Rate to errors in the gravity field and the functions upon which the recovery or error analysis procedures are based.

The least squares solution model developed in this chapter is used to undertake an error analysis from which one may infer the relative benefits of one possible mission over another. The normal matrix will be developed into a block diagonal form which makes this kind of analysis practical . The study of this matrix will indicate how the orientations of the satellites affect the accuracy of the recovered coefficients.

5.2 The Least Squares procedure

It has been assumed here for reasons of efficiency and simplicity that only gravitational errors are present. It is also assumed that the partials can be filtered of the once,twice and up to $k_m + 1$ times per revolution signal and of the secular part of the signal , leaving only the periodic part that is separable from initial state

error and resonant effects, without introducing errors in the result. This may be an inaccurate assumption but is thought that the relative effect of this assumption on different mission scenarios is small (Wiejak W., 1990) (Colombo, 1984).

The filtered signal is of the form

$$\Delta RR_{calc\,i} = \sum_{l=2}^{Lmax} \sum_{m=0}^{l} \sum_{\alpha=0}^{1} \frac{\partial RR_{o,f\,i}(c_{lm\alpha})}{\partial c_{lm\alpha}} \Delta c_{lm\alpha} \tag{5.2.1}$$

where the filtered partial derivatives are

$$\frac{\partial RR_{o,f\,i}}{\partial c_{lm\alpha}} = \sum_{j=-l-1-k_{max}}^{l+k_{max}} \left[\mathcal{A}_{lm\alpha j} \cos\left(\dot{\psi}_{jm} t_i\right) + \mathcal{B}_{lm\alpha j} \sin\left(\dot{\psi}_{jm} t_i\right) \right]. \tag{5.2.2}$$

The signal equation is given therefore by (5.2.1) and by the understanding that

$$\Delta RR_{obs\,i} = \Delta RR_{calc\,i} + \epsilon_i \quad i = 0, 1, .., N_{obs} - 1, \tag{5.2.3}$$

where ϵ_i, the model errors and noise of the i^{th} observation, are assumed to be normally distributed.

If (5.2.3) is written in vector form then

$$\Delta \mathbf{RR_{obs}} = \mathbf{Ac} + \epsilon \tag{5.2.4}$$

where $\Delta \mathbf{RR_{obs}}$ and ϵ are column vectors indexed by i and therefore of dimension N_{obs} , the number of observations in the dataset. **c** is also a column vector, made up of the coefficients $c_{lm\alpha}$ in some order. Since there are $(L_{max}+1)(L_{max}+2) - L_{max}$ coefficients up to degree and order L_{max} then **c** has that dimension. The matrix of partials **A** is of dimension $N_{obs} \times ((L_{max}+1)(L_{max}+2) - L_{max})$ and each of the $(L_{max}+1)(L_{max}+2) - L_{max}$ columns comprises the N_{obs} partials for some l, m, α.

Equation (5.2.4) gives the observation equations in matrix form. The least squares solution to these equations minimises the quadratic

$$q = \epsilon^{\mathrm{T}} \mathbf{W} \epsilon \tag{5.2.5}$$

with respect to the elements of **c** (Bomford, 1980). For a set of uncorrelated observations **W** is a diagonal matrix, elements of which are the weights attached

to each observation. The weights increase with the accuracy of the observation, eg $W_i = \frac{1}{\sigma_i^2}$ where σ_i is the standard error of the i^{th} observation.

The solution to the minimisation procedure is the normal equations

$$(\mathbf{A^T W A})\hat{\mathbf{c}} = \mathbf{A^T W \Delta RR_{obs}}. \tag{5.2.6}$$

In (5.2.6) $\hat{\mathbf{c}}$ is the best linear estimate of $\mathbf{c}$ and $(\mathbf{A^T WA})$ the normal matrix. If all observations have the same standard error σ then

$$(\frac{1}{\sigma^2}\mathbf{A^T A})\hat{\mathbf{c}} = \frac{1}{\sigma^2}\mathbf{A^T \Delta RR_{obs}}. \tag{5.2.7}$$

The normal matrix is then given by

$$\mathbf{N} = (\frac{1}{\sigma^2}\mathbf{A^T A}), \tag{5.2.8}$$

which is made up of the scalar products of columns of $\mathbf{A}$ and is obviously symmetric. It can easily be shown (Bomford, 1980) that the elements of the inverted normal matrix are the variances (diagonal elements) and covariances (non-diagonal elements) of the coefficients to be recovered. Therefore by examining the elements of the inverted normal matrix, information about the accuracy of the gravity field recovery is obtained without having to simulate data and carry out an actual recovery.

5.3 Efficient Least Squares Analysis

The problem in hand, that of finding the variances and covariances of the gravity coefficients from the inverted normal matrix is not straightforward as for high degree and order solutions, say 120x120, this matrix has size 14400x14400 with each element made up from contributions from each data point. This amounts to around a million data points for a month of measurements taken every 3 seconds and several million elements of the matrix. A considerable amount of computer time would be required to compute the matrix and invert it.

The problem can be greatly simplified by making a few assumptions about the distribution of the dataset. The data is distributed along the paths of the satellites which are assumed to be repeat orbits. Hence the orbital and nodal frequencies can be written as (eg (Koop, 1993), (Colombo, 1984))

$$\dot{F} = n_0 = \frac{2\pi N_{revs}}{T_{rep}} \tag{5.3.1}$$

and

$$\dot{L} = \dot{\Omega} - \dot{\theta}_G = -\frac{2\pi N_{days}}{T_{rep}}. \tag{5.3.2}$$

The repeat period is T_{rep} seconds and contains exactly N_{revs} orbital revolutions and N_{days} revolutions of the nodes, where N_{revs} and N_{days} are coprime integers, ie without any common divisors, the gravitational frequencies are therefore

$$\dot{\psi_{jm}} = \frac{2\pi N_{revs}}{T_{rep}} \left(j - m\frac{N_{days}}{N_{revs}} \right). \tag{5.3.3}$$

On using (5.2.2) and (5.2.8) a typical element of the normal matrix is given by

$$\begin{aligned} N^{lm\alpha}_{l'm'\alpha'} &= \frac{1}{\sigma^2} \sum_{i=0}^{N_{obs}-1} \frac{\partial RR_{o,fi}}{\partial c_{lm\alpha}} \frac{\partial RR_{o,fi}}{\partial c_{l'm'\alpha'}} \\ &= \frac{1}{\sigma^2} \sum_{j=-l-1-k_{max}}^{l+k_{max}} \sum_{j'=-l'-1-k_{max}}^{l'+k_{max}} \mathcal{A}_{lm\alpha j}\mathcal{A}_{l'm'\alpha'j'}\mathcal{I}^1_{jj'mm'} \\ &\quad + \mathcal{A}_{lm\alpha j}\mathcal{B}_{l'm'\alpha'j'}\mathcal{I}^2_{jj'mm'} \\ &\quad + \mathcal{B}_{lm\alpha j}\mathcal{A}_{l'm'\alpha'j'}\mathcal{I}^3_{jj'mm'} \\ &\quad + \mathcal{B}_{lm\alpha j}\mathcal{B}_{l'm'\alpha'j'}\mathcal{I}^4_{jj'mm'} \end{aligned} \tag{5.3.4}$$

where

$$\begin{aligned} \mathcal{I}^1_{jj'mm'} &= \sum_{i=0}^{N_{obs}-1} \cos\left(\dot{\psi}_{jm}t_i\right)\cos\left(\dot{\psi}_{j'm'}t_i\right) \\ \mathcal{I}^2_{jj'mm'} &= \sum_{i=0}^{N_{obs}-1} \cos\left(\dot{\psi}_{jm}t_i\right)\sin\left(\dot{\psi}_{j'm'}t_i\right) \\ \mathcal{I}^3_{jj'mm'} &= \sum_{i=0}^{N_{obs}-1} \sin\left(\dot{\psi}_{jm}t_i\right)\cos\left(\dot{\psi}_{j'm'}t_i\right) \\ \mathcal{I}^4_{jj'mm'} &= \sum_{i=0}^{N_{obs}-1} \sin\left(\dot{\psi}_{jm}t_i\right)\sin\left(\dot{\psi}_{j'm'}t_i\right) \end{aligned}$$

Now when:-

- the data points are equally spaced, ie $t_i = t_o + i\Delta t$
- the sampling frequency is greater than twice the highest significant frequency
- there are an integer number of cycles in the sampling period

the summations are zero except for a few special cases due to the orthogonality properties of trigonometric functions, from which similar results on trigonometric series can be inferred, subject to the conditions listed above.

The number of cycles that an arbitrary frequency term performs in one repeat period is $jN_{revs} - mN_{days}$ which is an integer. For a dataset of the required form this implies that

$$\mathcal{I}^1_{jj'mm'} = \mathcal{I}^2_{jj'mm'} = \mathcal{I}^3_{jj'mm'} = \mathcal{I}^4_{jj'mm'} = 0 \tag{5.3.5}$$

unless

$$|\dot{\psi}_{jm}| = |\dot{\psi}_{j'm'}| \tag{5.3.6}$$

in which case

$$\mathcal{I}^2_{jj'mm'} = \mathcal{I}^3_{jj'mm'} = 0 \tag{5.3.7}$$

for all j, j', m, m' , and

$$\mathcal{I}^1_{jjmm} = \mathcal{I}^4_{jjmm} = \frac{N_{obs}}{2}, \tag{5.3.8}$$

(Colombo, 1984).

This is the basis of all efficient numerical methods with equispaced data, and is analogous to the Fast Fourier Transform routine where the data is situated on a regular grid of points (Brigham, 1974), or to efficient harmonic analysis on a regular grid (Colombo, 1981).

Now equation (5.3.6) implies

$$j - m\frac{N_{days}}{N_{revs}} = \pm\left(j' - m'\frac{N_{days}}{N_{revs}}\right). \tag{5.3.9}$$

On examining the positive option first

$$\frac{j - j'}{m - m'} = \frac{N_{days}}{N_{revs}} \tag{5.3.10}$$

it is clear that,

$$\begin{aligned} -L_{max} &\leq m - m' \leq L_{max} \\ -2L_{max} &\leq j - j' \leq 2L_{max} \end{aligned}$$

and so if $N_{revs} > L_{max}$ then (5.3.10) cannot hold. Therefore (5.3.9) with the positive sign holds only when $m = m'$ and $j = j'$. This is a consequence of the assertion that N_{days} and N_{revs} are coprime. (Koop, 1993).

Similarly taking the negative option it can be shown that if $N_{revs} > 2L_{max}$ then non-zero series occur only for $m = m'$ and $j = j'$. The result is that (5.3.4) can be rewritten as

$$N^{lm\alpha}_{l'm'\alpha'} = \frac{N_{obs}\delta_{mm'}}{2\sigma^2} \sum_{j=-l-1-k_{max}}^{l+k_{max}} \sum_{j'=-l'-1-k_{max}}^{l'+k_{max}} \delta_{jj'}\left(\mathcal{A}_{lm\alpha j}\mathcal{A}_{l'm'\alpha' j'} + \mathcal{B}_{lm\alpha j}\mathcal{B}_{l'm'\alpha' j'}\right). \tag{5.3.11}$$

Thus elements of the normal matrix are non-zero only when the coefficients share the same value of m, and the summations over which these elements are obtained are limited by the fact that their values of j must also be equal. Only one summation is needed and its range is the intersection of the two summations above .

Further consideration requires a separate treatment of the $m = m' = 0$ case. There $j = -j'$ produces non zero series and therefore contributes to the elements of the matrix. Also when $j = j' = 0$

$$\mathcal{I}^1_{0000} = \mathcal{I}^4_{0000} = N_{obs}. \tag{5.3.12}$$

However, the contributions to the gravity signal from constant, and once up to k_m+ 1 times per revolution frequency terms have already been absorbed by $\tilde{A}^k, .., \tilde{D}^k$. Thus, as mentioned at the end of chapter 4, the j summation is limited to $|j| > k_m + 1$ for the zonals. The loss of these frequencies will have a degrading effect on the lower degree zonals. When $m = 0$ an element of the matrix can be written

$$N^{l0\alpha}_{l'0\alpha'} = \frac{N_{obs}}{\sigma^2} \sum_{j=-l-1-k_{max}}^{l+k_{max}} \sum_{j'=-l'-1-k_{max}}^{l'+k_{max}} \delta_{jj'} (\mathcal{A}_{l0\alpha j}\mathcal{A}_{l'0\alpha' j'} + \mathcal{B}_{l0\alpha j}\mathcal{B}_{l'0\alpha' j'} + \mathcal{A}_{l0\alpha j}\mathcal{A}_{l'0\alpha' -j'} + \mathcal{B}_{l0\alpha j}\mathcal{B}_{l'0\alpha' -j'}) \tag{5.3.13}$$

where $|j|, |j'| > k_m + 1$, (Colombo, 1984).

In consequence of (5.3.11) and (5.3.13) the normal matrix is block-diagonal if the coefficients are ordered within the vector $\mathbf{c}$ so that elements are grouped into those with the same order. The system now becomes a sparse block diagonal normal matrix with the advantage that one can invert each of the smaller sub blocks in turn and therefore reduce the computational effort. Further, there is no need to sum the elements over all observations as would normally be the case making the analysis much more efficient.

The results presented in this chapter are based on an analysis of this type. However, before looking at the results a few points should be made about earlier assumptions . A necessary simplification was made regarding the removal of secular and kn cycles per revolution signal for k less than k_{max} from the residuals. These terms would of course effect the errors in the coefficients to some extent but there are few of these compared to the thousands still considered. For this reason one could reasonably expect the errors to be dominated by the relationships between all the coefficients within each sub-block (Colombo, 1984). Furthermore the differential effect between two missions is likely to be small and the results can be viewed as accurate relative to each other.

In the remainder of this chapter the variances and covariances of the gravity

coefficients, that is the diagonal elements of the inverted normal matrix, are presented for a variety of possible mission scenarios. These give valuable information about how the orbits and orientations of the satellites would affect the recovery of the gravity field.

In addition to these results the eigenvalues of the inverted normal matrix are displayed providing limits within which the solution is expected to lie. The maximum eigenvalue is the maximum error that could exist in a linear combination of coefficients and as such illustrate where possible deficiencies in the recovery may lie. Which coefficients are involved in the linear combination and their proportions are given by the eigenvectors corresponding to each eigenvalue, these eigenvectors have dimension equal to the coefficient vector. Similarly the minimum eigenvalue is the lowest error that a linearly independent combination of coefficients is expected to have.

Because of the block diagonal nature of the normal matrix it is possible to solve for the eigenvalues of each block separately to see how coefficients of a particular order perform in the missions discussed. Together with the degree variance plots the eigenvalues allow one to pinpoint the strengths and limitations of each of the cases studied and can be of use in deciding what type of mission would be best in a gravity field determination using two satellites.

5.4 Discussion of the error analyses

5.4.1 Analysis of the normal matrix

The elements of each sub-block are indexed by l, α, l', α' and the sub-blocks themselves identified by m. Thus an element of the m^{th} order sub block can be written as (cf (5.3.11), (5.3.13))

$$\left(N^{l\alpha}_{l'\alpha'}\right)_m = \frac{N_{obs}}{2\sigma^2} \sum_{j=-min(l,l')-1-k_{max}}^{min(l,l')+k_{max}} \mathcal{A}_{lm\alpha j}\mathcal{A}_{l'm\alpha' j} + \mathcal{B}_{lm\alpha j}\mathcal{B}_{l'm\alpha' j} \qquad (5.4.1)$$

for $m \neq 0$, and

$$\left(N^{l\alpha}_{l'\alpha'}\right)_0 = \frac{N_{obs}}{\sigma^2} \sum_{j=-min(l,l')-1-k_{max}}^{min(l,l')+k_{max}} (\mathcal{A}_{l0\alpha j}\mathcal{A}_{l'0\alpha' j} + \mathcal{B}_{l0\alpha j}\mathcal{B}_{l'0\alpha' j} + \mathcal{A}_{l0\alpha j}\mathcal{A}_{l'0\alpha' -j} + \mathcal{B}_{l0\alpha j}\mathcal{B}_{l'0\alpha' -j}) \qquad (5.4.2)$$

when $m = 0$, where $|j| > k_m + 1$. Therefore to obtain the variances and eigenvalues from the normal matrix each sub-block is set up and inverted in turn, for a choice of initial parameters. These are

- The common height of the satellites.
- The common inclination of the satellites.(Bearing in mind the model, or at least Hill's equations, are accurate only for near polar orbits)
- The separation of the satellites whilst they share the same orbital plane.
- The separation of the orbital planes in right ascension.

For all the results presented it is assumed that the satellites are in repeat orbits in which they perform 323 orbital revolutions in 20 nodal days. This is consistent with the value $L_{max} = 120$ chosen here since $2 \times 120 < 323$.

The accuracy of the observations is assumed to be $\sigma = 0.1mm/sec$, the value quoted for the GAMES laser ranging mission proposal. Furthermore it is assumed

that varying the separation has no effect on this accuracy, therefore concentrating attention on the mathematical rather than the practical aspects of this problem. The time between the measurements was taken to be 3 seconds and thus there are $N_{obs} = 576000$ measurements in the 20 day period and approximately 1783 in each orbital period. This represents a sampling frequency of 1783 times per revolution compared to a highest observed frequency of a little over 120 times a revolution. The sampling rate is more than sufficient for the model as described previously.

Once the values of the parameters which describe the mission have been chosen, the non zero elements of the normal matrix can be calculated from (5.4.1) and (5.4.2). The complete matrix can be written

$$N = diag\left(N_0, N_1, .., N_m, ..., N_{L_{max}}\right) \tag{5.4.3}$$

wherein N_m is the m^{th} sub block. The inverse of (5.4.3) is given by

$$N^{-1} = diag\left(N_0^{-1}, N_1^{-1}, .., N_m^{-1}, ..., N_{L_{max}}^{-1}\right) \tag{5.4.4}$$

from which it can be seen that to invert the whole matrix it is necessary only to invert each of the smaller sub blocks.

To perform the inversions, use was made of the method of Cholesky factorisation (Burden and Clemence, 1989). The normal matrix and therefore all of the sub blocks are positive definite. A consequence of which is the possibility of writing

$$N_m = L_m L_m^T \tag{5.4.5}$$

where L_m is a lower triangular matrix called the Cholesky factor of N_m. The matrix L_m can be easily inverted and it's inverse used to calculate the inverse of N_m using (5.4.5). The elements of these inverted sub blocks are the variances and covariances of the coefficients and are used to determine the accuracy of the solution. Later in this chapter the diagonal elements of these matrices are used in the variance plots along with the eigenvalues of the covariance matrix.

If the eigenvalues of the matrix N^{-1} are λ_i with associated eigenvector $\mathbf{u}_i$, then

$$N^{-1}\mathbf{u}_i = \lambda_i \mathbf{u}_i. \tag{5.4.6}$$

and from elementary matrix theory

$$det\left(N^{-1} - \lambda_i I\right) = 0. \tag{5.4.7}$$

From the theory of determinants of block diagonal matrices this is equivalent to

$$\prod_{m=0}^{L_{max}} det\left(N_m^{-1} - \lambda_{i,m} I\right) = 0 \tag{5.4.8}$$

where $\lambda_{i,m}$ are the eigenvalues of the matrix N_m^{-1}. Therefore the eigenvalues can be considered independent of the eigenvalues of any other sub block. The eigenvalues of the covariance matrix are the extrema that the variance of a linear combination of coefficients can attain. Thus the maximum and minimum eigenvalues of a sub block N_m are bounds within which the variances of coefficients of order m lie.

Before presenting the results of these analyses approximate expressions for the signal equations for the planar and non planar cases will be obtained. They should be useful in helping to explain the results in later sections.

5.4.2 The signal for the planar case

For the planar case the satellites are assumed to be close so that the separation ΔF is small compared to an orbital revolution. For the purpose of discussion the simplification is made that the range rate residuals are due entirely to the difference in the along track velocity perturbations of the satellites. This implies that $\cos \Delta F = 1$ and $\sin \Delta F = 0$.

Hence, writing y and x for the minus along track and cross track coordinates

$$\frac{\partial RR_{calc\,i}}{\partial c_{lm\alpha}} = \frac{\partial \dot{y}_1}{\partial c_{lm\alpha}} - \frac{\partial \dot{y}_2}{\partial c_{lm\alpha}} \tag{5.4.9}$$

and differentiating equation (3.5.4)

$$\frac{\partial \dot{y}_\beta}{\partial c_{lm\alpha}} = \sum_{j=-l(2)}^{l} -\mathcal{Y}_{lmj} \sin\left(\dot{\psi}_{jm} t_i + \phi_{lm\alpha} + \psi_{jm}^{o\beta} + \frac{\pi}{2}\right) \tag{5.4.10}$$

where

$$\begin{aligned} \dot{\psi}_{jm} t_i &= \frac{2\pi N_{revs}}{T_{rep}} \left(j - \frac{N_{days}}{N_{revs}} m\right) i\Delta t \\ &= n_o \left(j - \frac{N_{days}}{N_{revs}} m\right) i\Delta t. \end{aligned} \tag{5.4.11}$$

The amplitude in (5.4.10) is derived from (3.5.8) as

$$\mathcal{Y}_{lmj} = \frac{\mu}{R^2} \left(\frac{R}{r}\right)^{l+2} F_{lmp} \left(\frac{j\left(\dot{\psi}_{jm}^2 + 3n_o^2\right) - 2\dot{\psi}_{jm} n_o (l+1)}{\dot{\psi}_{jm}\left(n_o^2 - \dot{\psi}_{jm}^2\right)} \right). \tag{5.4.12}$$

To develop (5.4.9) one takes

$$\begin{aligned} \psi_{jm}^{o1} + \psi_{jm}^{o2} &= 2\psi_{jm}^{o1} - \dot{\psi}_{jm} \frac{\Delta F}{n_o} \\ \psi_{jm}^{o1} - \psi_{jm}^{o2} &= \dot{\psi}_{jm} \frac{\Delta F}{n_o} \end{aligned} \tag{5.4.13}$$

where the temporal separation of the satellites is $\frac{\Delta F}{n_o}$. Substituting (5.4.10) in (5.4.9) and using (5.4.13)

$$\begin{aligned} \frac{\partial RR_{calc\,i}}{\partial c_{lm\alpha}} &= \sum_{j=-l(2)}^{l} \mathcal{Y}_{lmj} \left(\sin^2\left(\dot{\psi}_{jm} \frac{\Delta F}{2n_o}\right) \cos\left(\dot{\psi}_{jm} t_i + \phi_{lm\alpha} + \psi_{jm}^{o1}\right) \right. \\ &+ \left. \sin\left(\dot{\psi}_{jm} \frac{\Delta F}{2n_o}\right) \cos\left(\dot{\psi}_{jm} \frac{\Delta F}{2n_o}\right) \sin\left(\dot{\psi}_{jm} t_i + \phi_{lm\alpha} + \psi_{jm}^{o1}\right) \right). \end{aligned} \tag{5.4.14}$$

From equation (5.4.14) it can be seen that the important factors in determining the sensitivity of the range rate signal to an error in $c_{lm\alpha}$ are:-

- The functions $\mathcal{Y}_{lmj}$ which describe the relation between the amplitude and the frequency for a coefficient of degree l and order m. These determine the response of the along track velocity to oscillations in the radial and along track gravity forcing terms and depend critically on the height and inclination of a satellite in a circular orbit.

- The separation in the form of the factors $\sin^2\left(\dot{\psi}_{jm}\frac{\Delta F}{2n_o}\right)$ and $\sin\left(\dot{\psi}_{jm}\frac{\Delta F}{2n_o}\right)\cos\left(\dot{\psi}_{jm}\frac{\Delta F}{2n_o}\right)$. For certain separations ΔF and for certain frequencies determined by j and m the signal could, due to these factors, become greatly reduced.

In the non-planar case these formulae are not valid. In particular the additional cross track terms will depend on the cross track inclination functions discussed in chapter 3. Equations (5.4.13) are no longer valid either. A similar expression to (5.4.14) will now be derived for the non planar case.

5.4.3 Signal for the non planar case

It was seen in chapter 4 that the non-planar case is more complicated than when the satellites share the same plane as in the previous section. If the cross track separation is quite small compared to the along track separation then one can assume for the purposes of discussion that the signal is made up entirely of along track and cross track velocity errors. Using the result from chapter 3 this amounts to assuming

$$\begin{aligned} V_{X,i\beta} &= 0,\ \forall i,\beta \\ V_{ij} &= 0,\ \forall i,\beta \\ \mathbf{h}_{3\beta}.\mathbf{e}_{12} &= 0,\ \beta = 1,2. \end{aligned} \tag{5.4.15}$$

Furthermore it is assumed, after consideration of Figure 4.3.2, that

$$\begin{aligned} \mathbf{h}_{1\beta}.\mathbf{e}_{12} &= q\sin n_o t,\ \beta = 1,2. \\ \mathbf{h}_{2\beta}.\mathbf{e}_{12} &= -1,\ \beta = 1,2. \end{aligned} \tag{5.4.16}$$

Then from (4.4.34) and (4.4.35)

$$\begin{aligned}\mathcal{A}_{lm\alpha j} &= \Lambda^{11}_{lm\alpha j} - \Lambda^{12}_{lm\alpha j} + \Lambda^{21}_{lm\alpha j} - \Lambda^{22}_{lm\alpha j} \\ \mathcal{B}_{lm\alpha j} &= \Gamma^{11}_{lm\alpha j} - \Gamma^{12}_{lm\alpha j} + \Gamma^{21}_{lm\alpha j} - \Gamma^{22}_{lm\alpha j}.\end{aligned} \tag{5.4.17}$$

The last two terms in these equations are the along track contributions and are therefore in the form of (5.4.14) but in this case (5.4.13) are replaced by

$$\begin{aligned}\psi^{o1}_{jm} + \psi^{o2}_{jm} &= 2\psi^{o1}_{jm} - \dot{\psi}_{jm}\frac{\Delta F}{n_o} + m\Delta\Omega \\ \psi^{o1}_{jm} - \psi^{o2}_{jm} &= \dot{\psi}_{jm}\frac{\Delta F}{n_o} - m\Delta\Omega\end{aligned} \tag{5.4.18}$$

where $\Delta\Omega$ is the difference in right ascension of the satellites (positive for satellite 1 having greatest right ascension). Thus writing

$$\dot{\psi}_{jm}\frac{\Delta F}{n_o} - m\Delta\Omega = \hat{\phi}_{jm} \tag{5.4.19}$$

then the contribution from the along track terms can be written

$$\begin{aligned}\left(\frac{\partial RR_{calc\,i}}{\partial c_{lm\alpha}}\right)_{alongtrack} &= \sum_{j=-l(2)}^{l} \mathcal{Y}_{lmj}\left(\sin^2\left(\frac{\hat{\phi}_{jm}}{2}\right)\cos\left(\dot{\psi}_{jm}t_i + \phi_{lm\alpha} + \psi^{o1}_{jm}\right)\right. \\ &+ \left.\sin\left(\frac{\hat{\phi}_{jm}}{2}\right)\cos\left(\frac{\hat{\phi}_{jm}}{2}\right)\sin\left(\dot{\psi}_{jm}t_i + \phi_{lm\alpha} + \psi^{o1}_{jm}\right)\right).\end{aligned} \tag{5.4.20}$$

This leaves the cross track contribution

$$\begin{aligned}\left(\frac{\partial RR_{calc\,i}}{\partial c_{lm\alpha}}\right)_{acrosstrack} &= \left(\Lambda^{11}_{lm\alpha j} - \Lambda^{12}_{lm\alpha j}\right)\cos\left(\dot{\psi}_{jm}t\right) \\ &+ \left(\Gamma^{11}_{lm\alpha j} - \Gamma^{12}_{lm\alpha j}\right)\sin\left(\dot{\psi}_{jm}t\right)\end{aligned} \tag{5.4.21}$$

and from equations (4.4.36), (4.4.37), (4.4.42)

$$\begin{aligned}\Lambda^{1\beta}_{lm\alpha j} &= \frac{-q}{2}\left(\mathcal{X}_{lmj}\cos\left(\phi_{lm\alpha} + \psi^{o\beta}_{jm} + \frac{\pi}{2}\right) - \mathcal{X}_{lmj+2}\cos\left(\phi_{lm\alpha} + \psi^{o\beta}_{j+2m} + \frac{\pi}{2}\right)\right) \\ \Gamma^{1\beta}_{lm\alpha j} &= \frac{q}{2}\left(\mathcal{X}_{lmj}\sin\left(\phi_{lm\alpha} + \psi^{o\beta}_{jm} + \frac{\pi}{2}\right) - \mathcal{X}_{lmj+2}\sin\left(\phi_{lm\alpha} + \psi^{o\beta}_{j+2m} + \frac{\pi}{2}\right)\right)\end{aligned} \tag{5.4.22}$$

where, from (3.5.7) it can be deduced that

$$\mathcal{X}_{lmj} = \frac{\mu}{R^2}\left(\frac{R}{r}\right)^{l+2} F^*_{lmp}\left(\frac{\dot{\psi}_{jm}}{\left(n_o^2 - \dot{\psi}_{jm}^2\right)}\right). \tag{5.4.23}$$

After a little simplification (5.4.21) becomes

$$\begin{aligned}
\left(\frac{\partial RR_{calc\,i}}{\partial c_{lm\alpha}}\right)_{acrosstrack} &= \frac{q\mathcal{X}_{lmj}}{2}\left(\sin^2\frac{\hat{\phi}_{jm}}{2}\right)\cos\left(\dot{\psi}_{jm}t_i + \phi_{lm\alpha} + \psi^{o1}_{jm}\right) \\
&+ \frac{q\mathcal{X}_{lmj}}{2}\left(-\sin\frac{\hat{\phi}_{jm}}{2}\cos\frac{\hat{\phi}_{jm}}{2}\right)\sin\left(\dot{\psi}_{jm}t_i + \phi_{lm\alpha} + \psi^{o1}_{jm}\right) \\
&+ \frac{q\mathcal{X}_{lmj+2}}{2}\left(\sin^2\frac{\hat{\phi}_{j+2m}}{2}\right)\cos\left(\dot{\psi}_{jm}t_i + \phi_{lm\alpha} + \psi^{o1}_{j+2m}\right) \\
&+ \frac{q\mathcal{X}_{lmj+2}}{2}\left(-\sin\frac{\hat{\phi}_{j+2m}}{2}\cos\frac{\hat{\phi}_{j+2m}}{2}\right) \\
&\times \sin\left(\dot{\psi}_{jm}t_i + \phi_{lm\alpha} + \psi^{o1}_{j+2m}\right).
\end{aligned} \tag{5.4.24}$$

Equation (5.4.24) and (5.4.20) are the main terms that affect range rate residuals in this non planar case, namely

$$\begin{aligned}
\frac{\partial RR_{calc\,i}}{\partial c_{lm\alpha}} &= \left(\frac{\partial RR_{calc\,i}}{\partial c_{lm\alpha}}\right)_{alongtrack} + \left(\frac{\partial RR_{calc\,i}}{\partial c_{lm\alpha}}\right)_{acrosstrack} \\
&= \frac{\mathcal{Y}_{lmj} + q\mathcal{X}_{lmj}}{2}\left(\sin^2\frac{\hat{\phi}_{jm}}{2}\right)\cos\left(\dot{\psi}_{jm}t_i + \phi_{lm\alpha} + \psi^{o1}_{jm}\right) \\
&+ \frac{\mathcal{Y}_{lmj} - q\mathcal{X}_{lmj}}{2}\left(\sin\frac{\hat{\phi}_{jm}}{2}\cos\frac{\hat{\phi}_{jm}}{2}\right)\sin\left(\dot{\psi}_{jm}t_i + \phi_{lm\alpha} + \psi^{o1}_{jm}\right) \\
&+ \frac{q\mathcal{X}_{lmj+2}}{2}\left(\sin^2\frac{\hat{\phi}_{j+2m}}{2}\right)\cos\left(\dot{\psi}_{jm}t_i + \phi_{lm\alpha} + \psi^{o1}_{j+2m}\right) \\
&+ \frac{q\mathcal{X}_{lmj+2}}{2}\left(-\sin\frac{\hat{\phi}_{j+2m}}{2}\cos\frac{\hat{\phi}_{j+2m}}{2}\right)\sin\left(\dot{\psi}_{jm}t_i + \phi_{lm\alpha} + \psi^{o1}_{j+2m}\right).
\end{aligned} \tag{5.4.25}$$

Equation (5.4.25) explains the effect on the errors of the coefficients due to the choice of separations ΔF, $\Delta\Omega$.

5.5 Results for the planar case

Using the method outlined in section 5.4.1 the expected variances of the coefficients, and the eigenvalues of the inverted normal matrices were calculated and the results presented in the following sections for various mission orientations. The details of the repeat orbit used and the measurement accuracy assumed were discussed in section 5.4.1. The satellites are in repeat orbits in which they perform 323 orbital revolutions in 20 revolutions of the ascending node. The accuracy of the observations is $\sigma = 0.1mm/sec$ and they are made every 3 seconds. The orbital heights and inclinations are always common to both spacecraft, and unless it is stated otherwise the orbital height is taken to be $6605km$ above the geocentre. The inclinations will either be 91 or 96 degrees. Throughout this section only the coplanar case is discussed.

5.5.1 The height of the satellites

The effect of the height of the satellites on the coefficients is illustrated with the variances plotted in Figures 5.5.4, 5.5.5, 5.5.6 and 5.5.7 for heights of 6605, 6625, 6645, and 6665km. The separation is 2.0 degrees and the inclinations are 91 degrees for all cases . The factor $\left(\frac{R}{r}\right)^{l+2}$ affects the amplitudes of the Range Rate Residuals, so an increase in the common height will result in coefficients of higher degree having reduced effect on the signal to the extent that such coefficients should have greater errors. This is clear from Figures 5.5.4 to 5.5.7 where the errors of the high degree terms are seen to increase quite dramatically with a modest height increase, underlining the importance of low satellite orbits in this high resolution gravity recovery. The remainder of the error analyses are therefore only presented for a height of 6605km above the geocentre.

5.5.2 The inclination of the satellites

To examine what effect the inclination has on the recovery 4 error analyses were carried out. Since a near polar orbit is needed for a global recovery, values of 91 degrees (called a polar orbit) and 96 degrees (called a non polar orbit) were chosen for the inclinations. Separations of 2 and 4 degrees along track are used for each value of the inclination.

The variances of the coefficients are presented in Figures 5.5.4 and 5.5.15 for the polar orbit and 5.5.8 and 5.5.9 for the non polar orbit. For the non polar orbit all the $m = 0$ (zonal) coefficients have large variances and so would be poorly recovered. This is not the case when the orbits are polar. Comparing Figures 5.5.4 with 5.5.8 one can see a degradation in the accuracy of the high degree and order coefficients in 5.5.4, when the inclination is closer to 90°

Figure 5.5.1 show the eigenvalues of the inverted normal matrix for these missions. The Figures show that with a 2 degree separation the polar orbit solution is less well determinable for higher orders, since the eigenvalues of the higher order sub blocks are greater when the orbit is polar. The 4 degree separation cases show that the non polar orbit is not as good as the polar orbit for determining the lower order coefficients.

Putting the satellites into the non polar orbit affects the zonals partly because of the data gap in the polar regions. However the absence of data at the poles increases the density of data elsewhere and as a result the accuracy of the higher order coefficients evidently increases. This explains the effect of the inclination in part but a major influence is due to the inclination functions. The inclination functions help describe how a given spherical harmonic affects the perturbations of the satellite's motion in the orbital plane at a certain frequency. For a polar orbit the zonals have a strong effect in the orbital plane and none perpendicular to it. As the orbit becomes less polar , the proportion of the zonals power in the

orbital plane decreases.

p	$F_{20,0,p}$ (91°)	$F_{20,0,p}$ (96°)
0	0.8003	0.7192
1	-0.4056	-0.2140
2	0.3092	0.0723
3	-0.2625	-0.0007
4	0.2348	-0.0415
5	-0.2166	0.0682
6	0.2042	-0.0855
7	-0.1958	0.0967
8	0.1903	-0.1036
9	-0.1872	0.1074
10	0.1862	-0.1086
11	-0.1872	0.1074
12	0.1903	-0.1036
13	-0.1958	0.0967
14	0.2042	-0.0855
15	-0.2166	0.0682
16	0.2348	-0.0415
17	-0.2625	-0.0007
18	0.3092	0.0722
19	-0.4056	-0.2140
20	0.8003	0.7192

Table 5.5.1

zonal inclination functions

This can be seen by the fact that the F_{l0p} which account for the high frequency part of the range rate signal (high and low values of p) are generally greater as the orbital inclination tends to being polar, see Table 5.5.1, $p = 2, 3, .., 7, 13, ..20$. The zonal coefficients are therefore stronger in the higher frequency part of their Range Rate spectra for a polar orbit and weaker for a non polar orbit. These frequencies are important for the accurate recovery of the coefficients partly because the signal from equations (5.4.12) and (5.4.14) is sensitive to high frequency oscillations in the gravity field. If these oscillations are smaller along one orbit then with that orbit the recovery of the coefficients will be degraded.

More importantly the loss of signal at high frequencies may increase the correlations between the coefficients $c_{lm\alpha}, c_{l-2m\alpha}$ and $c_{l-4m\alpha}$ etc. The distinct frequencies which are important in the separation of these terms are those with j close to $\pm l$.

To choose the inclination for a gravity field recovery one must trade accuracy in the zonals with accuracy in the high order coefficients (cf Figures 5.5.4 and 5.5.8). The higher order terms and in particular the sectorials have a long wavelength variation with latitude and a short wavelength variation with longitude. For a polar orbit this longitude or cross track information is not represented in the orbital plane whereas for non polar orbits this signal does effect the in orbit perturbations. This could explain the higher errors in these near sectorials for the polar orbit. It seems however that the effect of the inclination on the zonals is so great it would be wise to use a polar orbit. The loss of accuracy in the high order coefficients could perhaps be reduced if the cross track velocities contributed to the line of sight velocity.

5.5.3 The separation of the satellites

The discussion on how a certain frequency can affect the recovery of a coefficient is related to how the along track separation affects the recovery because the higher frequency parts of the spectrum are attenuated first as the separation is increased. As ΔF approaches the wavelength of a gravity signal term, both satellites begin to be affected by these frequencies in harmony. Such in phase motion results in the relative velocity being unaffected at this frequency. The frequency is said to have been attenuated.

From equation (5.4.14) it is clear that this will occur when

$$\sin^2\left(\dot{\psi}_{jm}\frac{\Delta F}{2n_o}\right) = 0$$

and

$$\cos\left(\dot{\psi}_{jm}\frac{\Delta F}{2n_o}\right)\sin\left(\dot{\psi}_{jm}\frac{\Delta F}{2n_o}\right) = 0.$$

That is

$$\sin\left(\dot{\psi}_{jm}\frac{\Delta F}{2n_o}\right) = 0 \tag{5.5.1}$$

and so

$$\dot{\psi}_{jm}\frac{\Delta F}{2n_o} = \pm k\pi. \quad k = 0, 1, 2, .. \tag{5.5.2}$$

Now from (5.4.11) this condition is

$$\left(j - \frac{N_{days}}{N_{revs}}m\right)\Delta F = \pm 2k\pi, \quad k = 0, 1, 2, .. \tag{5.5.3}$$

Writing $\Delta F = \frac{2\pi}{N}$ then for the case in hand

$$j - \frac{20}{323}m = \pm kN, \quad k = 0, 1, 2, .. \tag{5.5.4}$$

For $k = 0$ slowly varying gravity terms are weak in the Range Rate signal regardless of the separation chosen. When $k = 1$ attenuation will occur for frequencies $\dot{\psi}_{jm}$ for which Equation (5.5.4) holds.

The common heights of the satellites are all $6605km$ and all have an inclination of 91 degrees. To illustrate a full range of separations Equation (5.5.4) is used to find the critical separation at which attenuation of the highest frequencies will occur. For $L_{max} = 120$ the maximum frequency is, using (5.5.4) $|-120-\frac{20}{323}120| \approx$ 127.5 cycles per revolution. Using k=1 in (5.5.4) gives $N \approx 128$. From Table 5.5.2 this implies that $\Delta F = 2.8$ degrees is the lowest separation at which attenuation will occur. The inverse normal matrices were calculated, and the variances and eigenvalues obtained, for separations of 1.2, 1.6, 2.0, 2.4, 2.8, 3.0 4.0 and 6.0 degrees. The variances are displayed in Figures 5.5.4 and 5.5.10 to 5.5.17 and the eigenvalues in figures 5.5.2, 5.5.3. When the separation is less than 2.8 degrees there is no attenuation and from Figures 5.5.4 and 5.5.10 to 5.5.16 the coefficients which are determined with the least accuracy are those with high degree and order, that is when $m > 50$ or so. This is a consequence of the polar orbit. However it seems from Figures 5.5.4 and 5.5.12 that the variances of the coefficients with greater order are reduced by increasing the separations to $\Delta F = 2.0$ and 2.4 degrees. The eigenvalues displayed in Figure 5.5.2 also indicate an improved solution for higher orders as the separation reaches those values.

ΔF (degrees)	N
1.2	300
1.6	225
2.0	180
2.4	150
2.8	128.6
3.0	120
4.0	90
5.0	75
6.0	60

Table 5.5.2

N versus ΔF

When the separation is greater than or equal to 2.8 degrees, the variances in Figures 5.5.13 to 5.5.17 show that certain coefficient's accuracies are strongly degraded. Other coefficients are determined with greater accuracy for these separations. In Figures 5.5.13 and 5.5.14 the separations are 2.8 and 3 degrees. These graphs show that the coefficients of degree near 120 and order close to zero are affected. The eigenvalues for these cases show in Figure 5.5.3 that the lower orders are poorly determined.

As the separation is increased to 4, 5 and 6 degrees in Figures 5.5.15, 5.5.16, 5.5.17 the degree at which the zonal coefficients are affected most strongly have $l \approx N$ for each case. Thus these coefficients have their highest frequencies attenuated since the highest frequencies in each case satisfy equation (5.5.4) with $k = 1$, ie for $\Delta F = 4°, N = 90$ the zonals have their frequency $\dot{\psi}_{\pm 90,0}$ attenuated. This is the maximum frequency of the $l = 90$ zonal coefficients. In section 5.5.2 the importance of these largest frequencies in the recovery of a coefficient was discussed, the same reasoning applies here to explain why the loss of just one frequency can so adversely affect the recovery of certain coefficients.

The higher order coefficients are attenuated at a higher degree than the zonals. In fact from Figures 5.5.15, 5.5.16, 5.5.17 the so called attenuation bands are U-shaped. This can be explained by remembering that for the polar orbits used here, the highest frequencies of the higher order coefficients are weak. Therefore the loss of a frequency due to attenuation will not affect the higher order coefficients at the same degree as the lower order coefficients. The coefficients of higher order

for a given degree will rely on the same frequencies (values of j) as a lower degree zonal. In Figure 5.5.17 there are two attenuation bands corresponding to $k = 1, 2$. Therefore the frequencies affected are 60 and 120 times per revolution (Table 5.5.2 and Equation (5.5.4)). For $m = 0$ this gives $j = \pm 60, \pm 120$ and these two groups of frequencies will affect coefficients of degree 120 in a similar way to the 3° case, and will also affect the U-shaped band of coefficients containing the zonals of degree 60. Whilst some coefficients are more poorly determined with larger separations ,the lower frequency terms and therefore lower degree coefficients are better determined than with smaller separations. In the $\Delta F = 6$ case (figure 5.5.17 there is a zone of coefficients with lower errors between the attenuation zones. For these terms it seems the separation best suits their important frequencies.

The eigenvalues for these examples are shown in Figures 5.5.3. They all show the low order deficiencies and indeed that beyond a 3.0° separation the mid and even higher orders can be severely affected.

From these analyses one could say that if a single separation was to be used, then for recovery of coefficients up to degree and order 120 a separation along track of 2.4° would be best overall. Some coefficients would be better determined with a greater separation but only at the expense of others. Perhaps the best overall solution would be obtained with a number of different separations within the same mission.

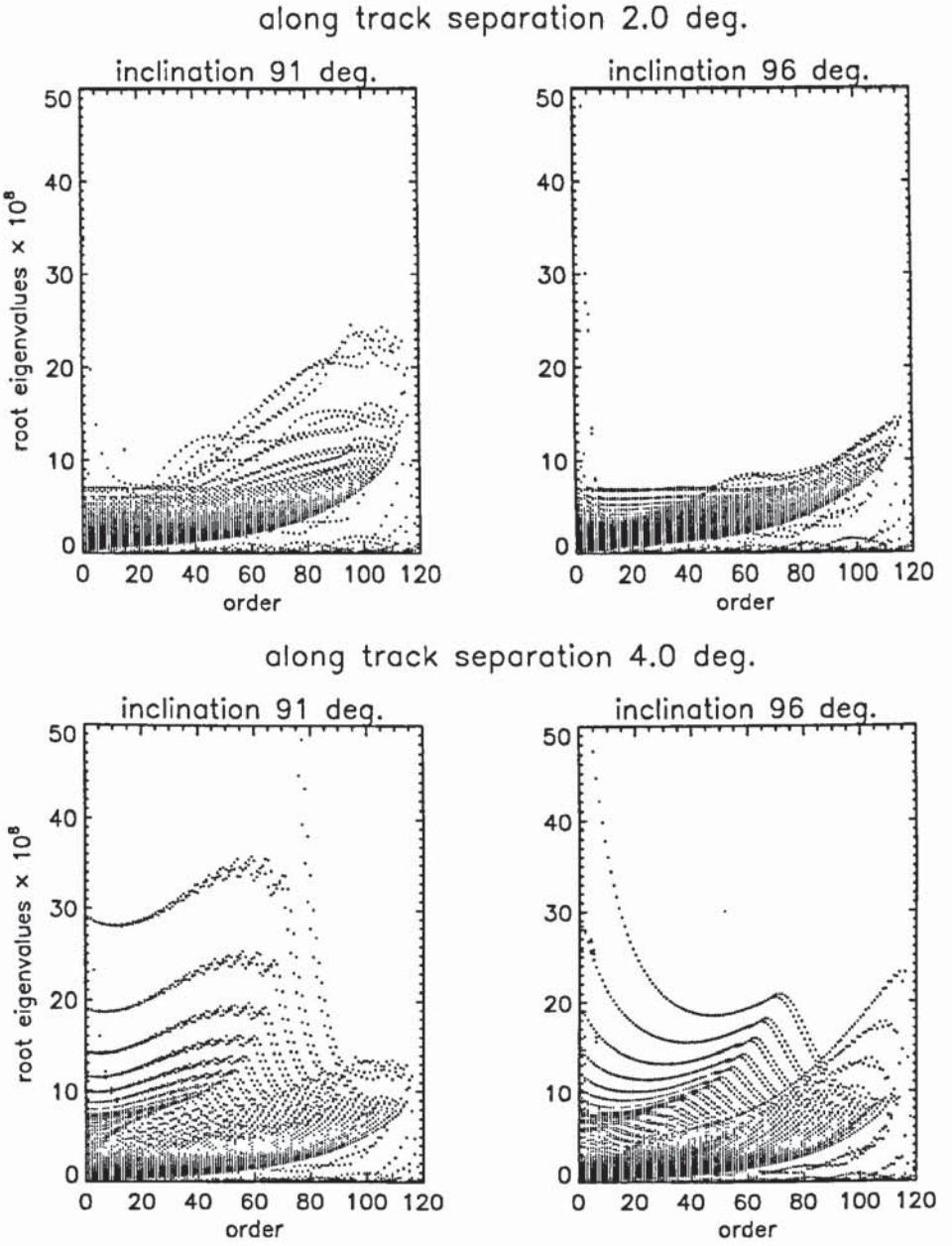

FIGURES 5.5.1 These eigenvalue plots illustrate the effect of a non polar orbit on the eigenvalues of the coefficients to be recovered.

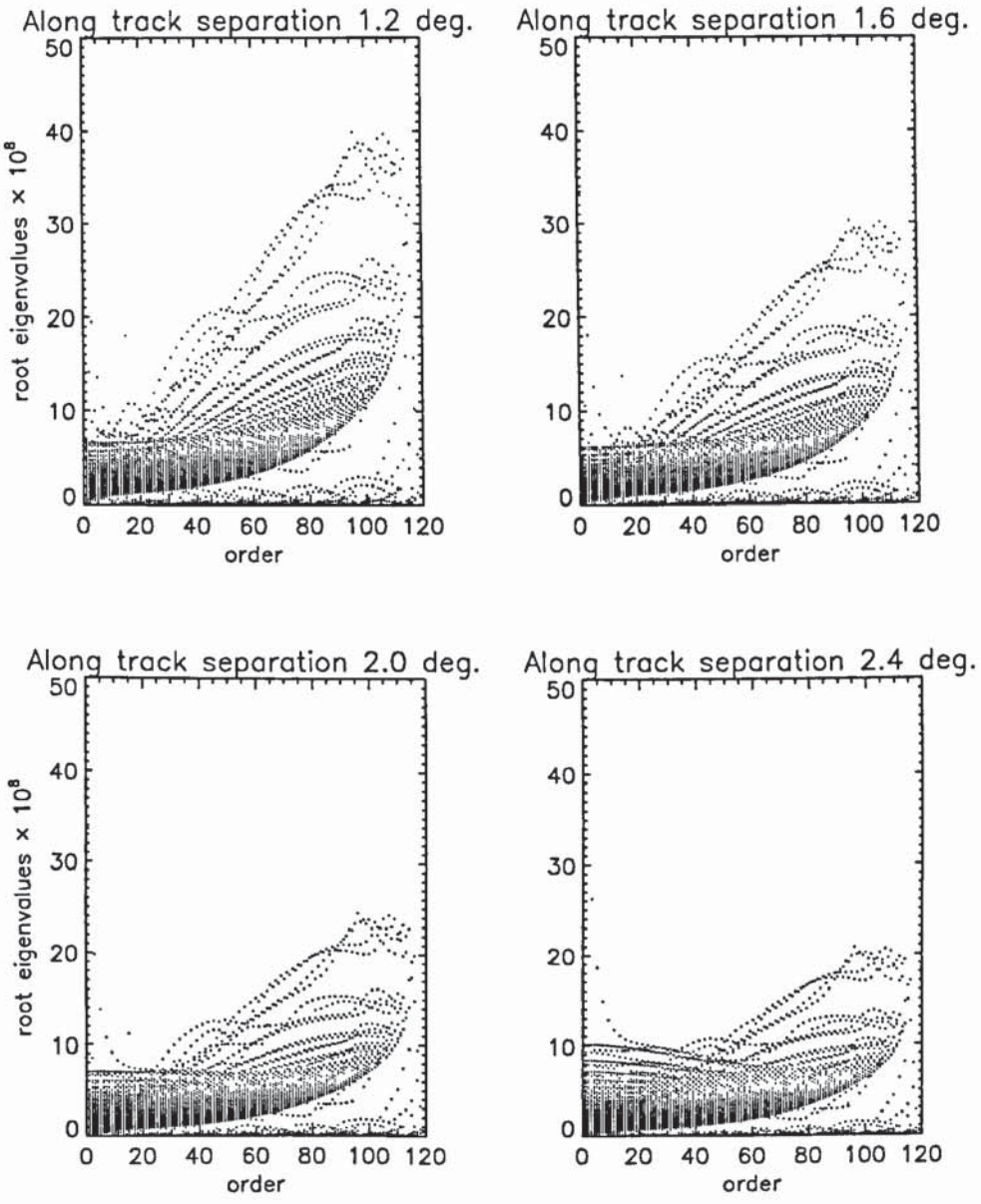

FIGURES 5.5.2 The eigenvalues for a range of separations less than the wavelengths measured. The inclinations are all 91 degrees.

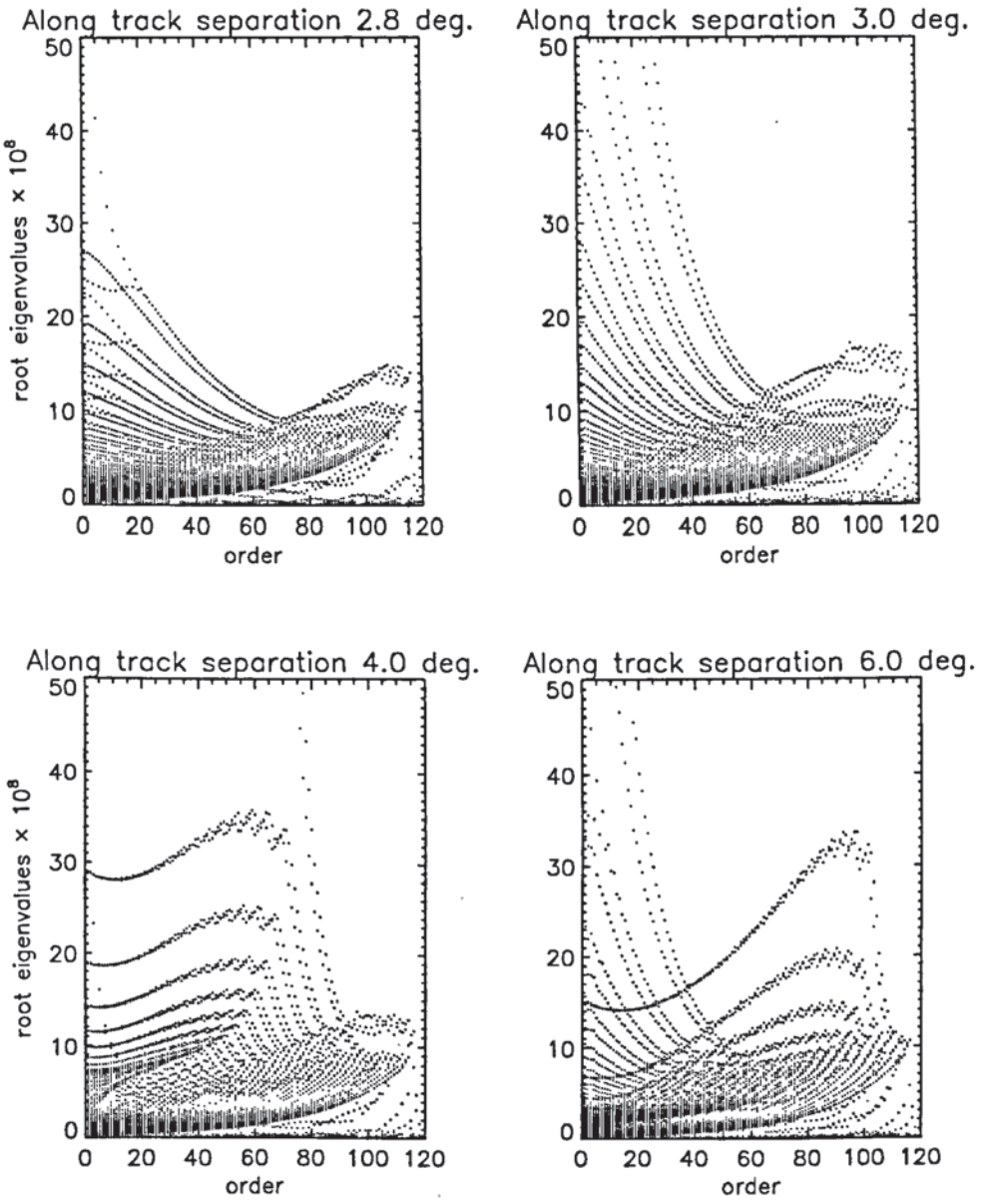

FIGURES 5.5.3 The eigenvalues for a range of separations equal to or greater than the wavelengths measured. The inclinations are all 91 degrees.

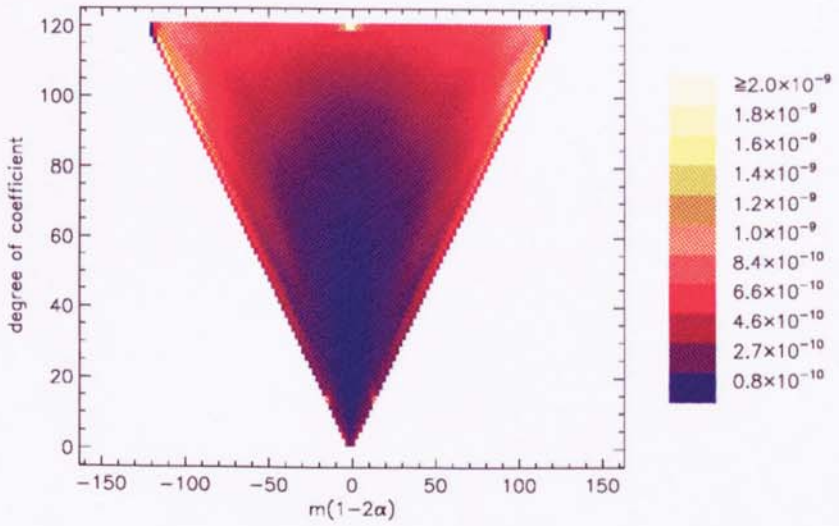

Figure 5.5.4

Root Variances of Gravity coefficients. $\Delta F = 2.0°, \Delta\Omega = 0.0°$ (height above geocentre=6605km)

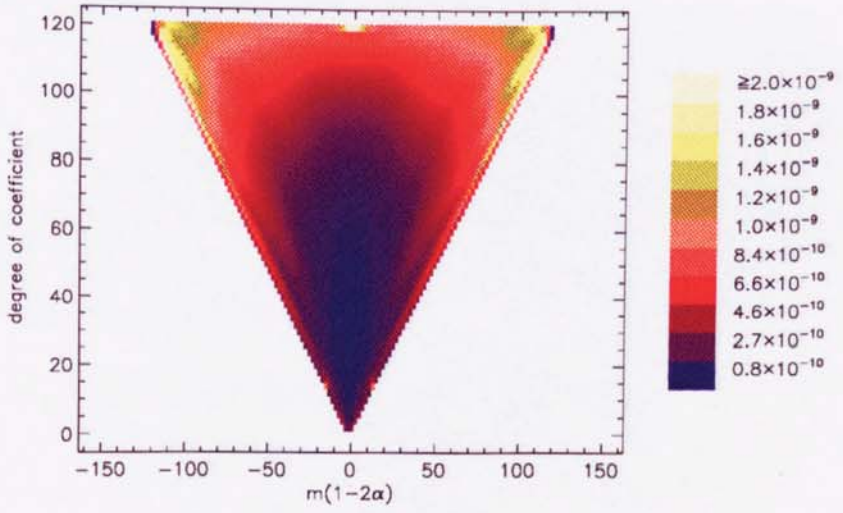

Figure 5.5.5

Root Variances of Gravity coefficients. $\Delta F = 2.0°, \Delta\Omega = 0.0°$ (height above geocentre=6625km)

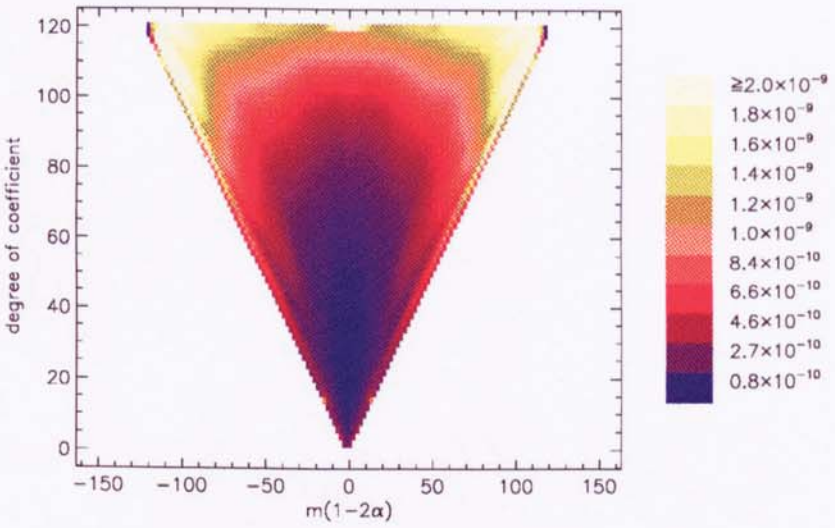

Figure 5.5.6

Root Variances of Gravity coefficients. $\Delta F = 2.0°, \Delta\Omega = 0.0°$ (height above geocentre=6645km)

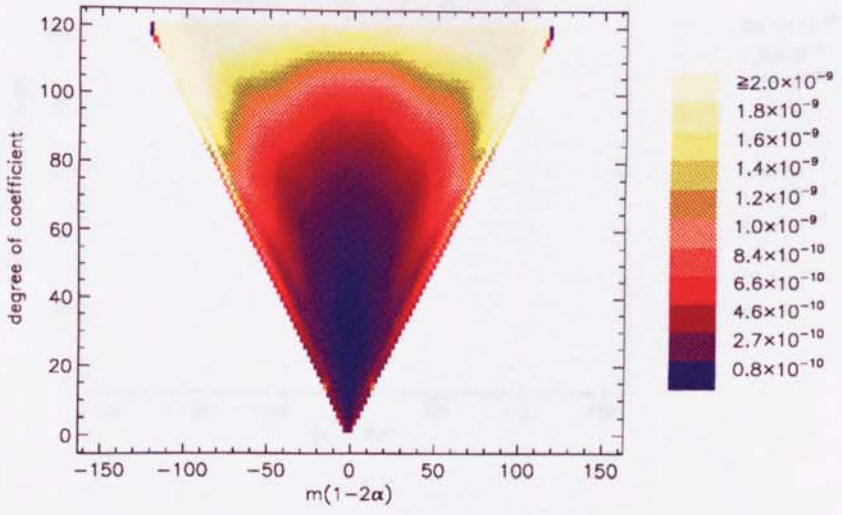

Figure 5.5.7

Root Variances of Gravity coefficients. $\Delta F = 2.0°, \Delta\Omega = 0.0°$ (height above geocentre=6665km)

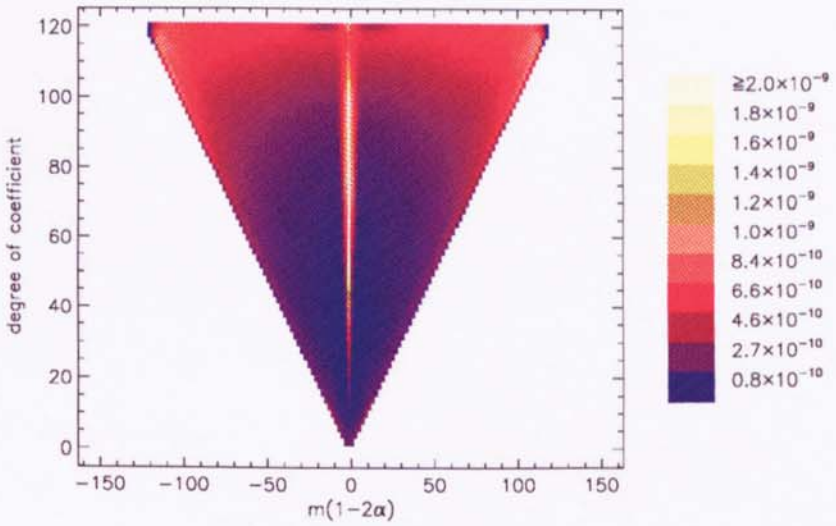

Figure 5.5.8

Root Variances of Gravity coefficients.$\Delta F = 2.0°, \Delta\Omega = 0.0°$ (inclination=96°)

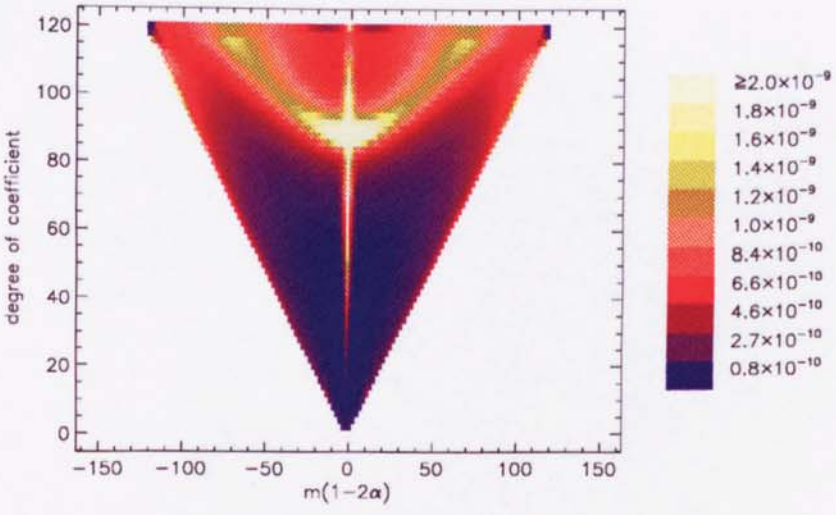

Figure 5.5.9

Root Variances of Gravity coefficients.$\Delta F = 4.0°, \Delta\Omega = 0.0°$ (inclination=96°)

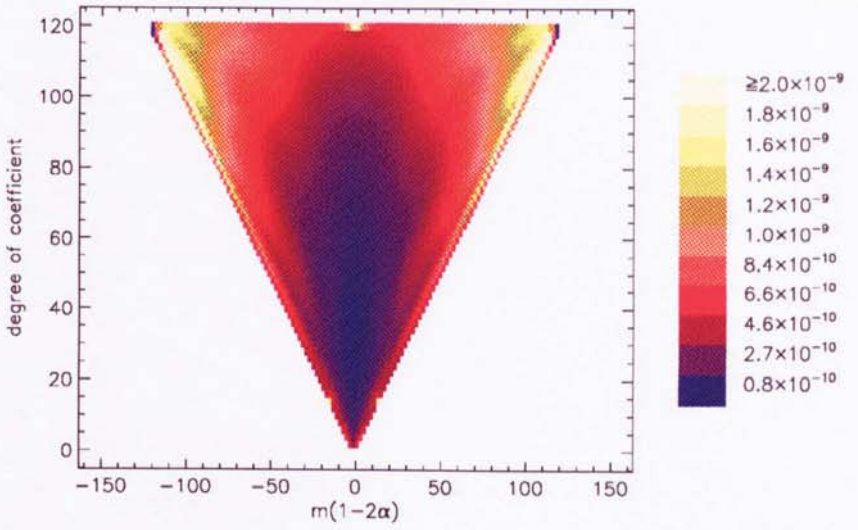

Figure 5.5.10

Root Variances of Gravity coefficients.$\Delta F = 1.2°, \Delta\Omega = 0.0°$

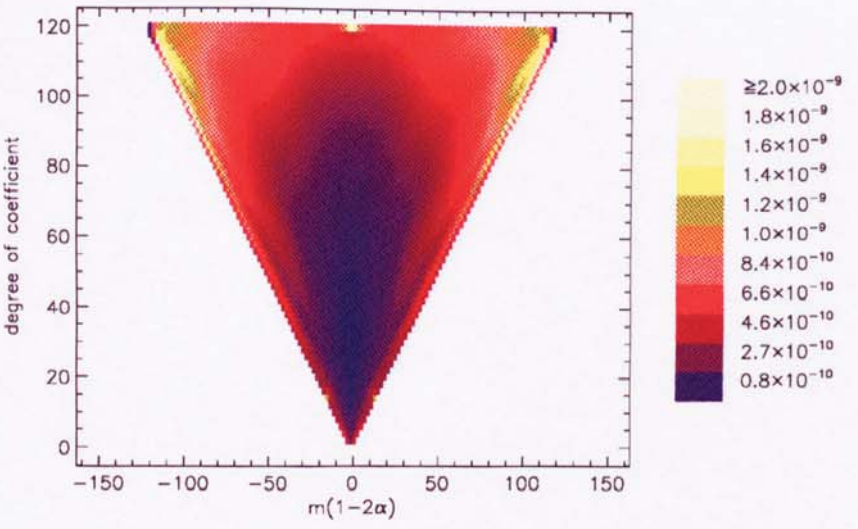

Figure 5.5.11

Root Variances of Gravity coefficients.$\Delta F = 1.6°, \Delta\Omega = 0.0°$

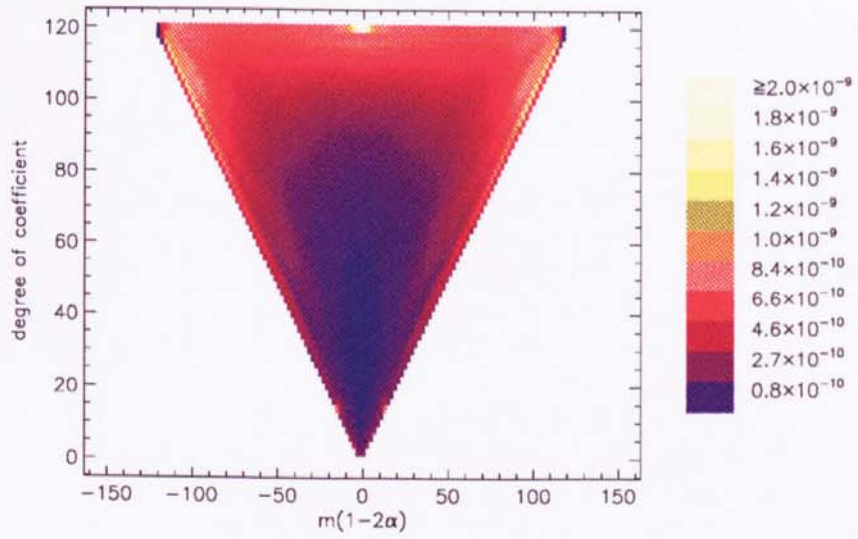

Figure 5.5.12

Root Variances of Gravity coefficients.$\Delta F = 2.4°, \Delta\Omega = 0.0°$

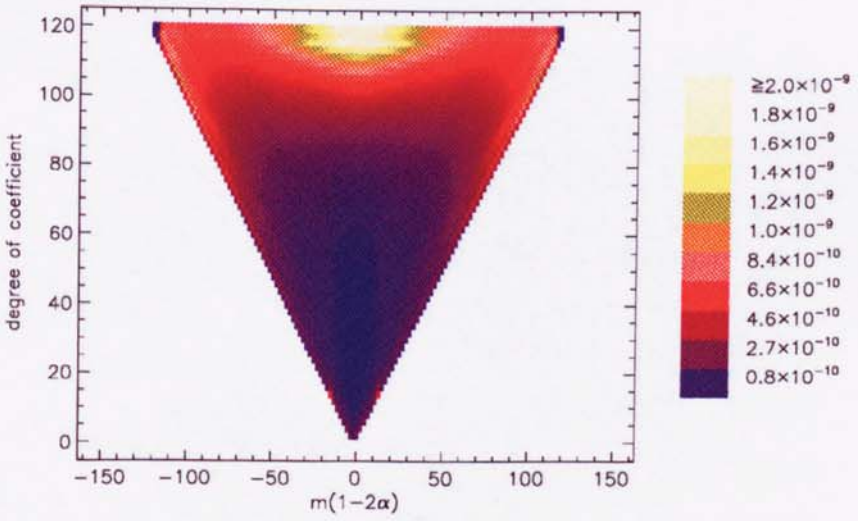

Figure 5.5.13

Root Variances of Gravity coefficients.$\Delta F = 2.8°, \Delta\Omega = 0.0°$

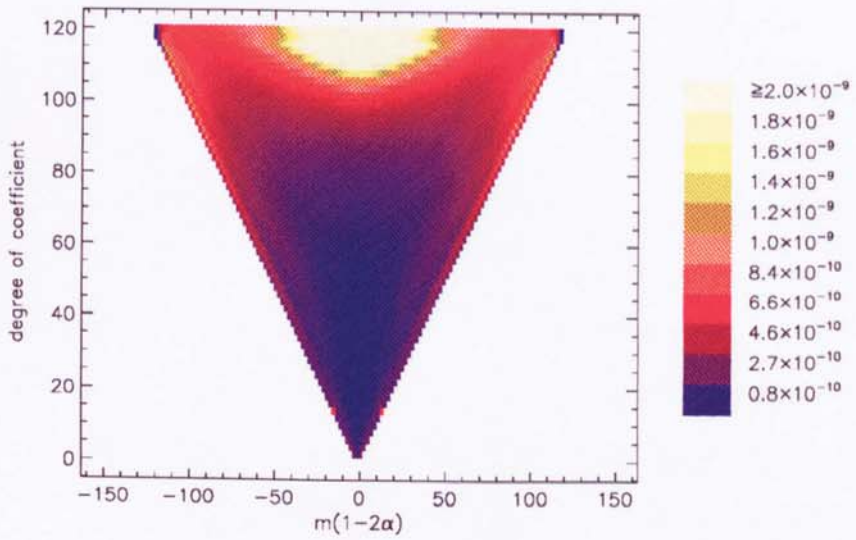

Figure 5.5.14

Root Variances of Gravity coefficients.$\Delta F = 3.0°, \Delta\Omega = 0.0°$

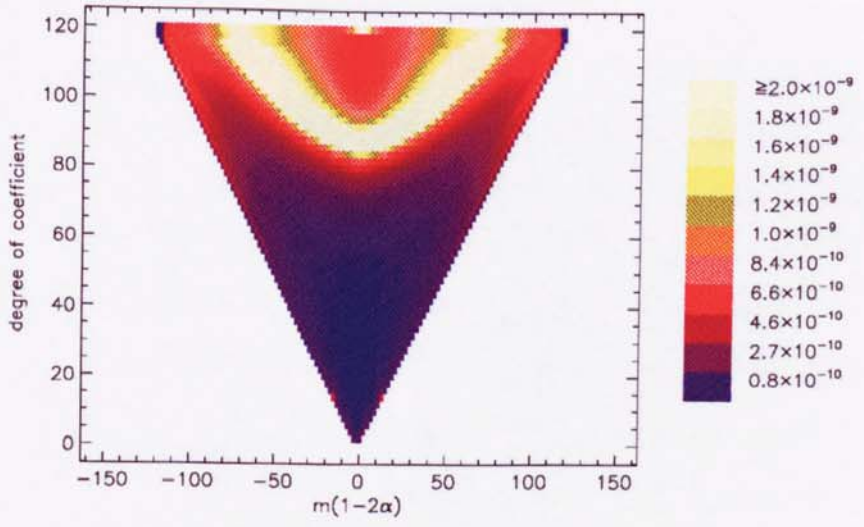

Figure 5.5.15

Root Variances of Gravity coefficients.$\Delta F = 4.0°, \Delta\Omega = 0.0°$

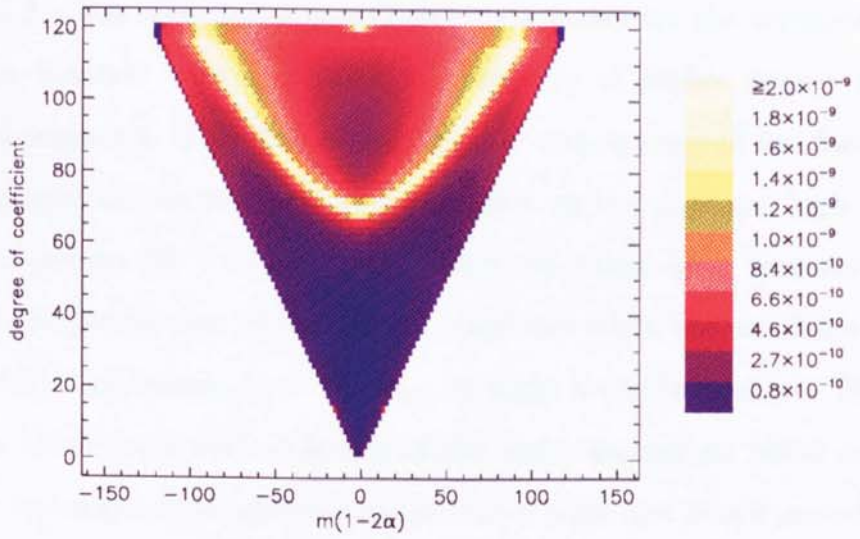

Figure 5.5.16

Root Variances of Gravity coefficients.$\Delta F = 5.0°, \Delta\Omega = 0.0°$

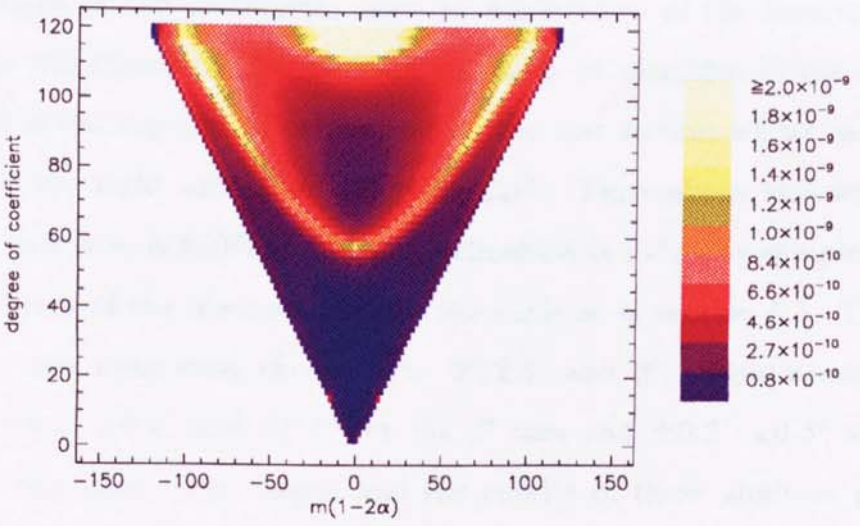

Figure 5.5.17

Root Variances of Gravity coefficients.$\Delta F = 6.0°, \Delta\Omega = 0.0°$

5.6 Results for the non planar case

In section 5.5.2 it was seen that a polar orbit is necessary for the accurate recovery of the zonals, however with this orbit the recovery of higher degree and order coefficients is degraded. This was explained as a consequence of the fact that the coefficients in question do not have a strong effect on the in-plane, high frequency orbital perturbations for a polar orbit. They do cause high frequency orbital perturbations perpendicular to the orbital plane but when the satellites share the same plane their contribution to the line of sight velocity is zero. By putting the satellites into orbits with different initial right ascensions these cross track velocities are no longer perpendicular to the line of sight and hence provide a useful contribution to the range rate signal. In particular this means that if the satellites are in polar orbits and have different right ascensions of their ascending nodes then the range rate has high frequency signal contributions from both higher order terms and zonals. To determine the extent that this helps the recovery procedure is the subject of this section.

The variances of the coefficients and the eigenvalues of the inverted normal matrices were calculated for Range Rate residuals of satellites in the same 323 revolution, 20 nodal day repeat orbits used in the last section whilst using a non zero value for the right ascension difference $\Delta\Omega$. Throughout this section the height of the satellites is 6605km and the inclination is 91°. The sample rate and the standard error of the observations are the same as in section 5.5. The values of the along track separation chosen were $2°, 2.4°$ and $3°$. Separations in right ascension of $\pm 0.1°, \pm 0.2°$ and $\pm 0.3°$ for the $2°$ case and $\pm 0.2°, \pm 0.3°$ and $\pm 0.4°$ for the other two cases were chosen and the results of these analyses presented as variances of coefficients in figures (5.6.4) to (5.6.21) and as eigenvalues of the inverted normal matrices in figures (5.6.1) to (5.6.3). These results should be compared to the planar cases of equal along track separation from the previous

section.

From Figures 5.6.5, 5.6.7 to 5.6.21 (odd nos.) one can see that there is a significant improvement in the expected errors of the higher degree and order coefficients when a negative right ascension difference is introduced, that is when the trailing satellites right ascension is increased beyond that of the first satellite. These cases also show that there is no improvement in the coefficients of low order. Furthermore as $\Delta\Omega$ becomes more negative, the better the improvement to these coefficients. The eigenvalues in Figures 5.6.1, 5.6.2, 5.6.3 of the higher order sub blocks for these cases are found to be reduced in size by separating the orbital planes. The eigenvalues also show that increasing the negative right ascension difference improves the errors of these high order coefficients.

When the right ascension of the leading satellite is increased beyond that of the trailing satellite then the situation is not as straightforward. For most of these examples, illustrated in Figures 5.6.4, 5.6.6 to 5.6.20 (even nos.)the improvement is of the same character and as significant as when the right ascension difference is negative eg compare Figures 5.6.8 and 5.6.9 or 5.6.20 and 5.6.21, between which the missions vary only in the sign of $\Delta\Omega$. Here once again there is no difference to the errors in the coefficients of lower order, when compared to the planar case. Only the coefficients of higher order are affected.

There are certain results which show that a degree of caution must employed. These are evident in Figures 5.6.6 and 5.6.7, and 5.6.10 and 5.6.11, where ΔF and $\Delta\Omega$ are $2.0°$ and $\pm 0.2°$,$2.4°$ and $\pm 0.2°$ respectively. No improvement in the variances of the coefficients is made and some groups of coefficients seem to have their accuracies degraded eg. the coefficients with high degree and mid to high order. Figures 5.6.4, and 5.6.6, where ΔF and $\Delta\Omega$ are $2.0°$ and $+0.1°$ and $2.0°$ and $+0.2°$ can be compared to illustrate how for this case increasing the difference in right ascension does not improve the results.

The reasons why one could expect an improvement in the general case were

outlined at the beginning of this section. The orientations of the satellites allow the sectorial's cross track velocities of high frequency to contribute to the line of sight. These cross track velocities are characterised by the cross track amplitudes $\mathcal{X}_{lmj}$ and are chiefly affected by the cross track inclination functions, which are related to the derivatives of the ordinary inclination functions. From the discussion in section 5.5.2 the near sectorial ordinary inclination functions have the property that the high order spherical harmonics they represent have little contribution to the planar Range Rate signal for polar orbits. The result is a deficiency in the accuracy of these coefficients.

An important characteristic of the cross track amplitudes seems to be that they are more sensitive to the near sectorial coefficients than the along track amplitudes as Table 5.6.1 shows. In Table 5.6.1 the proportion of the power of the inclination functions at a given order is displayed. The cross track inclination functions have more power in the higher values of m than the ordinary inclination functions. This will be realised in the equations by the higher order terms producing greater cross track velocities than in plane ones. Hence the errors in the near sectorial coefficients would be lower when the satellites are in different planes than in the planar case, and indeed with the exception of the anomalous results listed above this seems to be true. Precisely why these results do not concur with the others is not clear, but confirms the use of this kind of analysis in choosing the orbital parameters. For a different inclination the improvements may be less significant for some other value of $\Delta\Omega$ and another error analysis would be necessary to discover what orientations are best and those that should be avoided for an accurate recovery of the high order coefficients.

In summary it has been shown that it is possible to make significant improvement to the coefficients of high degree and order by separating the orbital planes of the two satellites. It was also shown that not all cross track separations improve the results and increasing that separation does not necessarily improve the results

either. However by careful choice of the separations it is possible to recover accurately those coefficients which in the planar case have the worst errors. In fact of all the results displayed in this chapter the best overall have been obtained when different orbital planes were used.

m	$\frac{\sum_{p=0}^{20} \lvert F_{20,m,p}(91°)\rvert}{\sum_{m=0}^{20}\sum_{p=0}^{20} \lvert F_{20,m,p}(91°)\rvert}$	$\frac{\sum_{p=0}^{20} \lvert F^{*}_{20,m,p}(91°)\rvert}{\sum_{m=0}^{20}\sum_{p=0}^{20} \lvert F^{*}_{20,m,p}(91°)\rvert}$
0	0.0583	0.0150
1	0.0564	0.0583
2	0.0541	0.0525
3	0.0546	0.0510
4	0.0559	0.0506
5	0.0562	0.0504
6	0.0540	0.0507
7	0.0515	0.0529
8	0.0516	0.0530
9	0.0513	0.0523
10	0.0487	0.0539
11	0.0481	0.0534
12	0.0464	0.0540
13	0.0461	0.0524
14	0.0428	0.0557
15	0.0425	0.0531
16	0.0408	0.0518
17	0.0391	0.0509
18	0.0373	0.0489
19	0.0341	0.0470
20	0.0302	0.0423

Table 5.6.1 Power of inclination functions vs. order

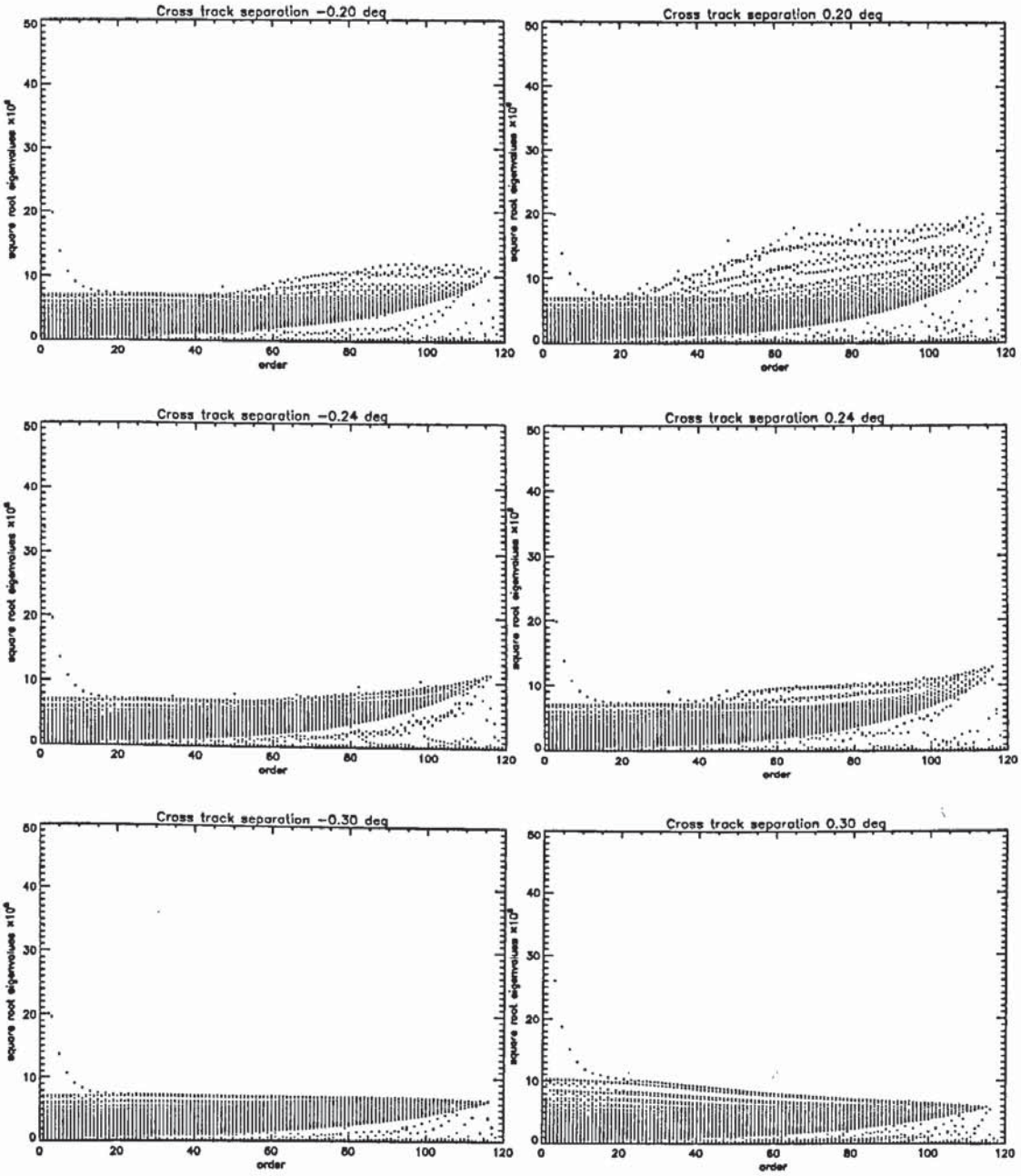

FIGURES 5.6.1 The eigenvalues for a range of cross track separations. The along track separation is 2.0°.

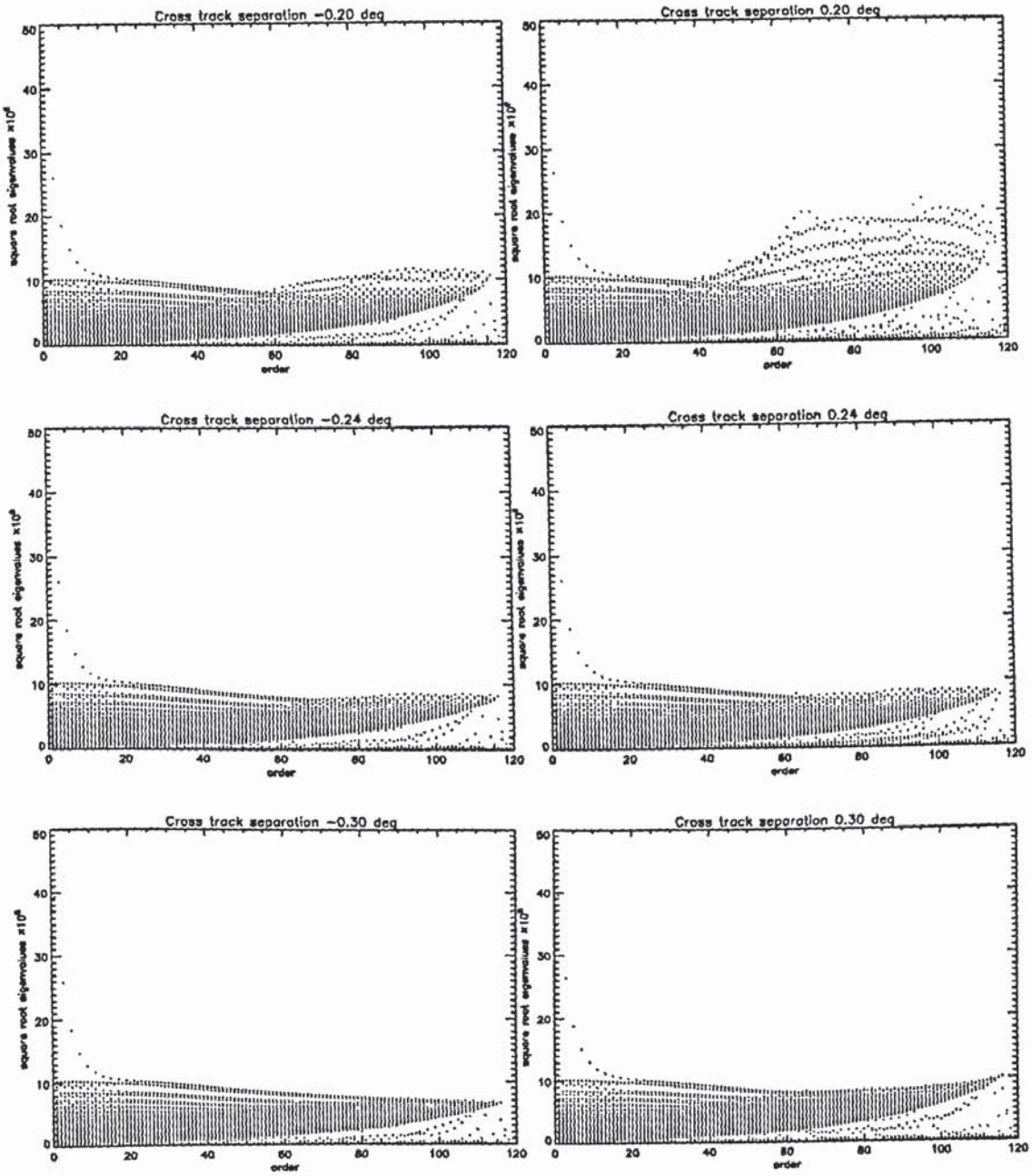

FIGURES 5.6.2 The eigenvalues for a range of cross track separations. The along track separation is 2.4°.

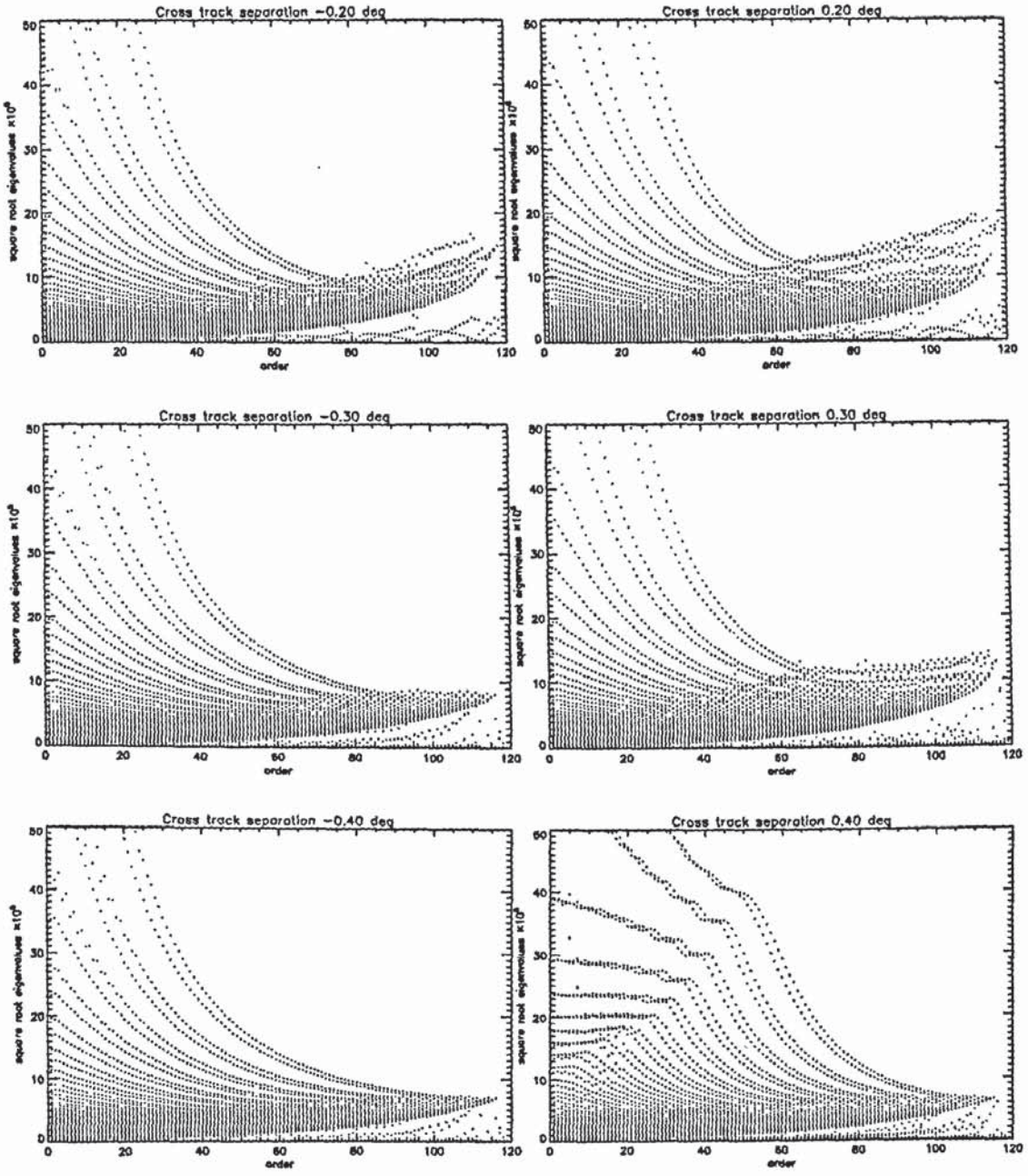

FIGURES 5.6.3 The eigenvalues for a range of cross track separations. The along track separation is 3.0°.

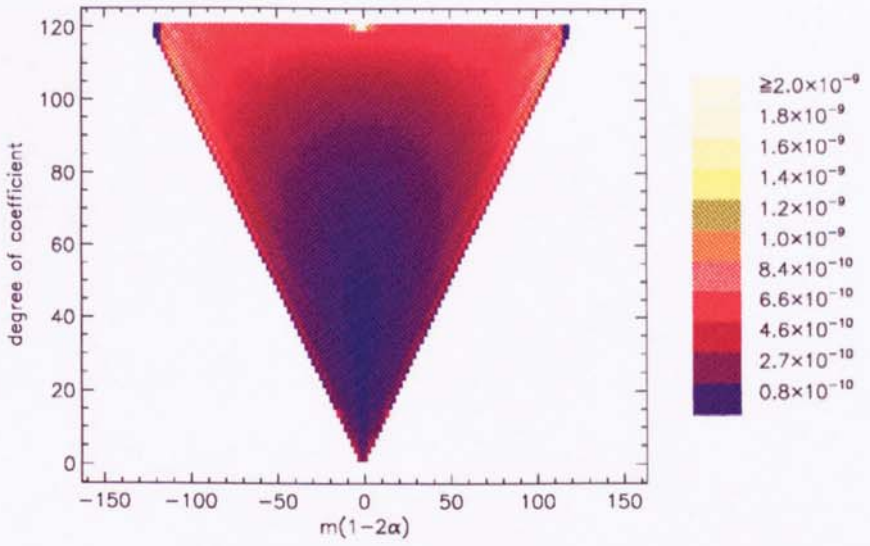

Figure 5.6.4

Root Variances of Gravity coefficients.$\Delta F = 2.0°, \Delta\Omega = 0.1°$

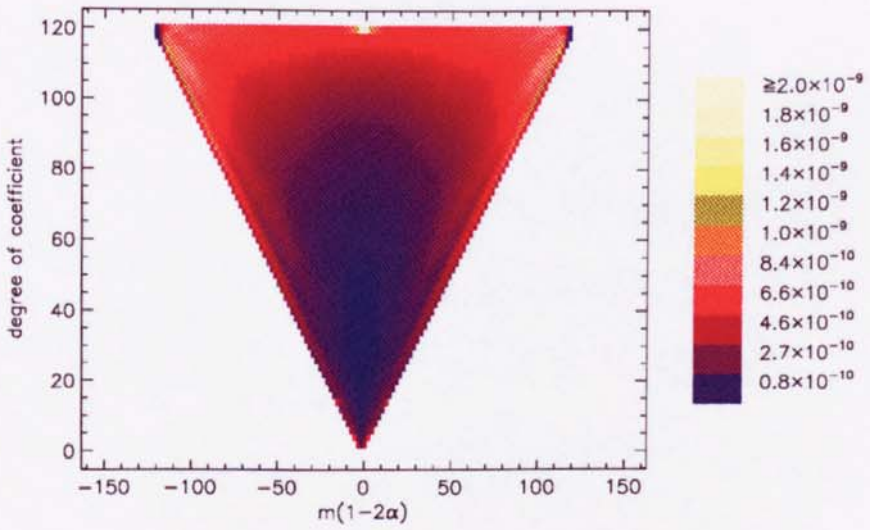

Figure 5.6.5

Root Variances of Gravity coefficients.$\Delta F = 2.0°, \Delta\Omega = -0.1°$

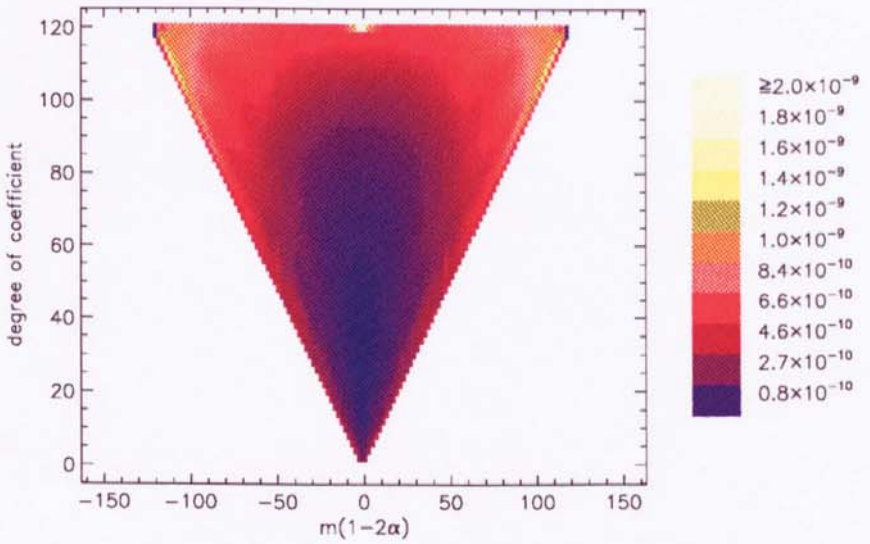

Figure 5.6.6

Root Variances of Gravity coefficients.$\Delta F = 2.0°, \Delta\Omega = 0.2°$

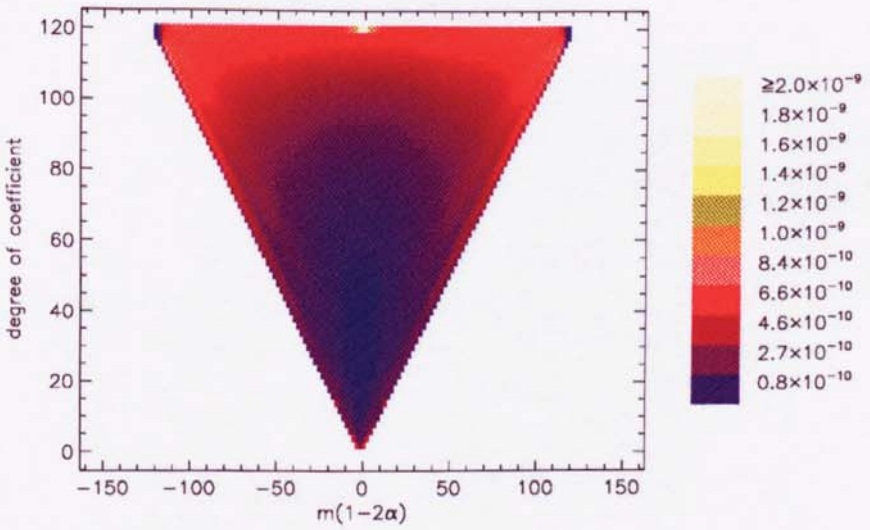

Figure 5.6.7

Root Variances of Gravity coefficients.$\Delta F = 2.0°, \Delta\Omega = -0.2°$

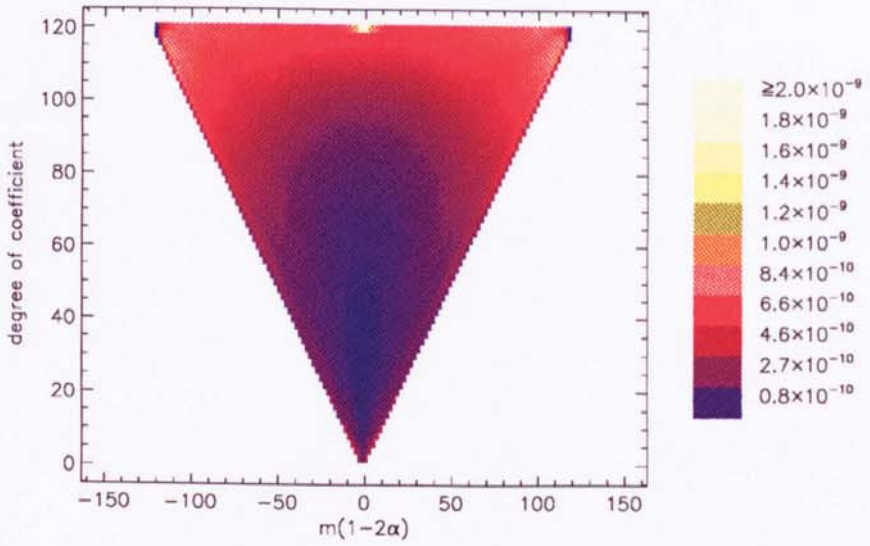

Figure 5.6.8

Root Variances of Gravity coefficients.$\Delta F = 2.0°, \Delta\Omega = 0.3°$

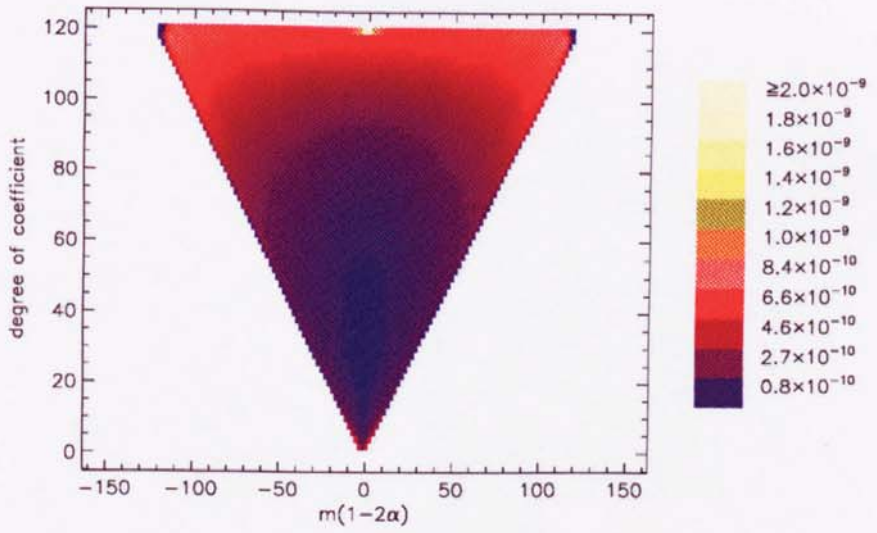

Figure 5.6.9

Root Variances of Gravity coefficients.$\Delta F = 2.0°, \Delta\Omega = -0.3°$

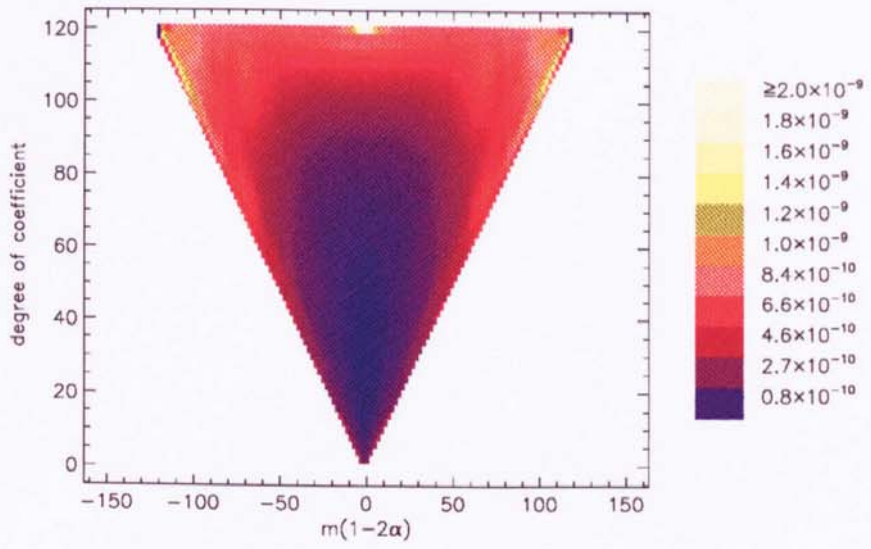

Figure 5.6.10

Root Variances of Gravity coefficients.$\Delta F = 2.4°, \Delta\Omega = 0.2°$

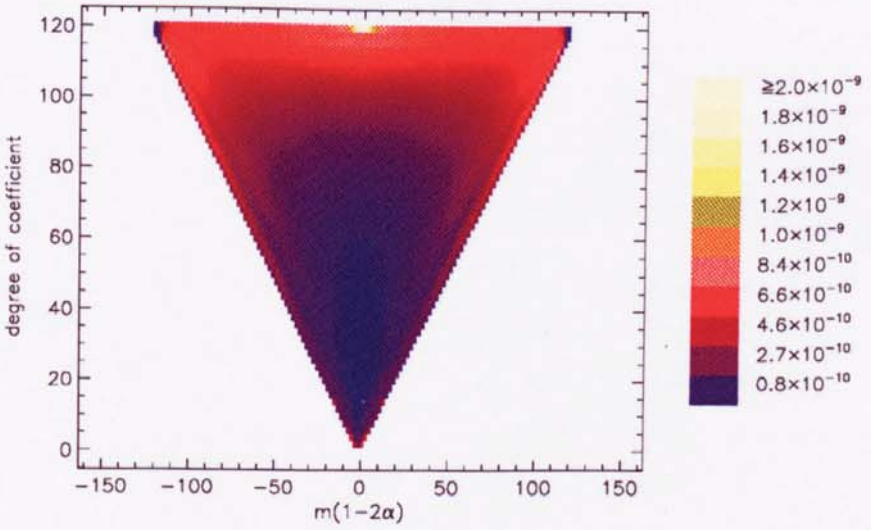

Figure 5.6.11

Root Variances of Gravity coefficients.$\Delta F = 2.4°, \Delta\Omega = -0.2°$

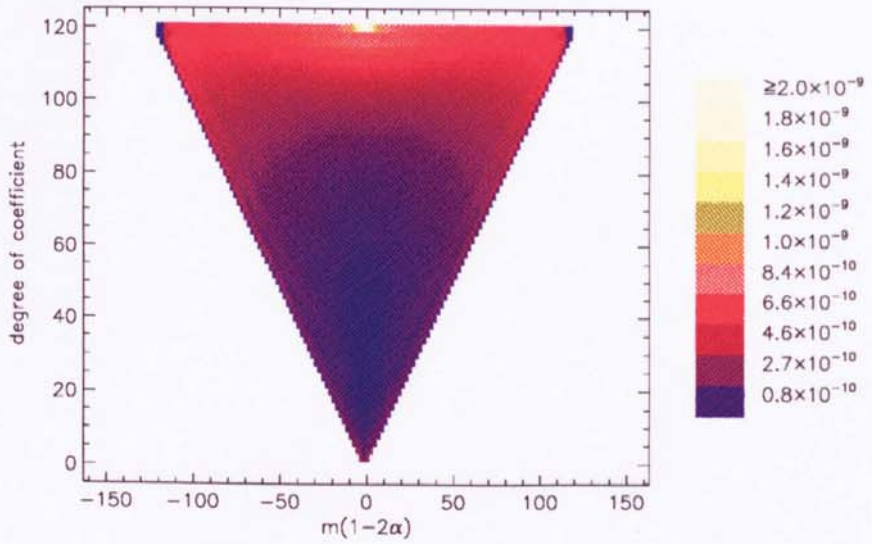

Figure 5.6.12

Root Variances of Gravity coefficients.$\Delta F = 2.4°, \Delta\Omega = 0.3°$

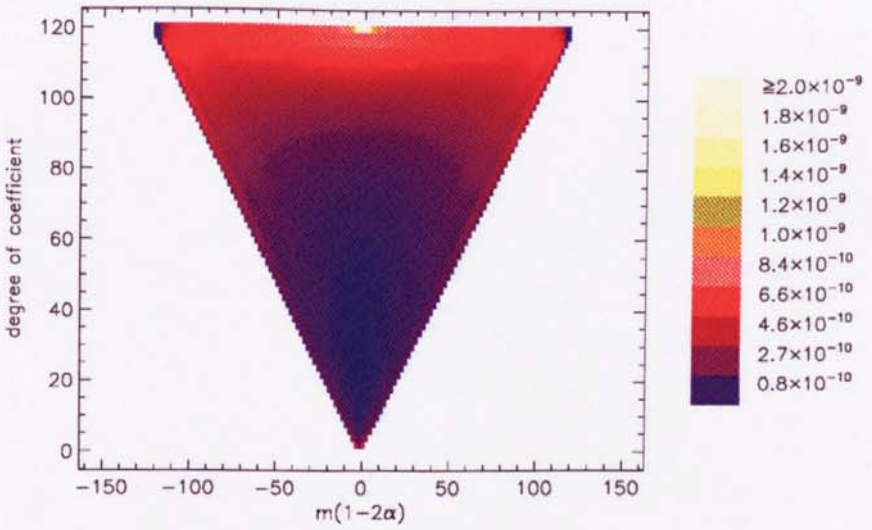

Figure 5.6.13

Root Variances of Gravity coefficients.$\Delta F = 2.4°, \Delta\Omega = -0.3°$

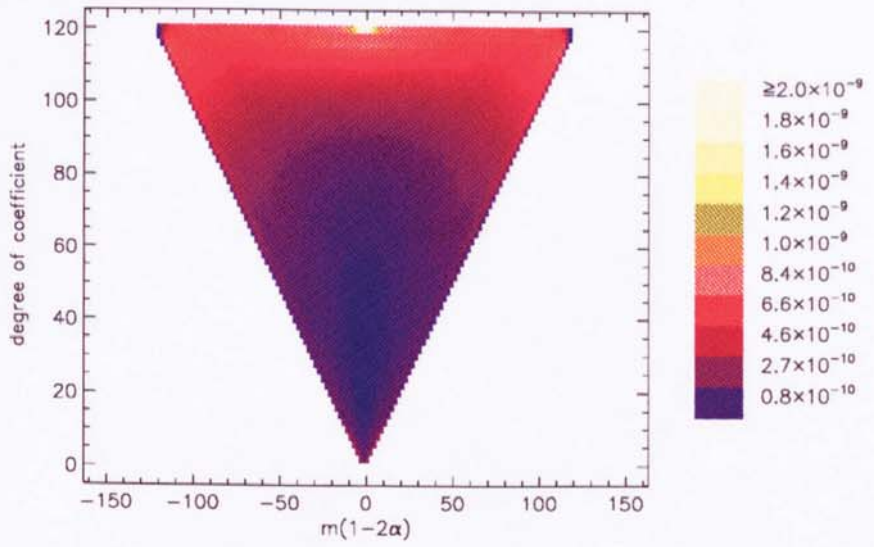

Figure 5.6.14

Root Variances of Gravity coefficients.$\Delta F = 2.4°, \Delta\Omega = 0.4°$

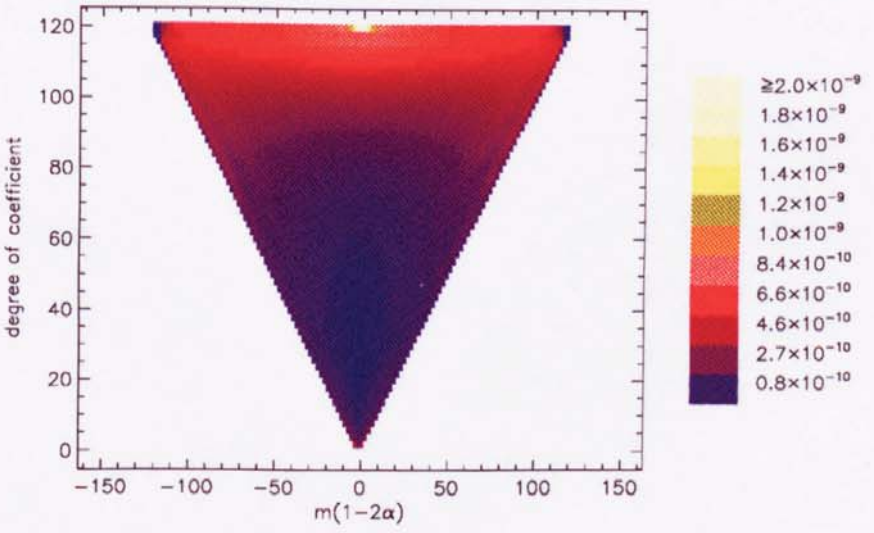

Figure 5.6.15

Root Variances of Gravity coefficients.$\Delta F = 2.4°, \Delta\Omega = -0.4°$

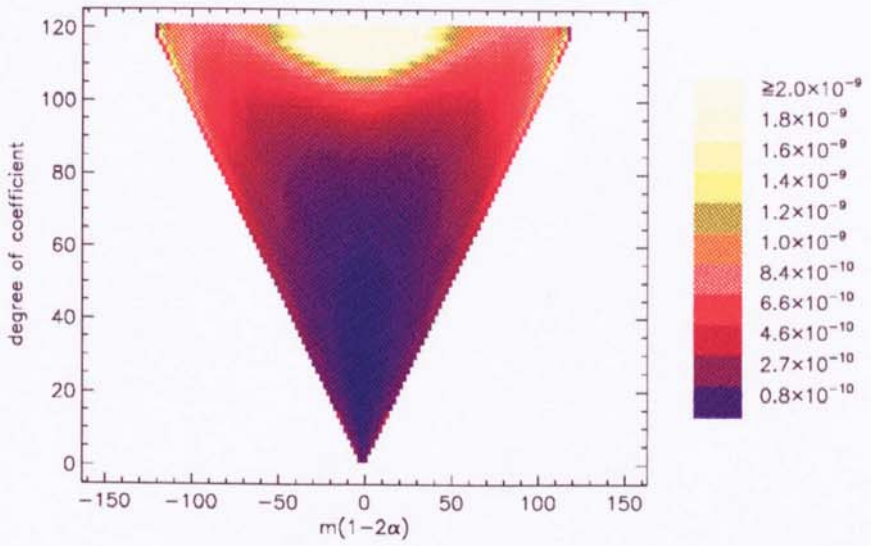

Figure 5.6.16

Root Variances of Gravity coefficients.$\Delta F = 3.0°, \Delta\Omega = 0.2°$

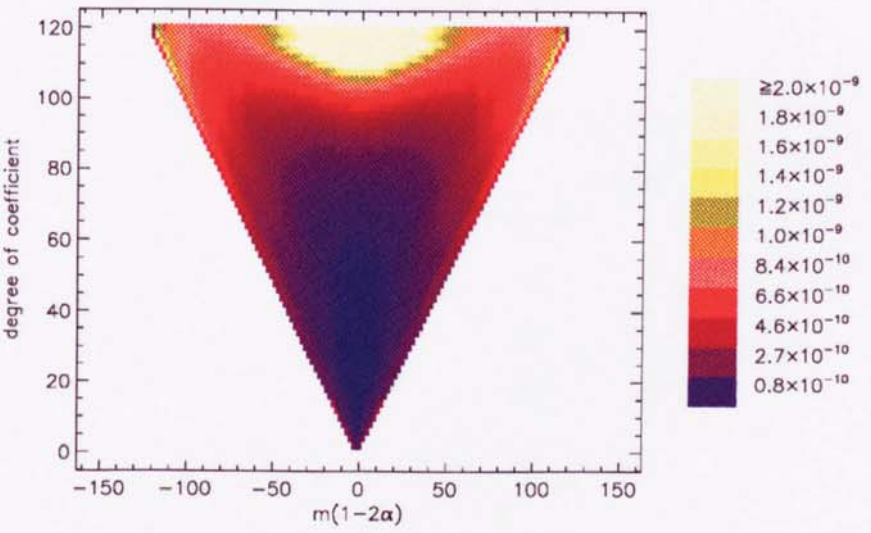

Figure 5.6.17

Root Variances of Gravity coefficients.$\Delta F = 3.0°, \Delta\Omega = -0.2°$

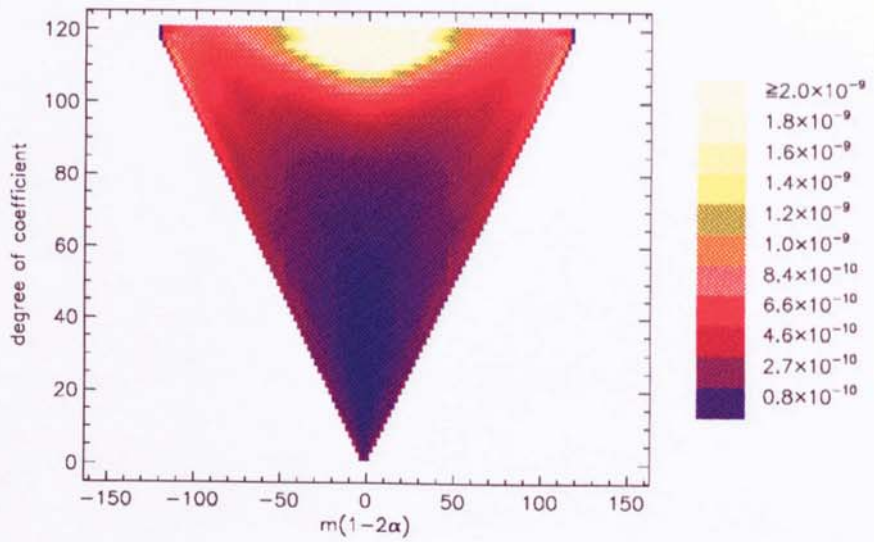

Figure 5.6.18

Root Variances of Gravity coefficients.$\Delta F = 3.0°, \Delta\Omega = 0.3°$

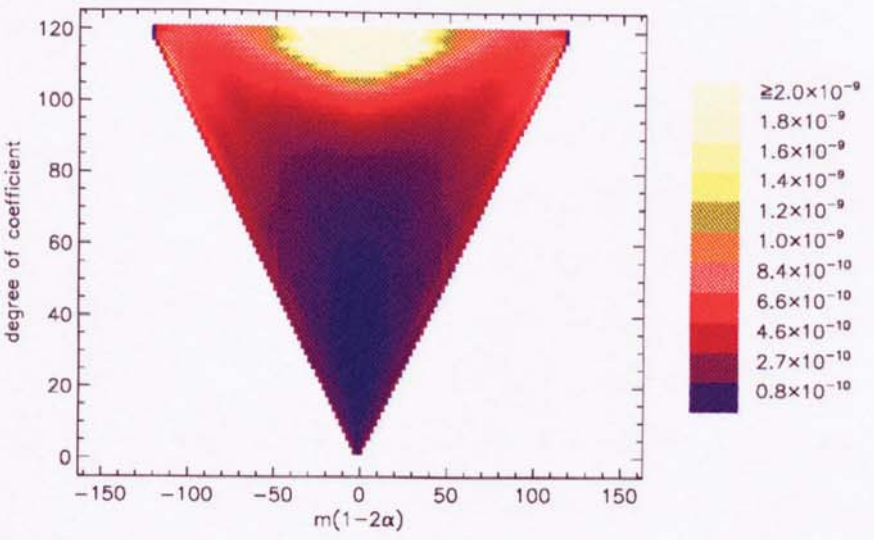

Figure 5.6.19

Root Variances of Gravity coefficients.$\Delta F = 3.0°, \Delta\Omega = -0.3°$

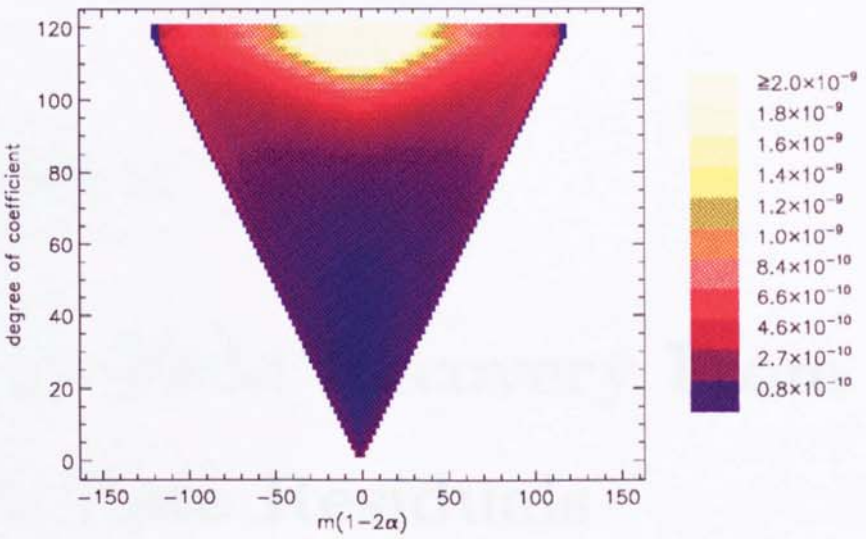

Figure 5.6.20

Root Variances of Gravity coefficients.$\Delta F = 3.0°, \Delta\Omega = 0.4°$

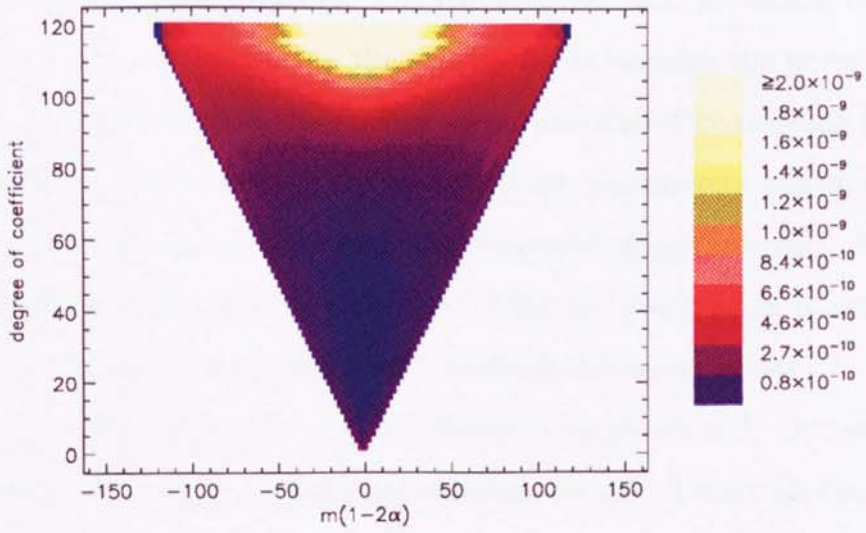

Figure 5.6.21

Root Variances of Gravity coefficients.$\Delta F = 3.0°, \Delta\Omega = -0.4°$

Chapter 6

Gravity Field Recovery From Range Rate Residuals

6.1 Introduction

In this chapter a number of gravity field recoveries will be performed using simulated Range Rate Residual datasets. The efficient methods presented in chapter 5 are not used explicitly in recovering the gravity fields because the preprocessing of the data would remove some of the gravity signal and therefore degrade the results. Instead of removing the effects of the so called arc parameters before solving for the gravity coefficients the whole system is recovered simultaneously. However as a result the purely block diagonal structure of the normal matrix is lost. A set of Range Rate Residuals is simulated by the method discussed below.

Multiple arc techniques are used to obtain a large enough dataset to make extensive recoveries possible without introducing round off error in the numerical integrator. All the recoveries presented here are however limited in their extent for reasons of efficiency and because of the difficulty in creating a long and accurate enough repeat orbit to make a full scale recovery possible.

A number of satellite orientations are experimented with in an attempt to verify the results of chapter 5.

6.2 The Least Squares Recovery Procedure

6.2.1 The Normal Equations

In this section the Least Squares model is developed with a more general form of signal equation than that considered in section 5.2. No assumptions are made regarding preprocessing of the data such as the filtering mentioned in chapter 5. The residuals are assumed to be the result of gravity field mismodelling which produces resonant and non resonant responses, and initial state mismodelling. Section 4.5 established a general form of analytical equation for this type of residual signal, namely equation (4.5.3), ie

$$\begin{aligned}\Delta RR_{calc}(t) &= \sum_{l=2}^{L_{max}} \sum_{m=0}^{l} \sum_{\alpha=0}^{1} \sum_{j=-l-1-k_{max}}^{l+k_{max}} \left[\mathcal{A}_{lm\alpha j} \cos\left(\dot{\psi}_{jm} t\right)\right. \\ &+ \left. \mathcal{B}_{lm\alpha j} \sin\left(\dot{\psi}_{jm} t\right)\right] \Delta c_{lm\alpha} \\ &+ \sum_{k=0}^{k_m+1} \left[\left(\tilde{A}^k + \tilde{B}^k t\right) \cos\left(k\dot{F}t\right) + \left(\tilde{C}^k + \tilde{D}^k t\right) \sin\left(k\dot{F}t\right)\right] \quad (6.2.1)\end{aligned}$$

where the amplitudes $\mathcal{A}_{lm\alpha j}$,$\mathcal{B}_{lm\alpha j}$ are derived in sections 4.3 and 4.4 and given by (4.4.34-43). The terms indexed by k are the so called arc dependent terms, that is they depend on initial state vector error. Additionally these terms contain gravity field signals that cannot be distinguished from this initial state error. Thus the arc dependent terms absorb any effects that may result from either source. The fact that some gravity signal is absorbed into these coefficients limits the summation over j in (6.2.1) to values for which the frequencies are not equal to $k\dot{F}$ for some k.

Equation (6.2.1) may be rewritten as

$$\begin{aligned}\Delta RR_{calc}(t) &= \sum_{l=2}^{L_{max}} \sum_{m=0}^{l} \sum_{\alpha=0}^{1} \sum_{j=-l-1-k_{max}}^{l+k_{max}} \left[\mathcal{A}_{lm\alpha j} \cos\left(\dot{\psi}_{jm} t\right)\right. \\ &+ \left.\mathcal{B}_{lm\alpha j} \sin\left(\dot{\psi}_{jm} t\right)\right] \Delta c_{lm\alpha} \\ &+ \sum_{k'=0}^{4k_m+4} A^{k'} f^{k'}(t) \end{aligned} \tag{6.2.2}$$

where the $A^{k'}$ are the $\tilde{A}^k, \tilde{B}^k$, etc. in some order and the $f^{k'}(t)$ are the appropriate functions of time. The $A^{k'}$ are called the arc parameters and the $f^{k'}(t)$ the arc functions. In any gravity field recovery it will be necessary to use more than one arc as the derived position would otherwise be subject to unreasonable round off errors in the numerical integrator whilst in a real mission orbital manoeuvers need consideration. The result is that one must calculate a start vector for each arc. In reality this is subject to error and therefore a new set of arc parameters must be calculated for each arc. If the number of arcs used is N_{arcs} and the arc parameters and arc functions for each arc are $A_I^{k'}$ and $f_I^{k'}(t)$ where $I = 1, .., N_{arcs}$, then the i_{th} measurement will be modelled by the equation

$$\begin{aligned}\Delta RR_{calc}(t_i) &= \sum_{l=2}^{L_{max}} \sum_{m=0}^{l} \sum_{\alpha=0}^{1} \sum_{j=-l-1-k_{max}}^{l+k_{max}} \left[\mathcal{A}_{Ilm\alpha j} \cos\left(\dot{\psi}_{jm} t_i\right)\right. \\ &\qquad \left. + \mathcal{B}_{Ilm\alpha j} \sin\left(\dot{\psi}_{jm} t_i\right)\right] \Delta c_{lm\alpha} \\ &+ \sum_{I=1}^{N_{arcs}} \sum_{k'=0}^{4k_m+4} A_I^{k'} f_I^{k'}(t_i), \end{aligned} \tag{6.2.3}$$

where the arc functions are non zero only for the arc on which they are defined. The amplitudes $\mathcal{A}_{Ilm\alpha j}$, and $\mathcal{B}_{Ilm\alpha j}$ are calculated using the initial angles $F_{o,I}, L_{o,I}$ of the arc I, F being the argument of latitude and L the longitude of the ascending node.

The least squares solution to the combined arc problem is derived from the solution to the single arc problem. In vector form for the I_{th} arc only, (6.2.3) may

be written as

$$\Delta \mathbf{RR}_{calc,I} = [\mathbf{A}_{c,I} : \mathbf{A}_{a_I}] \begin{bmatrix} \mathbf{c} \\ \mathbf{a}_I \end{bmatrix}. \tag{6.2.4}$$

If the observed Range Rate Residual vector is $\Delta \mathbf{RR}_{obs,I}$ and the vector of misclosures is ϵ_I then the observation equation for this arc is

$$\Delta \mathbf{RR}_{obs,I} = [\mathbf{A}_{c,I} : \mathbf{A}_{a_I}] \begin{bmatrix} \mathbf{c} \\ \mathbf{a}_I \end{bmatrix} + \epsilon_I. \tag{6.2.5}$$

The rows of $\mathbf{A}_{c,I}, \mathbf{A}_{a_I}$, $\Delta \mathbf{RR}_{obs,I}$ and ϵ_I are indexed by $i = 0, 1, ..N_{obs,I} - 1$ where $N_{obs,I}$ is the number of measurements in arc I. The columns of $\mathbf{A}_{c,I}$ are made up of the filtered partial derivatives for some l, m, α and those of $\mathbf{A}_{a_I}$, the arc functions for some value of k' and for arc I. The vectors $\mathbf{c}, \mathbf{a}_I$ are the corresponding gravity coefficients and arc parameters.

The least squares solution to (6.2.5) is given by the normal equations which are

$$\begin{bmatrix} \mathbf{N}_{11,I} & \mathbf{N}_{12,I} \\ \mathbf{N}_{21,I} & \mathbf{N}_{22,I} \end{bmatrix} \begin{bmatrix} \hat{\mathbf{c}} \\ \hat{\mathbf{a}}_I \end{bmatrix} = \begin{bmatrix} \mathbf{b}_{c,I} \\ \mathbf{b}_{a_I} \end{bmatrix} \tag{6.2.6}$$

where

$$\begin{aligned} \mathbf{N}_{11,I} &= \mathbf{A}_{c,I}^T \mathbf{W} \mathbf{A}_{c,I} \\ \mathbf{N}_{21,I}^T = \mathbf{N}_{12,I} &= \mathbf{A}_{c,I}^T \mathbf{W} \mathbf{A}_{a_I} \\ \mathbf{N}_{22,I} &= \mathbf{A}_{a_I}^T \mathbf{W} \mathbf{A}_{a_I} \\ \mathbf{b}_{c,I} &= \mathbf{A}_{c,I}^T \mathbf{W} \Delta \mathbf{RR}_{obs,I} \\ \mathbf{b}_{a_I} &= \mathbf{A}_{a_I}^T \mathbf{W} \Delta \mathbf{RR}_{obs,I}. \end{aligned} \tag{6.2.7}$$

In (6.2.7) $\mathbf{W}$ is the weight matrix of the observations and $\hat{\mathbf{c}}$ and $\hat{\mathbf{a}}_I$ are the estimated values of $\mathbf{c}$ and $\mathbf{a}_I$. Equations (6.2.6) do not have the block diagonal structure of the normal equations of chapter 5 as ,in general, the repeat period

cannot ensure the arc functions to be orthogonal to either the filtered partials or each other. As a result the sub matrices $\mathbf{N}_{22}$ and $\mathbf{N}_{12}$ do not have any special structure.

To combine the solutions from more than one arc the rows of the vector of unknowns are ordered so that the gravity coefficients are followed by the arc parameters of each arc in turn. The reordered normal equations in matrix form are then simply added together to give the combined solution. For example the combined solution for 3 arcs is given by

$$\begin{bmatrix} \sum_{I=1}^{3}\mathbf{N}_{11,I} & \mathbf{N}_{12,I=1} & \mathbf{N}_{12,I=2} & \mathbf{N}_{12,I=3} \\ \mathbf{N}_{21,I=1} & \mathbf{N}_{22,I=1} & \mathbf{0} & \mathbf{0} \\ \mathbf{N}_{21,I=2} & \mathbf{0} & \mathbf{N}_{22,I=2} & \mathbf{0} \\ \mathbf{N}_{21,I=3} & \mathbf{0} & \mathbf{0} & \mathbf{N}_{22,I=3} \end{bmatrix} \begin{bmatrix} \hat{\mathbf{c}} \\ \hat{\mathbf{a}}_{I=1} \\ \hat{\mathbf{a}}_{I=2} \\ \hat{\mathbf{a}}_{I=3} \end{bmatrix} = \begin{bmatrix} \sum_{I=1}^{3}\mathbf{b}_{c,I} \\ \mathbf{b}_{a_{I=1}} \\ \mathbf{b}_{a_{I=2}} \\ \mathbf{b}_{a_{I=3}} \end{bmatrix}. \quad (6.2.8)$$

The definitions (6.2.7) give the matrix sub-blocks in equation (6.2.8). For uncorrelated observations of equal variance the weight matrix is

$$\mathbf{W} = \frac{1}{\sigma^2}\mathbf{I}, \quad (6.2.9)$$

as in chapter 5. Therefore (6.2.7) becomes

$$\begin{aligned} \mathbf{N}_{11,I} &= \frac{1}{\sigma^2}\mathbf{A}_{c,I}^T\mathbf{A}_{c,I} \\ \mathbf{N}_{21,I}^T = \mathbf{N}_{12,I} &= \frac{1}{\sigma^2}\mathbf{A}_{c,I}^T\mathbf{A}_{a_I} \\ \mathbf{N}_{22,I} &= \frac{1}{\sigma^2}\mathbf{A}_{a_I}^T\mathbf{A}_{a_I} \\ \mathbf{b}_{c,I} &= \frac{1}{\sigma^2}\mathbf{A}_{c,I}^T\Delta\mathbf{RR}_{obs,I} \\ \mathbf{b}_{a_I} &= \frac{1}{\sigma^2}\mathbf{A}_{a_I}^T\Delta\mathbf{RR}_{obs,I}. \end{aligned} \quad (6.2.10)$$

6.2.2 Setting up the Normal Equations

Using equations (6.2.8) and (6.2.10) the normal equations for a set of arcs can be obtained. This requires that the blocks $\mathbf{N}_{11,I}, \mathbf{N}_{12,I}, \mathbf{N}_{22,I}$ and the vectors $\mathbf{b}_{c,I}$ and

$\mathbf{b}_{a,I}$ are calculated.

The blocks $\mathbf{N}_{11,I}$ are formed from the products of filtered partial derivatives summed over the measurements contained in the arc I, these measurements are indexed by $i_I = 0, 1, ..N_{obs,I} - 1$ where $N_{obs,I}$ is the the number of measurements for the I_{th} arc. The normal matrix discussed in Chapter 5 is equivalent to this block. Therefore if the assumptions of chapter 5. concerning the orbit and distribution of the measurements are made here, the matrix $\mathbf{N}_{11,I}$ will be block diagonal. Furthermore the elements will be given by the elements of $\left(N^{l\alpha}_{l'\alpha'}\right)_m$ in equations (5.4.1) and (5.4.2). Without these assumptions it is necessary to return to a previous point in the derivation of the normal matrix of chapter 5. The expression for a typical element of the matrix $\mathbf{N}_{11,I}$ is given by equation (5.3.4) which is rewritten in the notation of equation (6.2.8) as

$$\begin{aligned}
(\mathbf{N}_{11,I})^{lm\alpha}_{l'm'\alpha'} &= \frac{1}{\sigma^2}\sum_{i_I=0}^{N_{I,obs}-1}\frac{\partial RR_{calc\,i_I}}{\partial c_{lm\alpha}}\frac{\partial RR_{calc\,i_I}}{\partial c_{l'm'\alpha'}} \\
&= \frac{1}{\sigma^2}\sum_{j=-l-1-k_{max}}^{l+k_{max}}\sum_{j'=-l'-1-k_{max}}^{l'+k_{max}} \mathcal{A}_{Ilm\alpha j}\mathcal{A}_{Il'm'\alpha' j'}\mathcal{I}^1_{Ijj'mm'} \\
&\quad +\mathcal{A}_{Ilm\alpha j}\mathcal{B}_{Il'm'\alpha' j'}\mathcal{I}^2_{Ijj'mm'} \\
&\quad +\mathcal{B}_{Ilm\alpha j}\mathcal{A}_{Il'm'\alpha' j'}\mathcal{I}^3_{Ijj'mm'} \\
&\quad +\mathcal{B}_{Ilm\alpha j}\mathcal{B}_{Il'm'\alpha' j'}\mathcal{I}^4_{Ijj'mm'} \qquad (6.2.11)
\end{aligned}$$

where

$$\begin{aligned}
\mathcal{I}^1_{Ijj'mm'} &= \sum_{i_I=0}^{N_{I,obs}-1}\cos\left(\dot{\psi}_{jm}t_{i_I}\right)\cos\left(\dot{\psi}_{j'm'}t_{i_I}\right) \\
\mathcal{I}^2_{Ijj'mm'} &= \sum_{i_I=0}^{N_{I,obs}-1}\cos\left(\dot{\psi}_{jm}t_{i_I}\right)\sin\left(\dot{\psi}_{j'm'}t_{i_I}\right) \\
\mathcal{I}^3_{Ijj'mm'} &= \sum_{i_I=0}^{N_{I,obs}-1}\sin\left(\dot{\psi}_{jm}t_{i_I}\right)\cos\left(\dot{\psi}_{j'm'}t_{i_I}\right) \\
\mathcal{I}^4_{Ijj'mm'} &= \sum_{i_I=0}^{N_{I,obs}-1}\sin\left(\dot{\psi}_{jm}t_{i_I}\right)\sin\left(\dot{\psi}_{j'm'}t_{i_I}\right). \qquad (6.2.12)
\end{aligned}$$

The time of the i_I^{th} measurement t_{i_I} is taken from the beginning of the I^{th} arc.

Without assumptions about the distribution of the data the summations in equations (6.2.12) cannot be simplified in the manner of Chapter 5. Equations (6.2.11) and (6.2.12) are therefore used to calculate the matrix $\mathbf{N}_{11,I}$ in the recovery procedure when a non repeating orbit is used.

The other sub blocks of the normal matrix are formed in the same way. From (6.2.10) these are

$$\begin{aligned}
\left(\mathbf{N}_{12,I}\right)_{lm\alpha}^{k'} &= \frac{1}{\sigma^2}\sum_{i_I=0}^{N_{I,obs}-1}\frac{\partial RR_{calc\,i_I}}{\partial c_{lm\alpha}}f_I^{k'}\left(t_{i_I}\right) \\
&= \frac{1}{\sigma^2}\sum_{j=-l-1-k_{max}}^{l+k_{max}}\left(\mathcal{A}_{Ilm\alpha j}\sum_{i_I=0}^{N_{I,obs}-1}\cos\left(\dot{\psi}_{jm}t_i\right)f_I^{k'}\left(t_{i_I}\right)\right. \\
&\qquad \left. + \mathcal{B}_{Ilm\alpha j}\sum_{i_I=0}^{N_{I,obs}-1}\sin\left(\dot{\psi}_{jm}t_i\right)f_I^{k'}\left(t_{i_I}\right)\right) \qquad (6.2.13)
\end{aligned}$$

and

$$\left(\mathbf{N}_{22,I}\right)_{k_1'}^{k_2'} = \frac{1}{\sigma^2}\sum_{i_I=0}^{N_{I,obs}-1}f_I^{k_1'}\left(t_{i_I}\right)f_I^{k_1'}\left(t_{i_I}\right) \qquad (6.2.14)$$

Equations (6.2.11), (6.2.12), (6.2.13) and (6.2.14) are the general formulae for deriving the elements of the normal matrix.

To calculate the right hand side of the normal equations it is necessary to create the simulated dataset $\Delta RR_{i_I\,obs,I}$ for $i_I = 0, 1, .., N_{I,obs} - 1$. The method employed for this task is discussed in section 6.3. Once the residual data set is obtained the elements of the vectors $\mathbf{b}_{c,I}$ and $\mathbf{b}_{a,I}$ can be formulated, namely

$$\begin{aligned}
\left(\mathbf{b}_{c,I}\right)_{lm\alpha} &= \frac{1}{\sigma^2}\sum_{i_I=0}^{N_{I,obs}-1}\frac{\partial RR_{calc\,i_I}}{\partial c_{lm\alpha}}\Delta RR_{i_I\,obs,I} \\
&= \frac{1}{\sigma^2}\sum_{j=-l-1-k_{max}}^{l+k_{max}}\left(\mathcal{A}_{Ilm\alpha j}\sum_{i_I=0}^{N_{I,obs}-1}\cos\left(\dot{\psi}_{jm}t_i\right)\Delta RR_{i_I\,obs,I}\right. \\
&\qquad \left. + \mathcal{B}_{Ilm\alpha j}\sum_{i_I=0}^{N_{I,obs}-1}\sin\left(\dot{\psi}_{jm}t_i\right)\Delta RR_{i_I\,obs,I}\right) \qquad (6.2.15)
\end{aligned}$$

and

$$(\mathrm{b}_{a,I})_{k'} = \frac{1}{\sigma^2} \sum_{i_I=0}^{N_{I,obs}-1} f_I^{k'}(t_{i_I}) \, \Delta RR_{i_I\, obs,I} \tag{6.2.16}$$

6.3 Simulating the Range Rate Residuals

To form the right hand side of the normal equations a set of Range Rate residuals is required as data. This is the part of the line of sight velocity that cannot be accounted for by using existing models to determine the forces a satellite experiences as it orbits the Earth. This mismodelling is of the earths gravity field, atmospheric and radiation forces and errors within the methods used to determine the satellites motions from these models.

Since this thesis aims to discuss gravitational forces only that source of mismodelling is considered here. In reality the problem of determining surface forces must be overcome by the inclusion of an accelerometer on board the satellites, as discussed in section 2.3.

The first step in creating a simulated data set is to calculate the range rate between two satellites under the action of gravitional forces arising from a reference field called the true field. This is done by calculating the positions and velocities of two satellites in an inertial frame. Then after randomly perturbing the true field to obtain the so called perturbed field one uses this to determine another set of range rate residuals. The differences between corresponding measurements in the two data sets are the aforementioned Range Rate residuals.

The force models and the numerical integrator used to determine the satellite positions and velocities form a non linear set of second order differential equations which require for their solution an initial state vector. This vector must be calculated to allow the satellite to follow the near circular, near polar orbits that have been hitherto assumed. The method used to calculate these initial state vectors

is discussed in the next subsection. The equations of motion, method of solution and creation of the data set will be dealt with thereafter.

6.3.1 Calculating the initial state vectors

The kind of near circular orbit that allows the possibility of the exact repeat orbit discussed in the last chapter is known as a frozen orbit. The effect of the odd zonals on the argument of perigee becomes comparable to the effect of the equatorial bulge when the orbit is nearly circular. It is possible therefore that the combined effects of the odd zonals up to some degree and of the c_{20} term cancel out. This results in the orbit having a fixed orientation in its precessing orbital plane. Such an orbit was discovered by (Cook, 1966) and will result from the following initial values of the Keplerian elements e, ω

$$\begin{aligned} \omega &= \frac{\pi}{2} \\ e &= \frac{1}{3} \sum_{l=3}^{L(odd)} c_{l0} \left(\frac{R}{a}\right)^{l} \left(\frac{l-1}{l\,(l+1)}\right) P_{l1}\,(0)\, P_{l1}\,(\cos i) \\ &\qquad \cdot \left[c_{20} \left(\frac{R}{a}\right)^{2} \left(1 - \frac{5}{4}\sin^2 i\right)\right]^{-1}, \end{aligned} \tag{6.3.1}$$

where P_{l1} is the associated Legendre polynomial of order 1 and degree l, a i and e are the semi-major axis, inclination and eccentricity of the orbit and L is some sufficiently large odd number. If these initial conditions are fulfilled then $\dot{\omega} = 0$, and the value of the eccentricity will be constant. It is approximately given by

$$e \approx 1.182 \times 10^{-3} \left(\frac{R}{a}\right) \sin i + O\,(c_{50}) \tag{6.3.2}$$

which is small enough to classify the orbit as near circular. In this orbit it is possible to fix the semi major axis and inclination to ensure that the precession of the nodes and the mean motion fulfil equations (5.3.1) and (5.3.2), thereby ensuring a repeat orbit. Using arbitrary values for a,i,M_0 and Ω_0 , and with

equations (6.3.1) determining the other two Keplerian elements, the start vector is determined. It remains to transform the start vector to inertial, Cartesian coordinates X_{In}, Y_{In}, Z_{In} and $\dot{X}_{In}, \dot{Y}_{In}, \dot{Z}_{In}$ for use in the numerical integration, see (Kaula, 1966). X_{In} is in the direction of the first point of Aries and Z_{In} is in the north polar direction. The start vectors can be calculated for the two satellites required with the restriction that the mean values of their mean motions must be equal, thus ensuring that their separation is fixed. The separations ΔF along track and $\Delta\Omega$ cross track are chosen and start vectors calculated from the sets of Keplerian elements a,i,M_0 and Ω_0, and a,i,$M_0 + \Delta F$ and $\Omega_0 + \Delta\Omega$.

6.3.2 Creating the dataset

In the absence of surface forces and third body attractions the motion of the satellites is determined by the Earth's gravity field and the initial state vector. In an inertial frame of reference the acceleration of a satellite is equal to the gradient of the Earth's potential V,

$$\ddot{\mathbf{X}}_{In} = \nabla V. \tag{6.3.3}$$

These equations are integrated forward from the initial conditions

$$\begin{aligned} \mathbf{X}_{In}(t_0) &= \mathbf{X}_{In0} \\ \dot{\mathbf{X}}_{In}(t_0) &= \dot{\mathbf{X}}_{In0}. \end{aligned} \tag{6.3.4}$$

using the eighth order Gauss-Jackson numerical technique. The partial derivatives of the Earth's potential are calculated numerically along the 'true path' of the orbit and not the circular approximation used for Hill's equations in the analytical theory expounded in this thesis. This makes the resultant orbits more accurate but the equations of motion are no longer simple. Hence the need for the numerical procedure.

Using two start vectors corresponding to the two satellites separated along track and across track by ΔF and $\Delta\Omega$ respectively, but sharing the same mean mean motion, a pair of ephemerides can be calculated. These are the ephemerides corresponding to the gravity field V, which shall be called the reference field or true field, denoted by

$$\mathbf{X}_{In,True,1}\left(t_0 + i\Delta t\right) \quad , \quad \dot{\mathbf{X}}_{In,True,1}\left(t_0 + i\Delta t\right)$$

for the leading satellite, and

$$\mathbf{X}_{In,True,2}\left(t_0 + i\Delta t\right) \quad , \quad \dot{\mathbf{X}}_{In,True,2}\left(t_0 + i\Delta t\right)$$

for the trailing satellite. The set of Range Rate values corresponding to the true field are therefore, using equation (4.2.1)

$$RR_{True}\left(t_0 + i\Delta t\right) = \frac{\left(\dot{\mathbf{X}}_{In,True,1} - \dot{\mathbf{X}}_{In,True,2}\right) \cdot \left(\mathbf{X}_{In,True,1} - \mathbf{X}_{In,True,2}\right)\right)}{\left|\left(\mathbf{X}_{In,True,1} - \mathbf{X}_{In,True,2}\right)\right|}. \quad (6.3.5)$$

If the reference field is now randomly perturbed either in part or as a whole, and by a limited degree (eg each coefficient by a fraction of its standard error), then the result shall be called the perturbed field. The ephemerides and range rate are then calculated using this field,

$$RR_{Pet}\left(t_0 + i\Delta t\right) = \frac{\left(\dot{\mathbf{X}}_{In,Pet,1} - \dot{\mathbf{X}}_{In,Pet,2}\right) \cdot \left(\mathbf{X}_{In,Pet,1} - \mathbf{X}_{In,Pet,2}\right)\right)}{\left|\left(\mathbf{X}_{In,Pet,1} - \mathbf{X}_{In,Pet,2}\right)\right|}. \quad (6.3.6)$$

The range rate residuals, that is the mismodelling due to the perturbation of the true field are calculable from (6.3.5) and (6.3.6) as

$$\Delta RR_{i,obs} = RR_{Pet}\left(t_0 + i\Delta t\right) - RR_{True}\left(t_0 + i\Delta t\right) \quad (6.3.7)$$

These residuals are used to form the observation vectors in equations (6.2.15) and (6.2.16).

It may be necessary to perform a check on the ephemerides before initiating a recovery procedure. It is important that the satellites do not drift apart by any

significant amount during the course of the experiment, therefore one must check that their mean mean motions are the same. The mean mean motions of both true and perturbed ephemerides should be equal, and to that end their osculating semi major axes are trimmed.

Take an arbitrary gravity field and satellite, it's ephemeris is used to calculate the speed V_i and the radial height r_i at each time step i. Then from the energy integral (Roy, 1978) the instantaneous semi major axis is obtained, it is given by

$$a_i = \frac{1}{\frac{2}{r_i} - \frac{V_i^2}{\mu}} \tag{6.3.8}$$

from which the instantaneous value for the mean motion is calculated

$$n_i = \left(\frac{\mu}{a_i^3}\right)^{\frac{1}{2}}. \tag{6.3.9}$$

The mean mean motion is obtained by solving n_i by least squares for a constant term. This value of the mean mean motion may differ from a predetermined ideal by a small value Δn, and to improve this, a correction to the semi major axis is made. Equation (6.3.9) gives

$$\Delta a = -\frac{2a}{3n}\Delta n \tag{6.3.10}$$

as the required correction. Once the start vector for the satellite in question is improved the ephemerides are recalculated for use in the gravity field correction procedure

6.4 Recovering a gravity field with a single arc

Using the procedure outlined in section 6.3 the range rate residuals are calculated for a set of single six day arcs. The 'true' gravity field used was the JGM2 field up to degree and order 70 (Nerem, 1994). The 102 coefficients of order 20 in this field are randomly perturbed by a fraction of their standard errors and the result,

along with the unperturbed coefficients make up the perturbed field. The initial values of the independent Keplerian coordinates used to calculate the start vectors of the pairs of satellites in each case, with the semi major axes trimmed according to the procedure in section 6.3.2, are given in Tables 6.4.1 to 6.4.8. The result is eight sets of range rate residual datasets. The data points are calculated twelve seconds apart, and as a result the total number of data values in each six day arc is $N_{obs} = 43200$.

Subsection 6.2.2 describes how the elements of the normal equations (6.2.8) are calculated from the analytical partials and the simulated datasets. For each of the eight cases the normal equations are formed and solved to obtain the vectors of unknowns denoted in (6.2.8) by $\hat{\mathbf{c}}$. These solutions are the corrections to the perturbed gravity field. Once the corrections have been made the range rate residuals are recalculated with the new perturbed fields and the procedure continued until a suitable convergence is obtained.

The first four iterations in each of the eight cases are presented in Figures 6.4.1 to 6.4.8. They show the differences between the coefficients of the 'true' field and the successive perturbed fields for order 20 and degrees 20 up to 70 . For a pair of coefficient errors $\Delta c_{lm0}, \Delta c_{lm1}$ the difference displayed is $\frac{1}{2}\sqrt{\Delta c_{lm0}^2 + \Delta c_{lm1}^2}$ where $\Delta c_{lm\alpha}$ is the difference between corresponding coefficients in the true and perturbed fields . Figure 6.4.1 gives the recovery corresponding to the initial elements given in Table 6.4.1, and similarly Figure 6.4.2 corresponds to Table 6.4.2 and so on.

Figure 6.4.1 shows how the recovery performs when the satellites are in the same plane of inclination 96° and are separated by 4° along track. Figure 6.4.3 shows the planar case for the same inclination when the along track separation is 6°. These graphs both show similar rates of convergence. A significant characteristic of all the recoveries shown is the relatively poor convergence of the higher degree coefficients. This could be due to the fact that they are shorter wavelength features and require more data than the lower degree coefficients, but more important are

the inevitable errors that accompany an analytical model, in particular the partial derivatives were integrated along a circular path. The deviation of the actual satellite path from this circle is more significant for higher degree coefficients than for lower degrees. This could be why they are not recovered as efficiently.

Whilst the inclination remains at 96°, Figures 6.4.2 and 6.4.4 show the recoveries for non planar cases where the initial right ascensions of the two satellites are different. In Figure 6.4.2 the along track separation is 4° and the right ascension separation is 0.4° In Figure 6.4.4 the along track separation is 6° and the right ascension separation is 0.6°. When compared to the planar cases with the same along track separation, (Figure 6.4.2 compared with Figure 6.4.1 and Figure 6.4.4 compared with Figure 6.4.3) the non planar orientations seem to be beneficial to the recovery of the lower degree, near sectorial coefficients.

Figures 6.4.5 and 6.4.7 show the recoveries when the satellites are coplanar, of inclination 91° and with separations along track are 4° and 6° respectively. Figures 6.4.6 and 6.4.8 correspond to the non planar case, again of inclinations 91° ,with separations along track of 4° and 6° and in right ascension of 0.4° and 0.6° respectively. When these are compared to the recoveries obtained from the satellites in orbits of inclination 96° but with the same separations it can be seen that the lower degree coefficients are recovered better with the nearer polar orbit. This result seems to contradict the result of chapter 5. which indicated that the 96° orbit was better for these near sectorial coefficients. However the reason why one should expect the nearer polar orbit to produce a better recovery is a result of an assumption made in chapter 3 concerning Hill's equations, from which the partials are derived. This assumption was that the orbital plane of the satellites did not precess with respect to an inertial frame, which is only true for polar orbits. As a result Hill's equations will model the motions better as the orbit becomes more polar. This is likely to be a more important consideration in the recoveries than the indications borne out of the error analysis in chapter 5.

In comparing Figures 6.4.5 and 6.4.6, and 6.4.7 and 6.4.8 to see how the coplanar and non coplanar missions compare one can observe that there is no noticeable improvement in introducing a right ascension difference between the satellites at this inclination, neither however is there any degradation in the results. One may conclude from this that the analytical model works as well for the coplanar and non coplanar cases but the simplifications made to allow an efficient error analysis prevent one from drawing conclusions from the gravity field recoveries carried out.

The relatively poor convergence of the higher degree coefficients referred to earlier is probably due to a combination of factors. One is that the error analyses carried out in chapter 5 showed the higher degree coefficients would not be recovered as well as the lower degree ones. This is a fact of life in any recovery because of the attenuation factor $\left(\frac{R}{r}\right)^{(l+1)}$ in the expression for the potential in equation (2.1.7). Using the range rate compensates for this to a certain degree eg the amplitudes of the velocity partials are the position amplitudes multiplied by the frequencies $\dot{\psi}_{jm}$, thus the velocity measurements are more sensitive to higher frequencies than position measurements. Differencing the velocities of the two satellites has a similar effect, but the attenuation is still important.

Another factor is the aforementioned assumptions in the Hill's equations model concerning the circularity of the orbit. The fact that the orbit of a Earth satellite must exhibit a small eccentricity will affect the higher degree coefficients because their spherical harmonics will vary more over the distance between ellipse and circle. To see this one can take the differential of equation (2.1.7) with respect to r to obtain

$$\frac{\Delta V_{lm}}{V_{lm}} = \frac{-l-1}{r}\Delta r. \tag{6.4.11}$$

Assuming a circular orbit means $r = constant$ but the orbit is an ellipse with the eccentricity given by (5.3.2), approximately 1×10^{-3}. Thus Δr between perigee

and apogee will be

$$\Delta r = 2ae \approx 13.2km, \tag{6.4.12}$$

for an orbit with semi major axis $a = 6600km$. For small l the effect is small but the mismodelling increases linearly with l . For the same reason the truncation in q at zero of the gravity field expansion used to calculate the partials will affect the higher degree coefficients to a far greater extent than the lower degree ones.

There is also the possibility that these higher degree coefficients converge less quickly because there is not enough data to sample the shorter wavelength spherical harmonic functions associated with them. To test whether this could be so the gravity field recoveries with $i = 91°$ from this section are repeated with the addition of another six day arc in the solutions. Therefore a total of twelve days data is used in the recoveries. This is done in the next section.

Finally, as a verification of the model used to determine the gravity field, another recovery is performed. In Figure 6.4.9 the analysis of Figure 6.4.8 is repeated but now the cross track terms are suppressed. If these terms are not correctly modelled one would expect to see a similar rate of convergence for the two graphs. This is not the case. Figure 6.4.9 illustrates a poorer rate of convergence when the cross track terms are neglected.

Keplerian coordinates	satellite 1	satellite 2
F_o	94.0	90.0
Ω_o	0.0	0.0
a	6605.000	6605.000
i	96.0	96.0

Table 6.4.1

Keplerian coordinates	satellite 1	satellite 2
F_o	94.0	90.0
Ω_o	0.0	0.4
a	6605.000	6605.000
i	96.0	96.0

Table 6.4.2

Keplerian coordinates	satellite 1	satellite 2
F_o	96.0	90.0
Ω_o	0.0	0.0
a	6605.000	6605.000
i	96.0	96.0

Table 6.4.3

Keplerian coordinates	satellite 1	satellite 2
F_o	96.0	90.0
Ω_o	0.0	0.6
a	6605.000	6605.000
i	96.0	96.0

Table 6.4.4

Initial elements for Figures 6.4.1-4

Keplerian coordinates	satellite 1	satellite 2
F_o	94.0	90.0
Ω_o	0.0	0.0
a	6605.000	6605.000
i	91.0	91.0

Table 6.4.5

Keplerian coordinates	satellite 1	satellite 2
F_o	94.0	90.0
Ω_o	0.0	0.4
a	6605.000	6605.000
i	91.0	91.0

Table 6.4.6

Keplerian coordinates	satellite 1	satellite 2
F_o	96.0	90.0
Ω_o	0.0	0.0
a	6605.000	6605.000
i	91.0	91.0

Table 6.4.7

Keplerian coordinates	satellite 1	satellite 2
F_o	96.0	90.0
Ω_o	0.0	0.6
a	6605.000	6605.000
i	91.0	91.0

Table 6.4.8

Initial elements for Figures 6.4.5-9

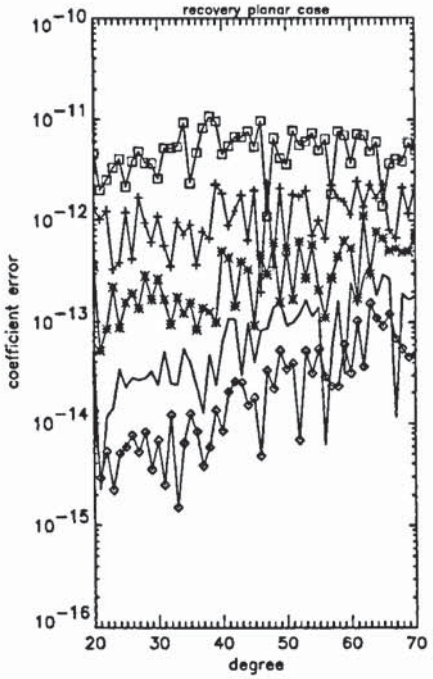

Figure 6.4.1

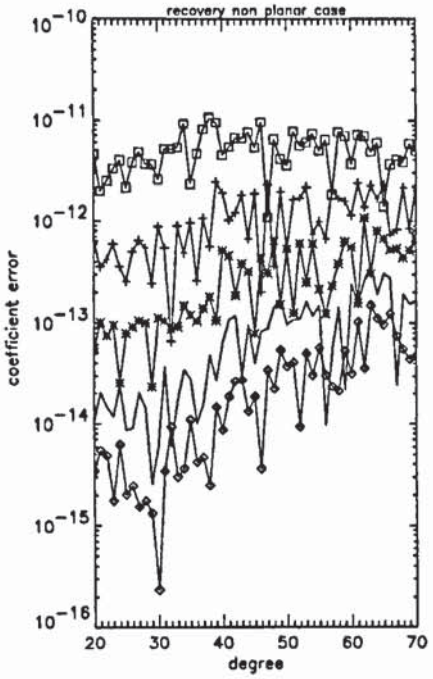

Figure 6.4.2

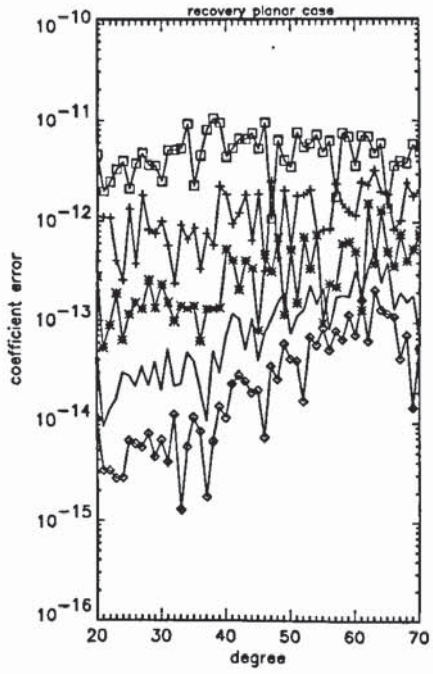

Figure 6.4.3

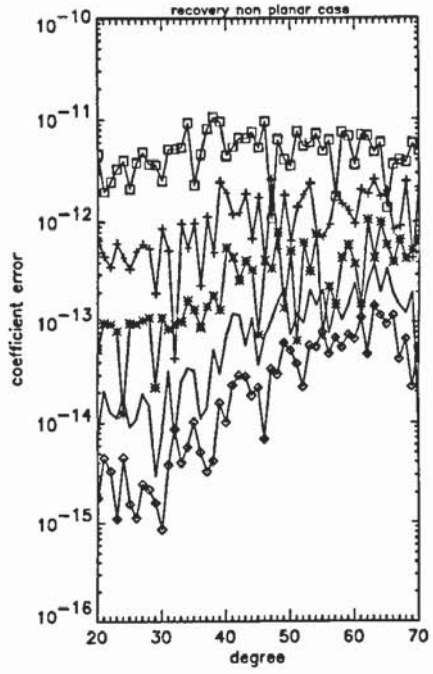

Figure 6.4.4

Successive iterations of Gravity field recoveries. The inclination for these simulations is 96°. Tables 6.5.1-4 show the other initial elements for each case.

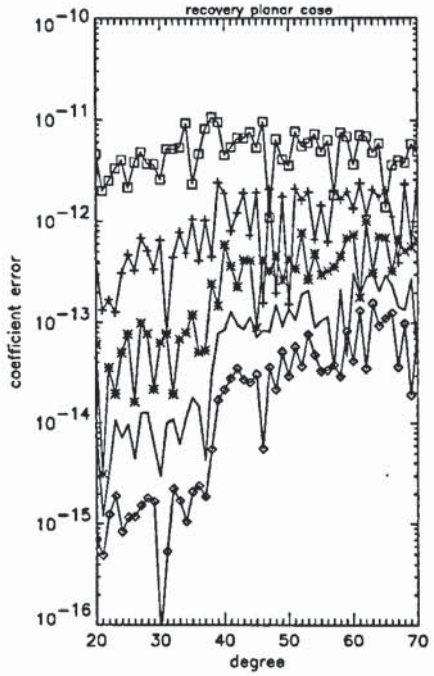

Figure 6.4.5

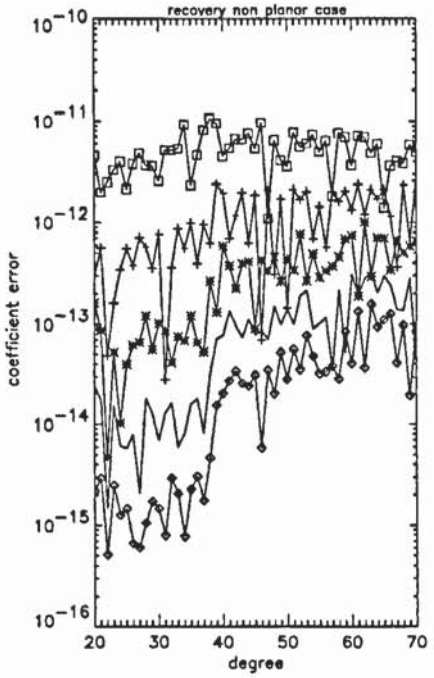

Figure 6.4.6

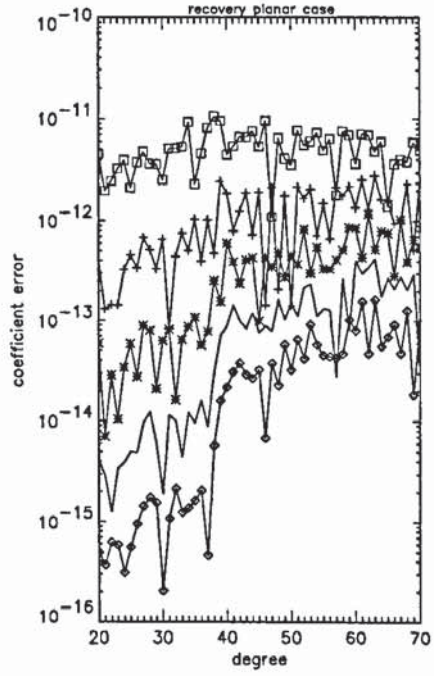

Figure 6.4.7

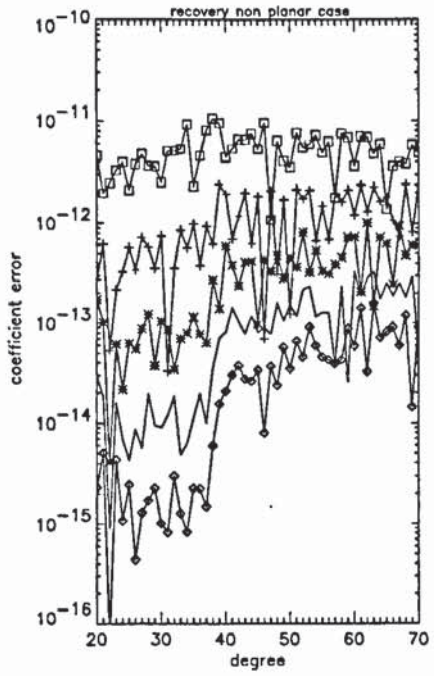

Figure 6.4.8

Successive iterations of Gravity field recoveries. The inclination for these simulations is 91°. See Tables 6.5.5-8 for the other initial elements for each case.

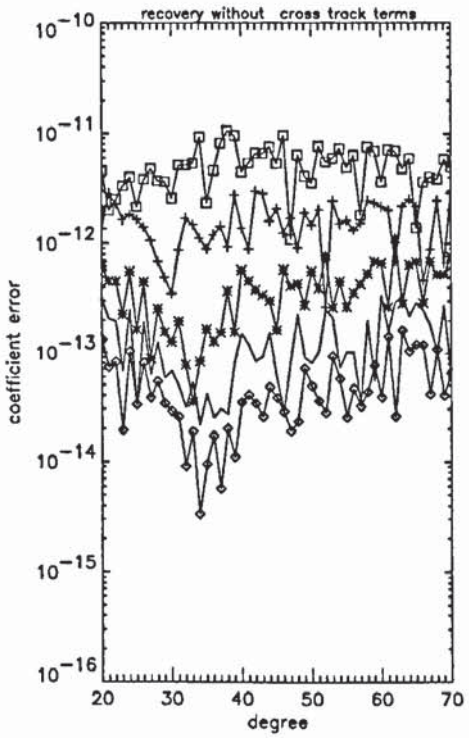

Figure 6.4.9

Recovered gravity field without cross track terms.

Same dataset as in Figure 6.4.8

6.5 Multiple arc gravity field recoveries

It is necessary to test whether the higher degree coefficients could be recovered more efficiently with the addition of more data. To that end some of the recoveries performed in the last section are repeated here with the existing six day arcs complimented with another six days range rate data.

The four recoveries performed use the same true and perturbed fields that were used in section 6.4. Four different satellite orientations with separations along track of 4° and 6°, and cross track of zero and 0.4°, and zero and 0.6° respectively are used. All the satellites in this section have inclination 91°. For each orientation two

arcs are used and the initial elements used to generate them are shown in Tables 6.5.1 to 6.5.4. The semi major axes were trimmed as in the previous section to eliminate any drift between the satellites and the data points are twelve seconds apart so that there are 43200 points per arc. The normal equations are calculated separately for each arc and the required corrections to the perturbed gravity field are the solution to the system obtained by adding together the normal equations for each arc as in equation (6.2.8). The corrections allow one to make a refinement to the perturbed field and successive iterations provide the improvements illustrated in Figures 6.5.1 to 6.5.4.

The results of this section when compared to Figures 6.4.5 to 6.4.8 show no improvement over the single arc recoveries. This indicates that the poorer determination of the higher degree coefficients is due to the increased amount of mismodelling they suffer. This mismodelling was attributed in section 6.4 to the circular orbit approximations in both the gravity field and in the solutions to Hill's equations. The fact that 91° recoveries were better than the 96° ones supports the assertion that the principle factor in the recovery performances discussed here is how well the partials are modelled.

Keplerian coordinates	Arc 1		Arc 2	
	satellite 1	satellite 2	satellite 1	satellite 2
$F_\circ$	94.0	90.0	94.0	90.0
$\Omega_\circ$	0.0	0.0	0.9	0.9
a	6605.000	6605.000	6605.000	6605.000
i	91.0	91.0	91.0	91.0

Table 6.5.1

Keplerian coordinates	Arc 1		Arc 2	
	satellite 1	satellite 2	satellite 1	satellite 2
$F_\circ$	94.0	90.0	94.0	90.0
$\Omega_\circ$	0.0	0.4	0.9	1.3
a	6605.000	6605.000	6605.000	6605.000
i	91.0	91.0	91.0	91.0

Table 6.5.2

Initial elements for Figures 6.4.1-2

Keplerian coordinates	Arc 1		Arc 2	
	satellite 1	satellite 2	satellite 1	satellite 2
F_o	96.0	90.0	96.0	90.0
Ω_o	0.0	0.0	0.9	0.9
a	6605.000	6605.000	6605.000	6605.000
i	91.0	91.0	91.0	91.0

Table 6.5.3

Keplerian coordinates	Arc 1		Arc 2	
	satellite 1	satellite 2	satellite 1	satellite 2
F_o	96.0	90.0	96.0	90.0
Ω_o	0.0	0.6	0.9	1.5
a	6605.000	6605.000	6605.000	6605.000
i	91.0	91.0	91.0	91.0

Table 6.5.4

Initial elements for Figures 6.4.3-4

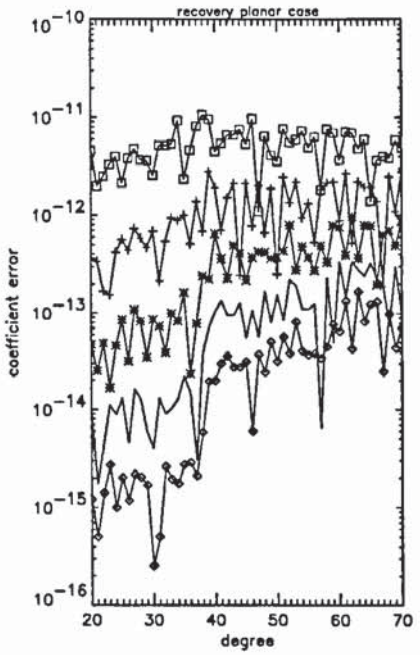

Figure 6.5.1

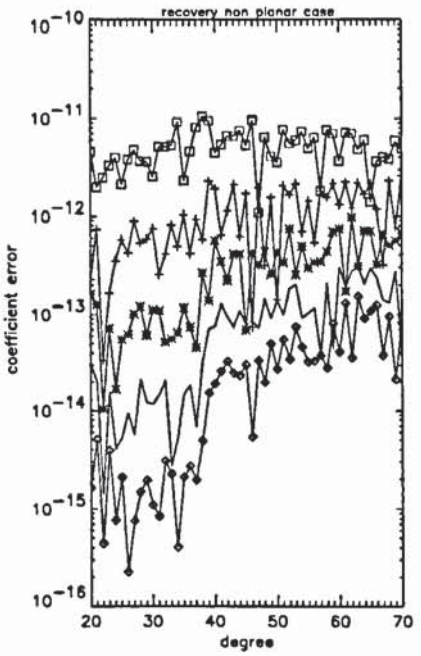

Figure 6.5.2

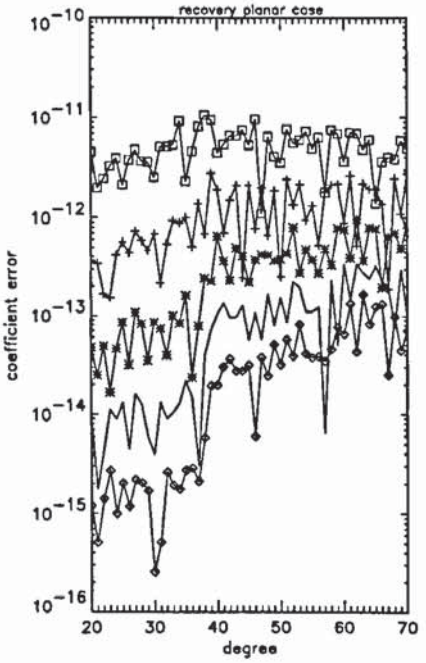

Figure 6.5.3

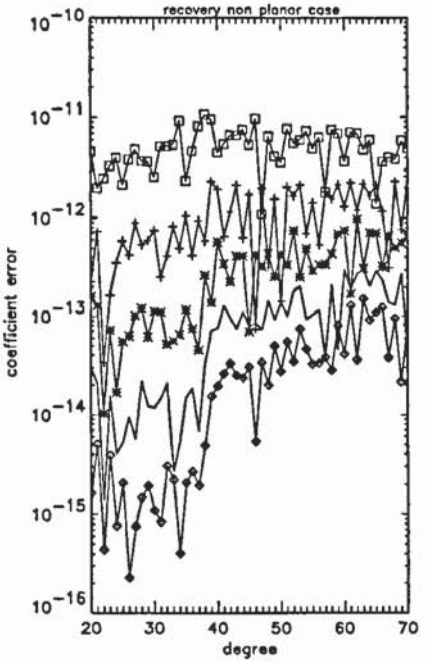

Figure 6.5.4

Successive iterations of Gravity field recoveries. The inclination for these simulations is 91°. See Tables 6.5.1-4 for the other initial elements for each case. Each recovery is performed with two 6 day arcs.

Chapter 7

Atmospheric Drag Problems

7.1 Introduction

The effects of air drag on a low satellite are significant but can be measured and accounted for with the use of an on board accelerometer as was discussed in section 2.3. Thus atmospheric perturbations do not cause problems in isolating the gravity signal but the possible differential decay rates of non coplanar orbits could result in the satellites moving apart at a non negligible rate. The possibility of a pair of drag free satellites would negate this problem but in the interest of economy many proposed missions eg GAMES, have only one active satellite and one passive target that is incapable of manoeuvering to avoid atmospheric decay.

In this chapter the effect on the mean motion due to a spherically symmetric atmosphere with a day to night variation will be discussed. It is this day to night variation which would cause two satellites with different right ascensions to decay at different rates and therefore drift apart. The possibility of varying the area to mass ratio of the spacecraft to combat the drift will be examined.

7.2 The Atmospheric Density model

The atmospheric density is assumed here to vary exponentially with height according to the equation

$$\rho = \rho_\circ \exp\left(-\frac{r - r_\circ}{H}\right), \tag{7.2.1}$$

(King-Hele, 1964), where $\rho_\circ$ is the density at some arbitrary point distance $r_\circ$ from the Earth's centre, the initial perigee point is usually chosen. H, assumed constant here is called the density scale height, it relates to how the quickly the density varies with altitude.

In this study any variation of drag with right ascension is of interest and the most important variation of this type is due to the effect of the sun on the upper atmosphere. This effect has been modelled by (Cook and King-Hele, 1965) as a change in the density which at a given height depends on the angle between the satellite and the centre of the so called diurnal bulge. This bulge is caused by solar warming of the atmosphere, it's centre is at the same declination as the sun but it lags behind the sub solar point by $\lambda \approx 30°$ in right ascension. If the angle between the centre of the bulge and the spacecraft is ϕ then the expression for the density of an atmosphere with day to night variation is

$$\rho = \rho_\circ (1 + F\cos\phi) \exp\left(-\frac{r - r_\circ}{H}\right), \tag{7.2.2}$$

where F is a constant.

In order to develop an analytical model for the orbital variations due to drag it is necessary to transform equation (7.2.2) to Keplerian coordinates. The argument of the exponential can be written in terms of the eccentric anomaly E, the semi major axis a, and eccentricity e, as

$$-\frac{r - r_\circ}{H} = \frac{1}{H}(r_\circ - a + ae\cos E). \tag{7.2.3}$$

Applying the equations of spherical trigonometry one can obtain the cosine of the angle ϕ in terms of the right ascension and declination of the sun α_s and δ_s, the

obliquity of the ecliptic ϵ, the angle λ defined earlier and the satellite's angular coordinates $E, i, \Omega, \omega,$. It is written

$$\cos\phi = A\left(\cos E - e\left(1-\cos^2 E\right) + O\left(e^2\right)\right) + B\left(1 + e\cos E + O\left(e^2\right)\right), \quad (7.2.4)$$

where

$$A = P\sin\omega + Q\cos\omega, \quad (7.2.5)$$

$$B = P\cos\omega - Q\sin\omega \quad (7.2.6)$$

and

$$P = \sin\epsilon\sin i\sin L - \cos i\left(\cos^2\frac{\epsilon}{2}\sin(\Omega-\lambda+L) - \sin^2\frac{\epsilon}{2}\sin(\Omega-\lambda+L)\right) \quad (7.2.7)$$

$$Q = \cos^2\frac{\epsilon}{2}\cos(\Omega-\lambda+L) + \sin^2\frac{\epsilon}{2}\cos(\Omega-\lambda+L), \quad (7.2.8)$$

(Cook and King-Hele, 1968). The angle L is defined in terms of α_s, δ_s and ϵ by the equations

$$\begin{aligned} \sin\delta_s &= \sin\epsilon\sin L \\ \cos L &= \cos\delta_s\cos\alpha_s, \\ \cos\epsilon\sin L &= \cos\delta_s\sin\alpha_s. \end{aligned} \quad (7.2.9)$$

The full expression for the density is therefore written

$$\rho = \rho_o\left(1 + FA\left(\cos E - e\left(1-\cos^2 E\right) + O\left(e^2\right)\right) + FB\left(1 + e\cos E + O\left(e^2\right)\right)\right)\exp\left(\frac{1}{H}\left(r_o - a + ae\cos E\right)\right). \quad (7.2.10)$$

In the next section the equation for the variation in the mean motion are discussed, allowing one to use (7.2.10) to obtain an explicit solution.

7.3 Orbital Variations due to Drag

To obtain the variation in the mean motion due to drag Lagrange's planetary equations in vector form are used. Differentiating the energy integral, namely

$$\frac{1}{2}\dot{\mathbf{r}}.\dot{\mathbf{r}} = \mu\left(\frac{1}{|\mathbf{r}|} - \frac{1}{2a}\right)$$

(Roy, 1978), and solving for $\dot{a}$ one obtains

$$\begin{aligned} \dot{a} &= \frac{2a^2}{\mu}\dot{\mathbf{r}}.\left(\ddot{\mathbf{r}} + \frac{\mu\mathbf{r}}{r^3}\right) \\ &= \frac{2a^2}{\mu}\dot{\mathbf{r}}.\mathbf{f}. \end{aligned} \tag{7.3.1}$$

Now $\dot{\mathbf{r}}.\mathbf{f}$ is the component of the drag acceleration in the direction of the satellite motion. It can be shown however that the dominant force per unit mass due to drag acts tangential to the orbit. Thus, where θ is the true anomaly and f_T is the component of $\mathbf{f}$ tangential to the orbit one can write

$$\dot{\mathbf{r}}.\mathbf{f} = r\dot{\theta}f_T. \tag{7.3.2}$$

The component f_T of $\mathbf{f}$ is given in (King-Hele, 1964) as

$$f_T = \frac{1}{2}\rho v^2\delta \tag{7.3.3}$$

where v is the motion of the satellite relative to the earth and

$$\delta = \left(1 - \frac{r_{p0}w\cos i}{v_{p0}}\right)\frac{SC_D}{m}. \tag{7.3.4}$$

S is the cross sectional area of the spacecraft, C_D and m it's drag coefficient and mass, w is the angular velocity of the atmosphere and the suffix $p0$ denotes initial values at perigee. After transforming (7.3.1-4) into Keplerian coordinates wherein one replaces the time derivative in (7.3.1) with

$$\frac{d}{dE} = r\sqrt{\frac{a}{\mu}}\frac{d}{dt}, \tag{7.3.5}$$

(7.3.1) can be rewritten

$$\frac{da}{dE} = a\rho\delta\frac{(1+e\cos E)^{\frac{3}{2}}}{(1-e\cos E)^{\frac{1}{2}}}. \tag{7.3.6}$$

By integrating equation (7.3.6) between 0 and 2π the variation in a over the course of one orbital revolution is obtained,

$$\Delta a = a\delta\int_0^{2\pi}\frac{(1+e\cos E)^{\frac{3}{2}}}{(1-e\cos E)^{\frac{1}{2}}}\rho dE. \tag{7.3.7}$$

Now (7.2.10) can be substituted into (7.3.7) and the integral explicitly solved. This is done by expanding the integrand as a power series in e, which for a near circular orbit can be truncated. Then using the integral representation of the Bessel function of the first kind and imaginary argument, namely

$$I_n(z) = \frac{1}{2\pi}\int_0^{2\pi}\cos n\theta\exp(zcos\theta)d\theta, \tag{7.3.8}$$

a solution can be obtained. The series expansion of these functions is given by

$$I_n = \sum_{m=0}^{\infty}\frac{\left(\frac{z}{2}\right)^{n+2m}}{m!\,(n+m)!}. \tag{7.3.9}$$

After some simplification, equation (7.3.7) is solved and the solution written, where $z = \frac{ae}{H}$, as

$$\begin{aligned}\Delta a &= -2\pi\delta a^2\rho_o\exp\left(\frac{r_o-a}{H}\right)\left[I_0(z)+2eI_1(z)\right.\\ &+ \left. FA\left(I_1(z)+\frac{e}{2}\left(I_0(z)+3I_2(z)\right)+O\left(e^2\right)\right)\right].\end{aligned} \tag{7.3.10}$$

Thus the variation in a after one orbital revolution is given by equation (7.3.10). Of interest to this work is the differential variation in the mean motion's of two satellites which have different right ascension. To that end one can apply a small change to Kepler's third law namely,

$$n_o^2 a^3 = \mu. \tag{7.3.11}$$

Hence

$$\Delta n_\circ = \frac{-3n_\circ \Delta a}{2a} \tag{7.3.12}$$

and therefore

$$\begin{aligned} \Delta n_\circ &= 3n_\circ \pi \delta a \rho_\circ \exp\left(\frac{r_\circ - a}{H}\right)\left[I_0(z) + 2eI_1(z)\right. \\ &+ \left. FA\left(I_1(z) + \frac{e}{2}\left(I_0(z) + 3I_2(z)\right) + O\left(e^2\right)\right)\right]. \end{aligned} \tag{7.3.13}$$

Only A in equation (7.3.13) is a function of the right ascension and therefore, if one wishes to compare the different rates of decay of two satellites with different values of Ω it is sufficient to compare the respective values of $\Delta n_\circ$ one obtains with $\Omega = \Omega_1$ and $\Omega = \Omega_2$ corresponding to $A = A_1$ and $A = A_2$. Furthermore since the satellites are not assumed to have identical area to mass ratios, they can also have different values of δ, so $\delta = \delta_1$ and $\delta = \delta_2$ correspond to satellites one and two respectively. In the following section the combined effects on the decay rates due to the diurnal bulge of two different satellites in different orbital planes are discussed.

7.4 Relative Decay Rates

Assuming the variations in δ and Ω between the two satellites is small one can take small changes in equation (7.3.13) to gauge the relative drift between the spacecraft due to the diurnal bulge. First of all however (7.3.13) is simplified by imposing a few restrictions.

- The orbit is nearly circular, ie $e \approx 0.001$
- The semi major axis is $a = 6600km$
- The orbit is polar, $i = 90°$

- The density scale height at this altitude is $H = 37km$ which means $z \approx 0.18$.
- The constant F has a value at this height of 0.2. (Cook and King-Hele, 1968)

Now equation (7.3.9) is used to evaluate the Bessel functions in (7.3.13), and only terms linear in z are retained. Thus (7.3.13) becomes

$$\Delta n_o = 3n_o\pi\delta a\rho_o \exp\left(\frac{r_o - a}{H}\right)\left[1 + FA\left(\frac{z+e}{2}\right)\right]. \tag{7.4.1}$$

Therefore for satellites one and two respectively

$$\Delta n_{o1} = 3n_o\pi\delta_1 a\rho_o \exp\left(\frac{r_o - a}{H}\right)\left[1 + FA_1\left(\frac{z+e}{2}\right)\right], \tag{7.4.2}$$

$$\Delta n_{o2} = 3n_o\pi\delta_2 a\rho_o \exp\left(\frac{r_o - a}{H}\right)\left[1 + FA_2\left(\frac{z+e}{2}\right)\right]. \tag{7.4.3}$$

Differencing (7.4.3) and (7.4.2) and defining $dA = A_1 - A_2$ and $d\delta = \delta_1 - \delta_2$ one obtains

$$\begin{aligned}\Delta n_{o1} - \Delta n_{o2} &= 3n_o\pi a\rho_o \exp\left(\frac{r_o - a}{H}\right) \\ &\quad \times \left[d\delta\left(1 + FA_1\left(\frac{z+e}{2}\right)\right) + FdA\delta_2\left(\frac{z+e}{2}\right)\right].\end{aligned} \tag{7.4.4}$$

In order that the two satellites do not drift apart (or together) because of the action of drag it is required that the left hand side of (7.4.4) is equated to zero. Then one has the condition of zero drift, namely

$$\frac{d\delta}{\delta_2} = \frac{-F\left(\frac{z+e}{2}\right)}{\left(1 + FA_1\left(\frac{z+e}{2}\right)\right)}dA. \tag{7.4.5}$$

Now applying the polar orbit restriction to (7.2.5-8) one obtains

$$A_\beta = \cos^2\frac{\epsilon}{2}\cos\left(\Omega_\beta - \lambda - L + \omega_\beta\right) + \sin^2\frac{\epsilon}{2}\cos\left(\Omega_\beta - \lambda + L + \omega_\beta\right) \tag{7.4.6}$$

where $\beta = 1, 2$ for satellites 1 and 2. The obliquity of the ecliptic, $\epsilon = 23.4°$ which means that

$$\begin{aligned}A_\beta &= 0.96\cos\left(\Omega_\beta - \lambda - L + \omega_\beta\right) + 0.04\cos\left(\Omega_\beta - \lambda + L + \omega_\beta\right) \\ &\approx \cos\left(\Omega_\beta - \lambda - L + \omega_\beta\right).\end{aligned} \tag{7.4.7}$$

Therefore for a small change $d\Omega$ in Ω between satellites one and two

$$dA \approx -\sin(\Omega - \lambda - L + \omega)\, d\Omega \tag{7.4.8}$$

where Ω and ω represent mean values of these angles for the two satellites. Applying (7.4.8) and the restrictions to the values of the constants to equation (7.4.5) realises,

$$\frac{d\delta}{\delta_2} \approx 0.018 \sin(\Omega - \lambda - L + \omega)\, d\Omega. \tag{7.4.9}$$

So for a value of $d\Omega$ of $0.6° = 0.0105\, radians$ this becomes

$$\frac{d\delta}{\delta_2} \approx 1.9 \times 10^{-4} \sin(\Omega - \lambda - L + \omega). \tag{7.4.10}$$

The definition of δ in (7.3.4) for a polar orbit, assuming the masses and drag coefficients of the satellites are equal gives,

$$\delta_\beta = \frac{S_\beta C_D}{m} \tag{7.4.11}$$

where S_β, $\beta = 1, 2$ are the surface areas of the two satellites. Now (7.4.10) becomes

$$\frac{dS}{S_2} \approx 1.9 \times 10^{-4} \sin(\Omega - \lambda - L + \omega). \tag{7.4.12}$$

Therefore to ensure that the satellites have the same mean motion when separated in right ascension by a value which in chapter 5 gave an improved solution, requires a temporal variation in the surface area of one satellite with only 0.02 percent maximum. This seems to suggest that the problem of differential air drag is of less significance than that of using two different satellites. Furthermore if two identical non spherical satellites were used then a small difference in the attitudes of satellites could bring about the same variation in the mean motion that the diurnal bulge would cause. The conclusion of this chapter is that for small differences in right ascension the differential air drag due to the diurnal bulge is not a major problem. Any drift could be negated by a small variation in the surface area of

one of the satellites, this could be brought about by extending flaps to increase, or retracting them to decrease the force of drag on the spacecraft to ensure constant separation.

Chapter 8

Conclusions

The work presented here has illustrated how an improvement in the accuracy of a gravity field recovered from Range Rate observations between two low satellites can be realised by separating their orbital planes. It has been explained that the relative motions of the satellites in the directions normal to the orbital planes allowed a significant cross track velocity component to contribute to the line of sight direction and therefore improved the signal content for gravity coefficients with a strong longitude variation.

In chapters 3 and 4 an analytical model was developed that proved flexible enough to model the gravitational perturbations in the range rate between two satellites at the same altitude and inclination but not necessarily the same right ascension. The model was based on Hill's equations which provided the sensitivities of the velocity and position of a spacecraft in it's local frame to errors in the gravity field coefficients. The relative motion of the two local frames was accounted for in a comprehensive manner that allowed for an efficient analysis.

Once this analytical model was developed it was used in chapter 5 to calculate the variances and covariances of the gravity coefficients by a least squares procedure. This procedure made use of a technique analogous to the Fast Fourier

Transform, whereby the assumption that the data set is made up of measurements of equal variance distributed at even intervals along a repeat orbit results in an extremely efficient analysis. To illustrate the benefit of this technique consider the recovery of a 120×120 gravity field. The normal matrix made up of a randomly distributed set of 100,000 measurements would be made up of around 2×10^8 elements, each the product of a summation over all the measurements in the dataset. Such a matrix would be a considerable task to create and this would be somewhat over taxing for an error analysis. With the dataset distributed as detailed above the matrix becomes block diagonal with the largest sub-block being of size 240×240. Furthermore each element of these sub blocks can be calculated without summing over each of the measurements. The difference in computing time between these two techniques is considerable.

The error analysis was carried out in order to illustrate how an optimum, planar, Satellite to Satellite Tracking range rate mission could be improved upon by allowing the orbital planes of the satellites to differ. First the need for a low, polar orbit was established for the recovery of the higher degree coefficients and zonal coefficients respectively. Then for a 120×120 field, a range of separations were tested using a $200km$ polar orbit. It was found that a separation of around 2.4° was best overall but that for some larger separations certain groups of coefficients were recovered better. As a result it was deduced that for a planar mission the best gravity field would be determinable from a mission combining a range of separations.

Separating the orbital planes of the satellites was shown to reduce the errors in the higher degree and order coefficients. These coefficients are associated with spherical harmonic functions which have short wavelength variations in longitude and long wavelength variations in latitude. Thus for a polar orbit they provide only a little along track signal and more cross track signal. Therefore the cross track velocities contributed significantly to the recovery process of these coefficients

which for a planar mission were quite poorly determined. This result underlined the desirability of a SST range rate mission with non coplanar satellites.

In chapter 6 recoveries of groups of coefficients were performed for coplanar and non coplanar missions in both polar and non polar orbits. Single six day arcs and pairs of these arcs were used for the recovery procedures. Using the single six day arcs the recoveries were better for polar orbits. This was due to the assumption in the derivation of Hill's equations that the orbital plane does not precess. Thus in the polar orbit the partials were more accurate.

The higher degree coefficients were not recovered as well as the lower degree ones. This was seen to be due to the circular orbit assumption in Hill's equations and in the forcing terms as well as the attenuation of gravity signal with height.

The introduction of a second arc into the analysis confirmed that the reason for poorer high degree recovery performance was not that the data was insufficient since the results did not alter.

Finally as a check of the model a recovery was performed for non coplanar satellites with the cross track velocities suppressed. This resulted in a poorer recovery than when the full model was used.

Chapter 7 was concerned with the possible drawback in putting the satellites in orbital planes with differing right ascensions. The existence of a bulge in the atmosphere due to the warming effects of the sun means that satellites in different planes will pass through different parts of the bulge and therefore be subject to different drag forces, and hence have different decay rates. This would result in the satellites drifting apart. After consideration of an analytic drag model and it's differential effects on a pair of satellites separated in right ascension by 0.6° the conclusion was drawn that the problem was not too significant. Indeed for such a cross track separation the differential drag would be negated by one of the satellites having a sinusoidal time variation in it's surface area (perpendicular to the direction of motion) with an amplitude of approximately 0.02% of it's mean.

As a result of the work carried out in this thesis the supremacy of non coplanar Satellite to Satellite tracking over the more frequently discussed planar case has been established. In particular it improves the recovery of those coefficients that are poorly recovered in a polar, planar mission, namely the high degree and order (near sectorial) coefficients. The possible problems with air drag have been seen to be rather small and techniques exist that could deal with them. Indeed when compared to that of using two different satellites, the air drag problems discussed here are quite insignificant.

This work would form an ideal basis from which more comprehensive simulations and recoveries could be performed. In particular the recovery of a full gravity field with the presence of the perturbing forces of air drag and solar radiation pressure would provide a more realistic test of the ideas formulated and discussed in this thesis.

Bibliography

CIGAR (1995). *Study of the gravity field determination using gradiometery and GPS.* CIGAR Consortium. ESA Contract 10713/93/F/FL.

Bomford, G. (1980). *Geodesy.* Clarendon Press, Oxford.

Brigham, E. (1974). *The Fast Fourier Transform.* Prentice-Hall, New Jersey, USA.

Burden, R. and Clemence, G. (1989). *Numerical Analysis.* PWS-Kent, Massachusetts, USA.

Colombo, O. (1981). Numerical methods for harmonic analysis on the sphere. Technical Report 310, Dept. of Geodetic Sciences, The Ohio State University.

Colombo, O. (1984). The global mapping of gravity with two satellites. *Netherlands Geodetic Commision, Publications on Geodesy, New Series*, 7(3).

Colombo, O. (1986). *Lecture notes in Earth sciences*, volume 7, chapter Notes on mapping the gravity field using satellite data, pages 263–315. Springer-Verlag.

Cook, G. (1966). Pertubations of near circular orbits by the earth's gravitational potential. *Planet. Space Sci.*, 14:433–444.

Cook, G. and King-Hele, D. (1965). The contraction of satellite orbits under the influence of air drag. v. with day to night variation in air density. *Phil. Trans. Roy. Soc.*, 259:33–67.

Cook, G. and King-Hele, D. (1968). The contraction of satellite orbits under the influence of air drag. vi. near circular orbits with day to night variation in air density. *Proc. Roy. Soc.*, 303:17–35.

Engelis, T. (1987). Radial orbit error reduction and sea surface topography determination using satellite altimetry. Technical Report 377, Dept. of Geodetic Sciences, The Ohio State University.

Fischell, R. and Pisacane, V. (1978). A drag free lo-lo system for improved gravity field measurement. In Mueller, I., editor, *Applications of geodesy to geodynamics, Rep. 280.* Ohio State University, Dept. of geod. sci., Columbus, Ohio.

Frey, H. et al (1993). Games :a gravity and magnetic experimental satellite for oceanography and solid earth science. In *Eos Trans., AGU*, volume 74.

Groten, E. (1987). Gravity field and gravimetric missions. Technical report, Dept. of Civ. Eng. University of Nottingham. Summer school in space and terrestrial geodesy.

Harries, J. (1990). *Earthwatch: The climate from space.* Ellis Horwood.

Hill, G. (1878). *American J. Math.*, 1:5–26.

Jekeli, C. and Upadhyay, T. (1990). Gravity estimation from stage, a satellite to satellite tracking mission. *J. Geophys. Res*, 95:10973,10985.

Kaula, W. (1966). *Theory of Satellite Geodesy.* Blaisdell Publishing Company, Massachusetts, USA.

Kaula, W. (1983). Inference of variations in the gravity field from satellite to satellite range rate. *J. Geophys. Res*, 88:8345–8349.

Keating T., et al (1986). Geopotential research mission,science, engineering and-program summary. Technical Report TM 86240, NASA Tech. memo.

King-Hele, D. (1964). *Theory of satellite orbits in an atmosphere.* Butterworths.

King-Hele, D. (1981). Lumped harmonics of 15^{th} and 30^{th} order in the geopotential, from the resonant orbit of the satellite 1971-54a. *Proc. Roy. Soc.*, 375:327–350.

King-Hele, D. (1983). Geophysical researches with the orbits of the first satellites. *Geophys. J. R. astr. Soc.*, 74:7–23.

King-Hele, D.G. and Walker D. (1985). Individual geopotential coefficients of order 15 and 30, from resonant satellite orbits. *Planet Space sci.*, 33:223–238.

Koop, R. (1993). *Global gravity field modelling using satellite gravity gradiometery.* PhD thesis, Technische Universiteit Delft.

Kozai, Y. (1966). The earth gravitational potential derived from satellite motion. *Space Science Review*, 88:8345–8349.

Nerem, R, Lerch F, Marshall J, Pavlis E, Putney B, Tapley B, Eanes R, Ries J, Schultz B, Shum C K, Watkins M, Klosko S, Chan J, Luthcke S, Patel G, Pavlis N, Williamson R, Rapp R, Biandale R, Nouel F (1994). Gravity model development for topex/poseidon: joint gravity models 1 and 2. *J. Geophys. Res*, 99,24:421–24,447.

Rosborough, G. and Tapley, B. (1987). Radial, transverse and normal satellite position pertubations due to the geopotential. *Celestial Mechanics*, 40:409–421.

Roy, A. (1978). *Orbit motion.* Adam Hilger LTD.

Rummel, R. and Colombo, O. (1985). Gravity field determination from satellite gradiometery. *Bulletin Geodesique*, 59:233–246.

Schrama, E. (1989). The role of orbit errors in processing of satellite altimeter data. Technical Report 33, Netherlands Geodetic Commission.

Stacy, F. (1977). *Physics of the Earth.* John Wiley and sons.

Torge, W. (1980). *Geodesy.* Walter de Gruyter.

Wagner, C. (1983). Direct determination of gravitational harmonics from low-low gravsat data. *J. Geophys. Res.*, 88:10309–10322.

Wakker K., Ambrosius B. and Leenman, H. (1989). Satellite orbit determination and gravity field recovery from satellite to satellite tracking. Technical report, Technische Universiteit Delft.

Wiejak W., Schrama E.J.O., Rummel. R. (1990). Spectral representation of the satellite to satellite tracking observables. In *COSPAR XXVIII.*

Wolff, M. (1969). Direct measurements of the earth's gravity potential using a satellite pair. *J. Geophys. Res.*, 74:5295–5300.

Appendix A

The Inclination Functions

The inclination functions allow one to express the gravitational potential in Keplerian coordinates. Their normal method of calculation is from the expression for the potential in spherical harmonics. Thus the inclination functions are derived from the Legendre polynomials and the sine and cosine terms in (2.1.7). The direct calculation of the Legendre polynomials and therefore of the inclination functions is unstable at high degree and order and requires an alternative method. Recurrence relations exist from which the Legendre polynomials and their derivatives are derived efficiently, which can be used in conjunction with the Fast Fourier Transform routine to provide a stable, efficient method to calculate the inclination functions. A similar method allows the calculation of the cross track inclination functions introduced in equation (3.3.22). Both cases will be outlined here.

The method has been described by [Wagner,1983], [Schrama,1989] and [Koop,1993] and makes use of the unit potential function. This is the potential of equations (2.1.7) and (2.1.8) with $c_{lm} = s_{lm} = \mu = R = r = 1$. It is calculated along a unit circular orbit with $a = 1$, $\Omega = \theta_G = e = \omega = 0$. Thus equating terms in (2.1.7) and (2.1.8) one obtains

$$V_{lm} = V_{lm0} + V_{lm1}$$

$$= \sum_{p=0}^{l} F_{lmp} \left[\left[\begin{array}{c} 1 \\ -1 \end{array} \right]_{l-m\,odd}^{l-m\,even} \cos\left((l-2p)F\right) + \sin\left((l-2p)F\right) \right]$$

$$= P_{lm}(\cos\theta)\left[\cos m\lambda + \sin m\lambda\right]. \qquad \text{(A.1)}$$

The right hand side of equation (A.1) is expressed as a summation over $l-2p = j = 0\,or\,1, l$ in steps of two,

$$V_{lm} = \sum_{j=0,1[2]}^{l} \left[F_{lm\frac{(l-j)}{2}} + F_{lm\frac{(l+j)}{2}}\right] \left[\begin{array}{c} 1 \\ -1 \end{array} \right]_{l-m\,odd}^{l-m\,even} \cos jF$$
$$+ \left[F_{lm\frac{(l-j)}{2}} - F_{lm\frac{(l+j)}{2}}\right] \sin jF. \qquad \text{(A.2)}$$

Each V_{lm} can now be calculated in terms of the Legendre polynomials and sines and cosines of longitude times m, for which efficient and stable methods allow good accuracy to high values of l and m. The latitude θ and longitude λ are calculated at equidistant points along a unit circular orbit of inclination I. The V_{lm} are calculated at each point and the time series transformed to the frequency domain by application of the FFT. Comparison of the amplitudes of the frequencies in (A.2) with the amplitudes obtained by FFT allows one to solve for the inclination functions.

Obtaining the required Fourier expansion in terms of the cross track inclination functions is more complicated than for the normal inclination functions. From equation (3.3.22) with the rules for the unit potential applied

$$\frac{\partial V_{lm}}{\partial u} = \sum_{j=-l+2[2]}^{l} F^{*}_{lm\frac{(l-j)}{2}} \left[\cos\left((j-1)F\right) + \left[\begin{array}{c} -1 \\ 1 \end{array} \right]_{l-m\,odd}^{l-m\,even} \sin\left((j-1)F\right) \right]. \qquad \text{(A.3)}$$

Transforming the j summation to $k = j-1$ one obtains

$$\frac{\partial V_{lm}}{\partial u} = \sum_{k=0,1[2]}^{l-1} \left[F^{*}_{lm\frac{(l-1+k)}{2}} + F^{*}_{lm\frac{(l-1-k)}{2}}\right] \cos(kF) +$$

$$+\begin{bmatrix} -1 \\ 1 \end{bmatrix}_{l-m\,odd}^{l-m\,even} \left[F^*_{lm\frac{(l-1-k)}{2}} - F^*_{lm\frac{(l-1+k)}{2}}\right] \sin(kF). \qquad (A.4)$$

This is the cross track derivative of the l, m term in the unit potential function. To solve by FFT for the amplitudes of the fourier series (A.4) and from that determine the cross track inclination functions, a set of values of $\frac{\partial V_{lm}}{\partial u}$ are required around the unit circle of inclination I. In order to produce such a dataset the cross track derivative must be expressed in terms of the derivatives with respect to latitude and longitude.

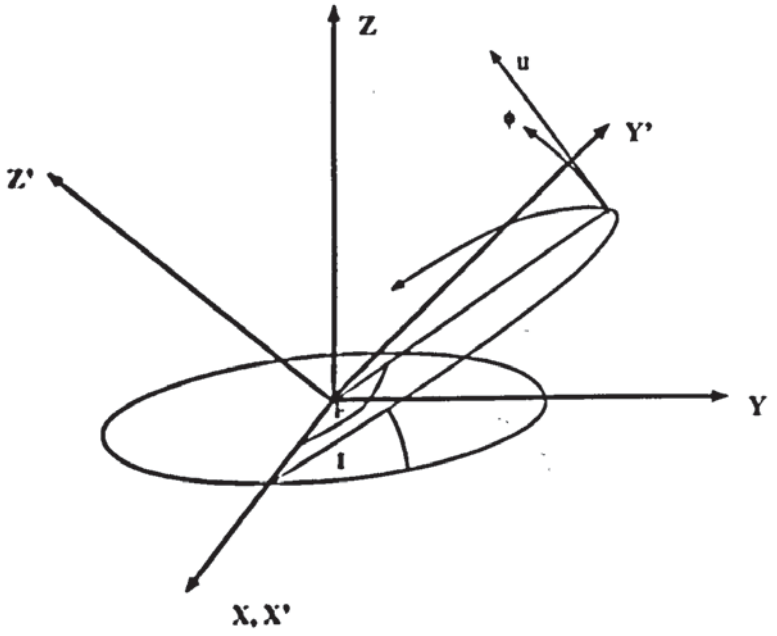

Figure A.1 Geocentric cartesian and orbital systems

From Figure A.1 the angle ϕ is defined as the 'latitude with respect to the orbital plane'. It can be seen that

$$\begin{aligned} \frac{\partial V_{lm}}{\partial u} &= \frac{1}{r}\frac{\partial V_{lm}}{\partial \phi} \\ &= \frac{\partial V_{lm}}{\partial \phi}, \end{aligned} \qquad (A.5)$$

for the unit potential.

The partial derivative with respect to ϕ is expanded by the chain rule as

$$\frac{\partial V_{lm}}{\partial \phi} = \frac{\partial V_{lm}}{\partial \theta}\frac{\partial \theta}{\partial \phi} + \frac{\partial V_{lm}}{\partial \lambda}\frac{\partial \lambda}{\partial \phi}. \tag{A.6}$$

From (2.1.7) one can show

$$\begin{aligned} \frac{\partial V_{lm}}{\partial \theta} &= P'_{lm}(\cos\theta)\,[\cos m\lambda + \sin m\lambda] \\ \text{and} & \\ \frac{\partial V_{lm}}{\partial \lambda} &= mP_{lm}(\cos\theta)\,[\cos m\lambda - \sin m\lambda] \end{aligned}$$

from which it is clear that we must find $\frac{\partial \theta}{\partial \phi}$ and $\frac{\partial \lambda}{\partial \phi}$ in order to calculate the required time series.

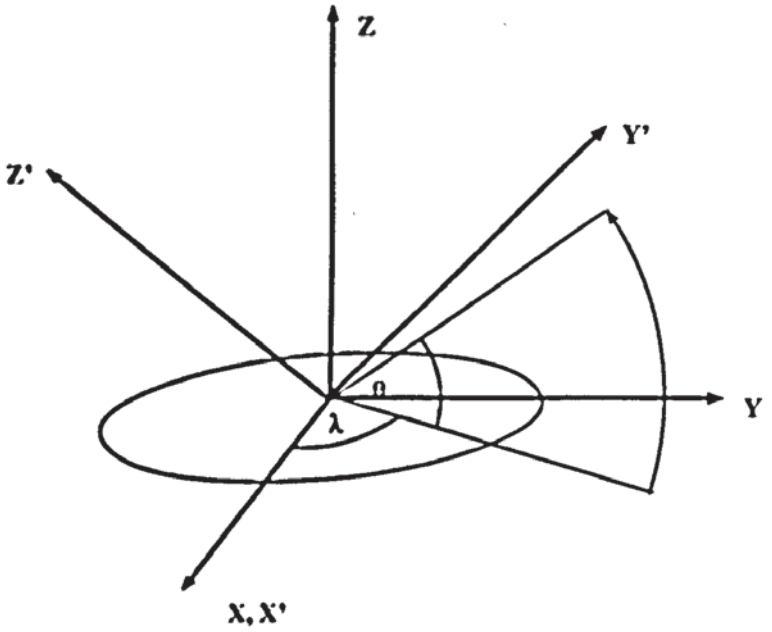

Figure A.2 Geocentric cartesian and polar systems

From Figure A.2 it can be seen that the geocentric cartesian coordinates on the unit sphere, in terms of the polar coordinates are

$$\begin{aligned} X &= \cos\theta\cos\lambda \\ Y &= \cos\theta\sin\lambda \\ Z &= \sin\theta. \end{aligned} \tag{A.7}$$

From Figure A.1 the X', Y', Z' coordinates on the unit sphere give

$$\begin{aligned} X' &= \cos\phi\cos F \\ Y' &= \cos\phi\sin F \\ Z' &= \sin\phi, \end{aligned} \tag{A.8}$$

and the relationship between the two geocentric coordinate systems is (for the case where the longitude of the ascending node is zero)

$$\begin{bmatrix} X \\ Y \\ Z \end{bmatrix} = \begin{bmatrix} 1 & 0 & 0 \\ 0 & \cos I & -\sin I \\ 0 & \sin I & \cos I \end{bmatrix} \begin{bmatrix} X' \\ Y' \\ Z' \end{bmatrix}. \tag{A.9}$$

Combining (A.7), (A.8) and (A.9) results in

$$\cos\theta\cos\lambda = \cos\phi\cos F \tag{A.10}$$

$$\cos\theta\sin\lambda = \cos\phi\sin F\cos I - \sin\phi\sin I \tag{A.11}$$

$$\sin\theta = \cos\phi\sin F\sin I + \sin\phi\cos I. \tag{A.12}$$

From (A.12), for $\phi = 0$,

$$\frac{\partial\theta}{\partial\phi} = -\frac{\cos I}{\cos\theta}, \tag{A.13}$$

and from (A.10) and (A.11)

$$\frac{\partial\lambda}{\partial\phi} = -\frac{\sin I\cos\lambda}{\cos\theta}. \tag{A.14}$$

Thus the time series necessary to calculate the cross track inclination functions is calculated from

$$\begin{aligned} \frac{\partial V_{lm}}{\partial\phi} = &-\frac{\cos I}{\cos\theta} P'_{lm}(\cos\theta)\left[\cos m\lambda + \sin m\lambda\right] \\ &-\frac{\sin I\cos\lambda}{\cos\theta} m P_{lm}(\cos\theta)\left[\cos m\lambda - \sin m\lambda\right]. \end{aligned} \tag{A.15}$$

Equation (A.4) is used to obtain these functions from the FFT of the time series of (A.15), calculated at discrete points along a unit circle of inclination I.